

CONTENTS

FAST NEUTRON STUDIES: A PROPORTIONAL COUNTER

| CHAPTER | METHOD OF FAST NEUTRON SPECTROSCOPY | PAGE |
|--------------|--|------|
| I | Introduction | 1 |
| II | Development of Fast Neutron Spectroscopy | 3 |
| III | The Fast Neutron Spectrometer. | 22 |
| | Absorbers | 32 |
| | Radiators Thesis | 34 |
| | Electronic Circuits | 38 |
| | Measurement of Coincidence Resolving Time | 44 |
| | The Neutron Source | 49 |
| IV | Submitted for the degree of | 52 |
| | The Proportional Counter | 52 |
| | Testing of Amplifier and Deflection Linearity | 59 |
| V | Calibration of the Spectrometer | 62 |
| | Doctor of Philosophy | |
| | The D-D Reaction | 68 |
| | Be ⁹ Spectrum from Monoenergetic Neutron Bead | 72 |
| | Polythene Film of Finite Thickness | 77 |
| | Be ⁹ Energy Spectrum from D-D Neutrons | 78 |
| VI | GEORGE C. REID, B.Sc. | |
| VII | Submitted for the degree of | 87 |
| VIII | Summary | 100 |
| Appendix I | University of Edinburgh | 105 |
| Appendix II | October, 1953. | 113 |
| Appendix III | The Level Scales of | 117 |



CONTENTS

| <u>CHAPTER</u> | | <u>PAGE</u> |
|---------------------|--|-------------|
| I | Introduction | 1 |
| II | Development of Fast Neutron Spectroscopy | 8 |
| III | The Fast Neutron Spectrometer. | 22 |
| | Absorbers | 32 |
| | Radiators | 34 |
| | Electronic Circuits | 38 |
| | Measurement of Coincidence Resolving Time | 44 |
| | The Neutron Source | 49 |
| IV | Testing of the Instrument | 52 |
| | The Proportional Counters | 52 |
| | Testing of Amplifier and Deflection Linearity | 59 |
| V | Calibration of the Spectrometer | 62 |
| | The D-D Reaction | 68 |
| | Recoil Spectrum from Monoenergetic Neutron Beam | 72 |
| | Polythene Film of Finite Thickness | 77 |
| | Recoil Energy Spectrum from D-D Neutrons | 78 |
| VI | Neutrons from Deuteron Bombardment of Beryllium | 87 |
| VII | The 4.9 MeV Excited State of Be^8 | 100 |
| VIII | Summary | 108 |
| <u>Appendix I</u> | Derivation of the Reaction Formulae | 110 |
| <u>Appendix II</u> | Computation of Energy Spread of Recoils from D-D Neutrons at 110° | 113 |
| <u>Appendix III</u> | The Level Scheme of B^{10} | 116 |
| | Acknowledgements | 120 |
| | References | 121 |

CHAPTER I.

INTRODUCTION

Since the discovery of the existence of discrete energy levels in atomic nuclei, which gave rise to the science of nuclear spectroscopy, a considerable amount of work has been devoted to the improvement of available techniques, and to the correlation of the data collected, in order to obtain a coherent picture of the structure of at least some nuclei, and of the laws of force existing between their constituent particles. Information about the low-lying energy levels of nuclei is most easily obtained from the study of the energies of particle groups and gamma-rays emitted on irradiation of a target material by a beam of particles whose energy is known. When a nuclear reaction of the type



occurs, a study of the energy distribution of the product b (usually an elementary nucleon) yields information about the energy level scheme of the product nucleus B . Similarly, the emission of gamma-radiation indicates the decay of one or more excited states in this nucleus, and measurement of the energies of the

gamma-rays yields further information on the level scheme.

Within the last few years, considerable progress has been made in the refinement of techniques for measuring the energies of gamma-rays and charged particle groups, notably by the development of the magnetic spectrometer. By the use of thin converters and magnetic analysis of the resulting photoelectrons, Compton electrons, or pairs, the energy of a gamma-ray can now be determined to an accuracy better than 1%.

Unfortunately, this technique cannot be applied directly to the particle most frequently emitted in nuclear reactions, the neutron, and methods of a rather cruder type must be resorted to. The techniques which have been used so far will be summarised in Chapter 2.

When a 1.25 MeV Cockroft-Walton particle accelerator was installed in the University of Edinburgh in 1950, it was decided to undertake a programme of fast neutron research, and one of the first problems to be tackled was the design of a fast neutron spectrometer which could be used both for the investigation of energy level structure in light nuclei, and as an auxiliary instrument in other fast neutron

work. In order to satisfy the first of these conditions, the instrument must be capable of at least as good energy resolution as the photographic plate and cloud-chamber methods, while the second condition necessitates the ability to obtain at least an approximate measurement of the spectrum during the period of irradiation, or very shortly afterwards. After an examination of methods of fast neutron spectroscopy which had previously been developed, it was decided to follow up a suggestion originally due to Kinsey⁽¹⁾, Amaldi, Bocciarelli, Ferretti & Trabacchi⁽²⁾, and later, independently, Kinsey, Cohen & Dainty⁽³⁾ used a triple coincidence proportional counter telescope to detect proton recoils from fast neutron bombardment of thin films of polythene $[(CH_2)_n]$, and hence to measure the fast neutron flux, knowing the n-p scattering cross-section, the thickness of the polythene film and the telescope solid angle. Kinsey later suggested that the device might be used as a fast neutron spectrometer by measuring the pulse-height produced in the second counter when a triple coincidence occurred. This would give a measure of specific ionisation, and hence of proton energy. In this form, however, the resolution would be poor for all but low energy neutrons, due to the

decreasing variation in specific ionisation with energy as the energy increases. It was thought, however, that by the use of variable absorption between the first and second counters, this difficulty could be overcome. The use of a coincidence telescope is necessitated by the very large background counting rate during neutron bombardment due to light nuclei, mainly protons, recoiling from the counter walls, an effect which would entirely swamp the genuine counting rate from a thin hydrogenous film.

Such an instrument, which might be called a 'recoil-coincidence-absorption spectrometer', ought to be capable of energy resolution of the same order of magnitude as the photographic plate, while at the same time, simply by measuring the coincidence counting rate as a function of absorber thickness, it would be possible to obtain rough knowledge of a neutron spectrum during irradiation.

The simplest method of measuring the pulse-height distribution on the middle counter would be to employ some form of multi-channel electronic pulse-height analyser, or 'kicksorter', the input to which could be 'gated' by the output of the coincidence mixer, so that only those pulses which gave rise to a coincidence were registered. However such instruments are subject to the drawback of possible

instability of channel settings and widths, besides being extremely costly, and it was decided to attempt a somewhat simpler method. The pulses from the middle counter are fed on to one of the deflection plates of a cathode-ray oscilloscope, and the output of the coincidence unit is applied to the grid, which is normally held at such a potential relative to the cathode that only a faint spot is visible on the screen. When a coincidence occurs, the beam is brightened for a short period, and the corresponding pulse from the middle counter becomes visible. No time-base is applied to the oscilloscope beam, and the pulses are recorded by a moving-film camera, and subsequently analysed.

This method has the great advantage over electronic counting methods that a permanent record of the pulse height spectrum is obtained, which can be re-analysed if necessary, while a visual indication of the performance of the amplifier is afforded. It also helps to eliminate the effect of chance coincidences between the counters, since, as will be shown later, these often give a type of pulse which is noticeably different from that produced by a genuine coincidence. In addition, the channel heights and widths can be varied at will in separate analyses of a film, and the question of stability does not arise.

The programme of work which can be carried out with an instrument of this type is very extensive, even with the limited bombarding voltage available. Most of the known stable isotopes produce neutrons with a positive energy release when bombarded by deuterons, but the neutron yield falls off quite rapidly with increasing atomic number of the target nucleus, due to the increasing Coulomb barrier against deuteron penetration. Hence the most useful field of investigation would appear to be the neutron spectra resulting from deuteron bombardment of light nuclei, say with atomic number less than about 10. In this region, only three stable isotopes suffer endothermic (d, n) reactions, namely He^4 , C^{12} and O^{16} . Of the remainder, several have been investigated, though even yet it can be said that the only neutron spectrum resulting from a (d, n) reaction which is known completely is that from the deuteron bombardment of deuterium, the well-known D-D reaction.

Three target materials have been used in the work to be described here - deuterium (for calibration purposes), beryllium and lithium. The latter two elements were chosen partly because some interesting information has come to light recently concerning their neutron spectra, and partly because certain features of these spectra are well known already, and

CHAPTER II.

afford an interesting comparison with the results obtained by other workers using different techniques. A further reason for investigating the neutron spectrum from deuteron bombardment of beryllium was the intended use of this reaction for fast neutron dosimetry experiments in the same laboratory.

The instrument can also be used as a neutron flux measuring device, and can give information on the angular distributions and excitation functions of (d, n) reactions, while the directional properties of the counter telescope can be used in conjunction with some simple form of gamma-ray spectrometer to investigate angular correlations between neutrons and their associated gamma-rays, leading to a knowledge of the spins and parities of the excited states of the residual nucleus. No work of this nature has yet, however, been carried out, and the instrument will be considered purely from the point of view of neutron energy measurement and the allocation of the positions of the excited states.

CHAPTER II.

DEVELOPMENT OF FAST NEUTRON SPECTROSCOPY.

The neutron, being a non-ionising particle, presents serious obstacles to accurate energy measurement, all methods being necessarily somewhat indirect. There are two main types of method available, broadly described as the 'recoil' and the 'reaction' methods. The recoil method is the one which has been most frequently used up to the present; in outline it consists in measuring the energy of a nucleus, usually a proton, recoiling from elastic collision with a neutron. If the direction of recoil is known, the original neutron energy is easily deduced. For a collision of a neutron of energy E_n with a stationary proton, the energy, E_p , imparted to the proton at angle θ to the direction of the incident neutron is given by

$$E_p = E_n \cos^2 \theta .$$

Hence the energy spectrum of the incident neutrons can be deduced from the recoil proton energy spectrum.

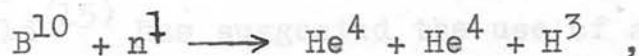
The reaction method yields rather less accurate results, and has not been widely used. Briefly, it consists in studying nuclear reactions produced in some substance by the neutrons, some feature of the reactions being energy dependent. It falls into two

subdivisions:

- (1) the measurement of the total energy release in a neutron-induced reaction whose Q-value is known; and
- (2) the use of the threshold phenomenon in reactions of negative Q-value producing a radioactive end-product. Here the presence of the activity in question indicates bombardment by neutrons of energy greater than the threshold, which is known from the mass-values of the nuclei taking part in the reaction. Theoretically, a range of substances having thresholds of this type would suffice to measure many neutron spectra; unfortunately, this is not possible. The method has been suggested by Feld, Scalettar and Szilard⁽⁴⁾ and by Bretscher and Wilkinson⁽⁵⁾, and these latter authors measured the excitation functions of four suitable (n, p) reactions. They state that as a method of exact spectroscopy, it is virtually useless, but that changes in the activity of the irradiated foil would provide a sensitive indication of changes in the incident neutron spectrum. There still, however, seem to be serious uncertainties in the energies of some of the thresholds themselves. For example

the cross-section for the reaction $S^{32}(n,p)P^{32}$ has been measured by Klema & Hanson⁽⁶⁾ for incident neutron energies between 1 and 6 MeV, giving a value for the threshold of 1.5 MeV, whereas the isotopic mass values give 0.96 MeV.⁽⁷⁾ The highest useful threshold energy is that of the reaction $Fe^{56}(n,p)Mn^{56}$, and is 3 MeV, which effectively sets the upper limit of the energy scale using this method.

The method in which the total energy release is measured, however, has been successfully applied by several workers. Taylor⁽⁸⁾ used photographic emulsions impregnated with borax, and measured the tracks resulting from the reaction



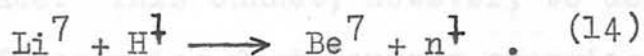
which has a Q-value of -0.4 MeV. The same method was later applied by Lattes & Occhialini⁽⁹⁾ to the measurement of the energy of fast neutrons occurring in cosmic rays.

Keepin & Roberts^{(10), (11)} have made use of the reaction

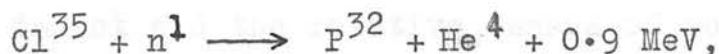


which has a Q-value of 4.64 MeV, and they claim an energy resolution for monoenergetic neutrons of at least ± 0.1 MeV from thermal energies up to 1.3 MeV.

However, for investigation of a continuous neutron spectrum, an accurate knowledge of both the excitation function and the angular distribution for the reaction would have to be known; at present the excitation function is known only approximately up to 0.8 MeV.⁽¹²⁾ One of the major advantages of this method is the fact that it can be applied to non-collimated incident neutrons, though the energy resolution appears to depend to some extent on the degree of collimation.⁽¹³⁾ The method has been applied to the study of the excited state in Be^7 resulting from the reaction



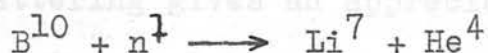
Feld⁽¹⁵⁾ has suggested the use of a proportional counter containing a gas which undergoes an exothermic (n,p) reaction, such as N^{14} or Cl^{35} . The Q-value in each case is about 0.5 MeV, but nitrogen would appear to be unsuitable as the cross-section for the reaction shows strong resonances corresponding to the excited states of the compound nucleus N^{15} . In the case of chlorine there is a competing reaction



but for neutron energies up to 1 MeV (the upper limit proposed for such a spectrometer by Feld) this

process is much less probable, since the alpha-particle has to penetrate a much higher potential barrier than the proton. Chlorine itself is unsuitable as a counter filling gas, being strongly electro-negative, but a polyatomic vapour such as CCl_4 might be used. There are no reports of this having been tested so far.

The reaction method has long been used as a detector of neutrons in BF_3 counters, in which the slow neutron reaction



takes place. This cannot, however, be used as a method of measuring fast neutron energies, as the cross-section is very small at energies above 1 keV.⁽¹⁶⁾

By far the greater part of the work carried out up to the present in the field of fast neutron spectroscopy has been concerned with the recoil method. When a neutron beam passes through any substance, any of the nuclei present can be 'struck' by a neutron, and projected with an energy whose value depends on the energy of the incident neutron, the angle of impact and the relative masses of nucleus and neutron. In most practical cases, the substance is hydrogen or a hydrogen compound, and recoil protons

are observed. After a collision between a neutron of energy E_n and a stationary proton, owing to the approximate equality in mass of the neutron and proton, they travel in directions at right angles, the proton having energy

$$E_p = E_n \cos^2 \theta .$$

For the (n,p) collision, the scattering is known to be isotropic in centre of gravity space if the neutron energy is less than about 10 MeV, since only S-wave scattering gives an appreciable contribution. By transferring to laboratory space, it can be shown from this that recoils of all energies from 0 up to the maximum, E_n , are equally probable.

Various methods of measuring the recoil proton ranges have been used. The cloud-chamber was used in the first attempt made to measure a neutron spectrum by Curie & Joliot⁽¹⁷⁾, and was used in most of the early neutron energy determinations, and even as recently as 1950⁽¹⁸⁾. One of the principal disadvantages of the method lies in the length of running time of the neutron source necessary to provide enough photographs for accurate measurements. Perhaps the most important single discovery made using the cloud-chamber technique was that of the monoenergetic

neutron group resulting from the so-called D-D reaction⁽¹⁹⁾; in this case the chamber was filled with helium, and the recoil alpha-particle tracks measured.

Since about 1940, the cloud-chamber has been almost entirely superseded by the photographic emulsion technique, with which by far the greatest amount of work in this field has been carried out. The earliest report of such work is by Blau & Wambacher⁽²⁰⁾ who used recoil protons either produced in the emulsion itself or in a paraffin block placed between the neutron source and the photographic plate. Their neutron sources, however, were relatively weak, and even long exposures gave so few tracks per unit area of plate that the analysis was extremely tedious. In 1935 Taylor⁽²¹⁾ examined the possibility of investigating neutron spectra by measuring recoil proton tracks in emulsions, but concluded that the method was too inaccurate for the purpose. The great resurgence of the photographic plate as a precise energy measuring device in all branches of nuclear physics has been almost entirely due to the work of Powell and his collaborators in the early 1940's, and the general technique, with applications to fast neutron spectroscopy, has been discussed by him.⁽²²⁾

Very good resolving powers have been obtained with this method⁽²³⁾ and the range of energy covered is from about 0.3 MeV⁽²⁴⁾ up to a value dependent to some extent on the thickness of emulsion used. Green and Gibson⁽²⁵⁾ have used 300 μ thick emulsions in the study of the high-energy neutrons from the bombardment of Li^7 by deuterons. The range of a proton of 15 MeV energy is about 120 μ).

The great advantages of the photographic plate method lie in its relative cheapness and simplicity and in the permanent records which it affords. However, it has serious drawbacks. The recording efficiency is energy dependent in two ways; besides the variation of the neutron-proton scattering cross-section with energy, which is inherent in all recoil measurements, a correction has to be applied for tracks which pass out of the emulsion at some point in their length, and are thus rejected. The probability of this occurring is obviously greater the longer the track, i.e. the greater the energy of the recoil proton, and consequently must be corrected for. The correction function has been computed by Richards.⁽²⁶⁾ A more grave disadvantage lies in the length of time which must necessarily elapse between the bombardment and the complete computation of the spectrum; this

period may amount to several months. Hence, while the photographic emulsion can provide very accurate and detailed descriptions of fast neutron spectra, it is of very little use where a rapid survey of a spectrum within a period of a few hours is desirable.

While the use of photographic plates cuts down considerably the exposure time to the neutron source when compared with the cloud-chamber method, this time must still be quite long. When measuring a photographic plate, it is standard practice merely to examine a fixed number of fields of view, and the total area examined is normally very much less than the area of the plate. Hence, in order to avoid waste of time, it is desirable to have at least one track per field of view on the average as a minimum criterion. In order to satisfy this condition, quite long periods of exposure are necessary, and usually only a fraction of the information available is used.

Among the most valuable work in this field carried out with photographic plates is the exhaustive study of the D-D neutron spectra at various angles of emission by Livesey & Wilkinson⁽²⁷⁾, the results of which have been used in the calibration of the spectrometer described here. Livesey and Wilkinson comment that despite the tedium, the photographic plate

technique is capable of giving more accurate results than any other method then available.

Proportional counters of various types have been used as recoil proton detectors. The simplest arrangement is a chamber containing hydrogen or methane at high pressure. Since a monoenergetic neutron beam produces recoils of all energies from zero up to the neutron energy with equal probability (see above), the resultant recoil proton spectrum will be rectangular. The neutron spectrum can be obtained by differentiation of the pulse-height distribution found with a pulse-height analyser. This method, which has been proposed by Baldinger, Huber and Staub⁽²⁸⁾ is not very reliable, owing to the necessity for numerical differentiation, although it is extremely simple from the instrumental point of view.

Alternatively, instead of depending on recoils from gas molecules, a thin hydrogenous radiator can be inserted in the counter, and recoils from it recorded. In this case, the counter gas will be as heavy as possible, so that recoil nuclei arising from collisions between neutrons and gas atoms may have as small an energy as possible and may be neglected. The energy sensitivity of such a counter has been predicted theoretically by Barschall and

Bethe⁽²⁹⁾, and the predictions have been tested experimentally by Coon and Nobles.⁽³⁰⁾ It is shown that this type of counter will act as a threshold detector when used in conjunction with a discriminator, and the effective threshold can be varied simply by varying the discriminator bias. From this device it is a simple step to the more generally useful proportional counter telescope described later.

A proportional counter technique of special application has been used by Willard and Preston⁽³¹⁾ for the detection of a very low energy neutron group occurring in the endothermic reaction



It consists in recording the ratio of the counting rate from a boron trifluoride chamber (whose sensitivity is proportional to $1/E_n^{1/2}$) to that from a long paraffin moderated chamber whose sensitivity is almost independent of energy.⁽³²⁾ This ratio shows a sharp increase at the threshold for production of a neutron group, and the energy of the corresponding excited state can be found from the bombarding proton energy. This method, however, can only be applied to such endothermic reactions. A similar technique, but using a single BF_3 counter, has been used by Bonner

and Butler.⁽³³⁾

Proportional counter telescopes have been used previously in this field. Worth⁽³⁴⁾, working with the Yale cyclotron, used two hydrogen-filled proportional counters in coincidence with variable absorption between them in determining the neutron spectra resulting from deuteron bombardment of gas targets of A^{40} and N^{15} . The geometry of his work was rather poor, however, owing to the low cyclotron beam current available. He states that this method of approach was used because of the greater ease of collecting data as compared with the photographic emulsion and cloud-chamber methods, though he does not believe it to be capable of greater accuracy than these methods, at least in the medium energy range. A similar instrument, in which four argon-carbon dioxide filled proportional counters with a fairly thick polythene foil are operated in coincidence-anticoincidence has been used by Baldwin⁽³⁵⁾ in the investigation of neutron-proton scattering in the 18 to 21 MeV range, and by Cohen and Falk⁽³⁶⁾, ⁽³⁷⁾ in the examination of neutron energies and angular distributions from (d,n) reactions with 15 MeV deuterons. In this work, absorbers are used to select a desired recoil proton energy range, and the counting rate measured.

In the last few years, rapid advances have been made in the technique of scintillation counter spectrometry, and several workers have applied these methods to fast neutron energy measurements. The crystal producing the scintillations is usually sufficiently rich in hydrogen to produce enough recoil protons of its own, so that a separate radiator is unnecessary. The reaction method could also be used with crystals enriched with, say, Li^6 . The recoil method has been discussed by Poole⁽³⁸⁾, and tested with 2.54 MeV neutrons from the D-D reaction using a crystal of anthracene. This substance has a high luminous efficiency, but has a relatively high gamma-ray sensitivity and its use is limited to measurements in the absence of gamma-radiation, or where the effect due to gamma-radiation can be subtracted by a 'background' run.

A coincidence method using crystals of stilbene, which has a highly linear energy-luminosity relationship⁽³⁹⁾, and sodium iodide, has been discussed and tested by Beghian, Allen, Calvert and Halban⁽⁴⁰⁾. The theoretical energy resolution and efficiency of this type of spectrometer has been discussed by the Pittsburgh cyclotron group⁽⁴¹⁾. A time-of-flight scintillation spectrometer has been tested by James

and Treacy⁽⁴²⁾, with so far inconclusive results. Methods involving the use of liquid scintillators are also under investigation in Glasgow University⁽⁴³⁾ but no definite results have been published at the time of writing.

1. The three proportional counter cathodes, shown at A, are sections of $\frac{1}{16}$ " wall brass tubing, the upper and lower thirds of which have been turned down to $\frac{1}{32}$ " to leave a $\frac{1}{32}$ " thick collar on which the cathode is supported. It is insulated from the surrounding metal by a ring of polystyrene into which the cathode is pushed. The polystyrene is then cemented to the top of the flange of the metal guard-ring, shown at B. The guard-ring flanges are necessary in order to protect the polystyrene from direct irradiation by recoil protons, which would cause deterioration in its insulating properties. The lower two cathodes are held in a brass container (c), whose interior wall is stepped in thickness by successive intervals of $\frac{1}{1600}$ th of an inch. The upper guard-ring is a push-fit on the upper section of the container, held in position by the 'civet' wire. The first polystyrene ring insulator is also a push-fit in this section, and is checked by the 'civet' wire flange. Pushed into this in turn, and checked by the collar mentioned above, is the middle counter cathode.

CHAPTER III.

THE FAST NEUTRON SPECTROMETER.

The fast neutron spectrometer is shown in section in Fig. 1. The three proportional counter cathodes, shown at A, are sections of $1/16$ " wall brass tubing, the upper and lower thirds of which have been turned down to $1/32$ " to leave a $1/32$ " thick collar on which the cathode is supported. It is insulated from the surrounding metal by a ring of polystyrene into which the cathode is pushed. The polystyrene in turn rests on the top of the flange of the metal guard-ring, shown at B. The guard-ring flanges are necessary in order to protect the polystyrene from direct irradiation by recoil protons, which would cause deterioration in its insulating properties. The lower two cathodes are held in a brass container (c), whose interior wall is stepped in thickness by successive intervals of $1/100$ th of an inch. The upper guard-ring is a push-fit in the upper section of the container, and is checked by the first 'step'. The first polystyrene ring insulator is also a push-fit in this section, and is checked by the guard-ring flange. Pushed into this in turn, and checked by the collar mentioned above, is the middle counter cathode.

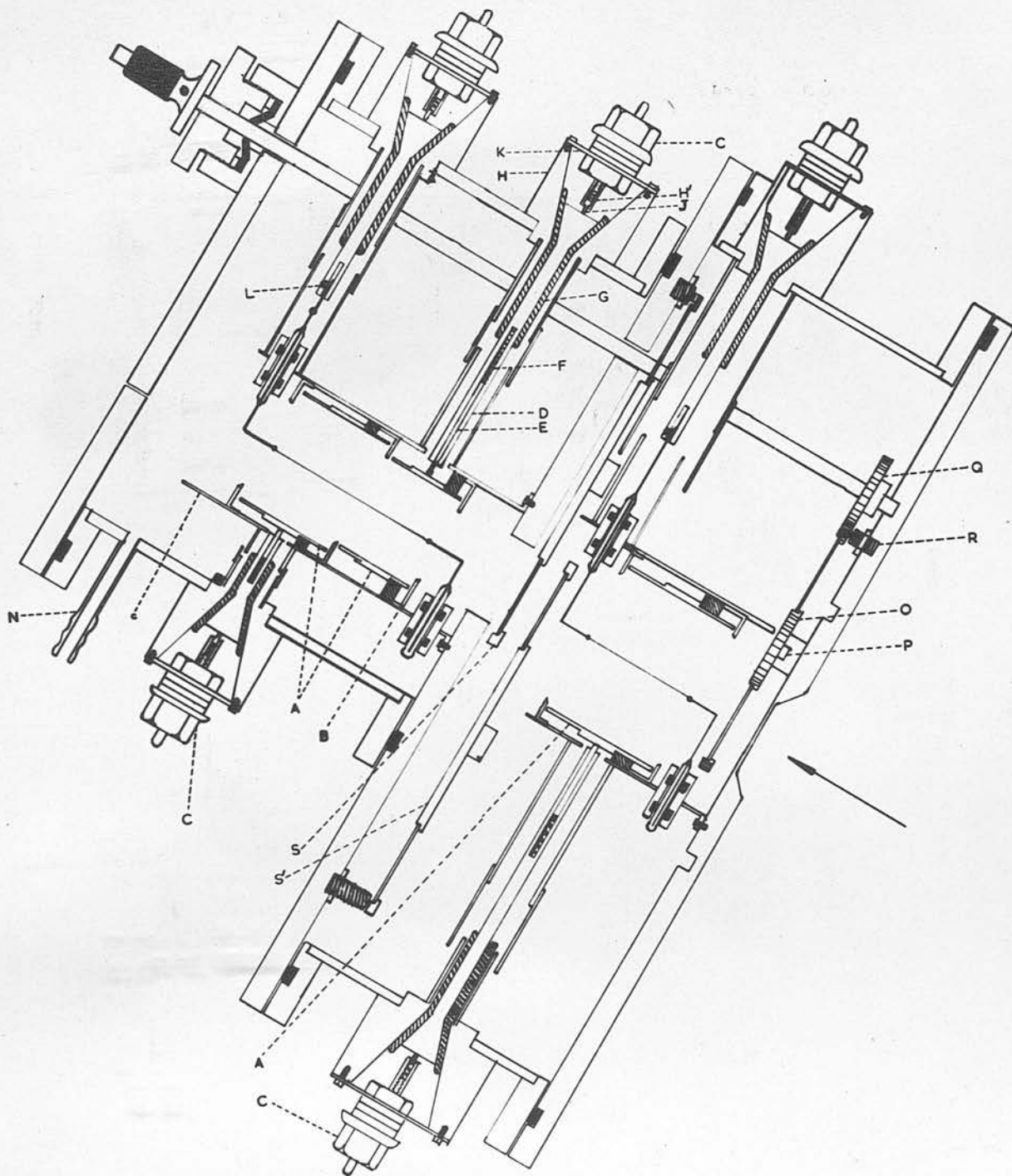


FIGURE I. Cross-section of fast neutron spectrometer.
The arrow indicates direction of incident neutrons.
(Note: In the text the 'upper' counter refers
to that nearest the target).

Below this, and checked by the second step, comes the other counter system, made up of guard-ring, insulator and cathode as before. Finally, the lower guard-ring rests on the third step, immediately above the high voltage lead. The cathode assembly for the uppermost counter, situated in the upper section of the spectrometer, is exactly similar.

Output pulses are taken directly from the cathodes, and the three output plugs are shown at C. It was thought advisable to avoid wherever possible rigid contacts in the construction of the instrument, since these present difficulties whenever dismantling and replacement are necessary, and usually involve the application of heat, which might cause deterioration in the insulator properties. Consequently, a form of lightly spring-loaded contact was used in the output systems, and was found to give completely satisfactory results where short voltage pulses are concerned. The arrangement will be illustrated by reference to the middle counter.

A brass barrel, D, carries the pulses to the exterior of the spectrometer via a length of brass rod, E, with highly polished flat ends, and a length of very light steel spring, F, both of which are free to move longitudinally in a cylindrical hole drilled

down the centre of the barrel D. D is insulated from the brass outer casing by a tube of polystyrene, G. The output ends of both the barrel and the polystyrene insulator are conical in cross-section, and the outer surface of the barrel cone and inner surface of the insulator cone are ground to ensure a close fit. The outer surface of the insulator cone is similarly ground to fit the conical interior surface of the output port, H. These cone-joints form a vacuum seal. It was found to be sufficient to apply a thin layer of Apiezon 'M' grease to the surfaces in order to make a good seal, but spontaneous leaks were found to develop from time to time, possibly due to the outward push of the spring-loaded contact at E when the interior of the spectrometer was let down to atmospheric pressure. A completely satisfactory seal was found to be made by applying to the ground surfaces a thin layer of a solution of Picien vacuum wax in chloroform. This set very rapidly, and yet had sufficient elasticity to afford a slight yield against the spring without giving rise to a leak, and could also be broken and re-made quite easily when the apparatus was dismantled.

The output plug itself is a simple coaxial cable connector modified to carry a small spring-loaded

contact at the end. This consists of a barrel, H', screwed on to the plug and carrying a short length of spring and a small brass button contact, J, bearing on the end-surface of the cone-joint. The plug is earthed to the spectrometer casing by means of a brass plate K, screwed on to the outer surface of the output port, H.

The output system is shielded throughout by means of three lengths of brass tubing. One is hard-soldered on to the counter container and the second on to the outer casing, while the third, which is a push-fit on the outer surface of the second, can be moved along to complete the shielding.

The high voltage input leads to the two axial wires are similar to the output leads, with the exception that no spring loaded contact is used at the counter end of the brass barrel, a small grub-screw, shown at L, being used instead.

The wire mounting will be described with reference to Fig. 2, where it is shown in rather more detail than in Fig. 1. The high voltage is carried into the counter container by a tungsten rod of 1 mm. diameter. This rod has sealed around it in the neighbourhood of the point where it enters the container a length of thin Pyrex tubing which acts as

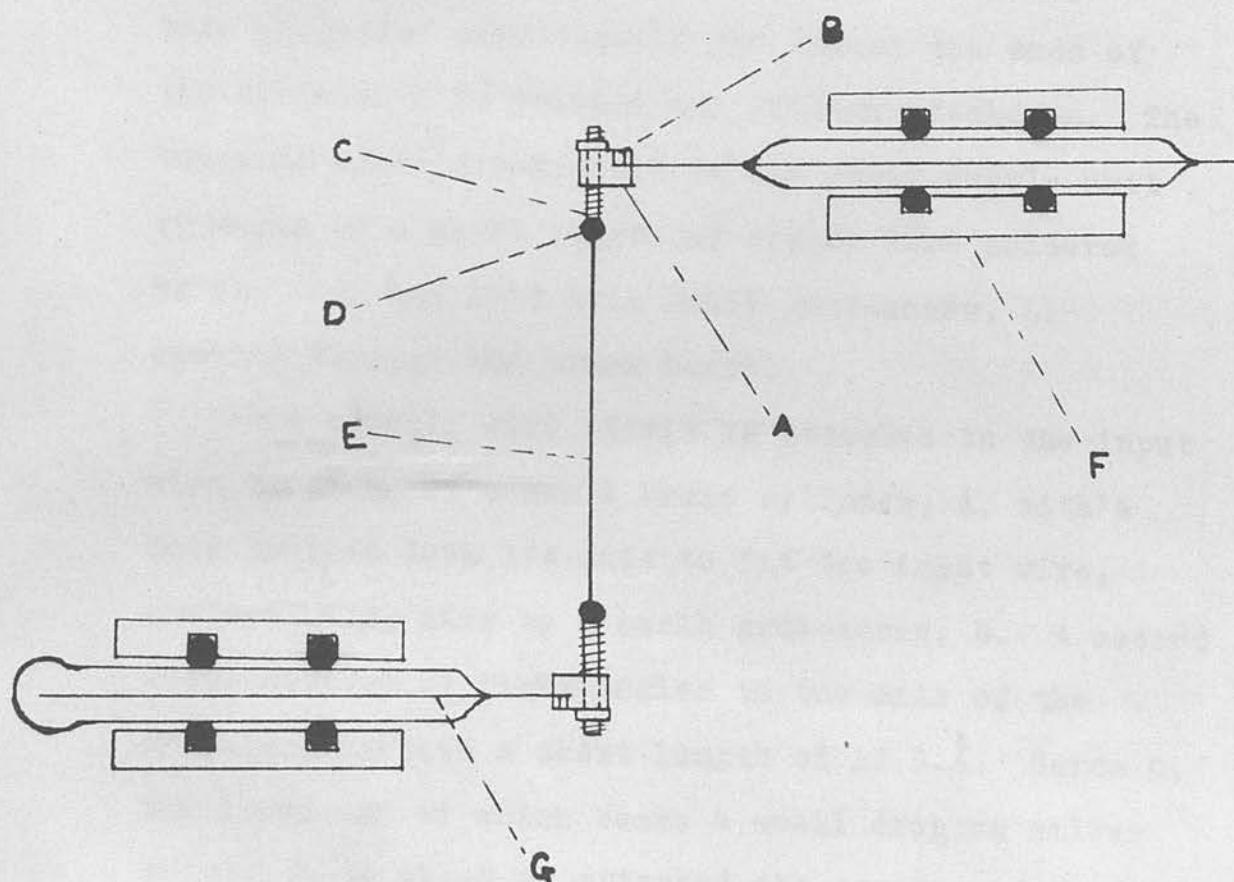


FIGURE 2. Proportional counter wire assembly.

both support and insulation. The Pyrex tubing is held in a small brass cylinder F, whose inner wall contains two grooves in which rest two Neoprene 'O' rings of $\frac{1}{8}$ th of an inch inside diameter. The Neoprene rings provide a fairly rigid, yet non-microphonic, support for the counter wire. The brass cylinder F is screwed into a hole in the wall of the counter container, so that the wire mounting can be easily dismantled as a unit. This arrangement was found to be completely satisfactory provided that the Pyrex tube projected sufficiently far beyond the ends of the cylinder F to prevent any voltage breakdown. The tungsten wire is connected to the power supply unit by means of a short length of copper wire soldered to its end, and held by a small grub-screw, L, passing through the brass barrel.

The counter wire itself is attached to the input wire by means of a small brass cylinder, A, with a hole drilled down its axis to fit the input wire, contact being made by a small grub-screw, B. A second hole, drilled at right angles to the axis of the cylinder, carries a short length of 12 B.A. Screw C, the lower end of which bears a small drop of silver solder, D, to which is attached the counter wire, E, which is of 0.1 mm. diameter tungsten. The

arrangement at the lower end of the wire is exactly similar, the rod G here terminating inside the Pyrex tube. The small 12 B.A. screws are held in position by means of nuts, which allow the tension in the counter wire to be adjusted and any kinks eliminated, and also allow easy replacement of the counter wire.

All sharp edges were eliminated in the input lead system in order to avoid disturbances from corona effects, and in practice no such trouble was experienced.

As is shown in Fig. 1, a common wire is used for the two lower counters, and a separate wire for the upper counter. This is necessary because of the positioning of the two absorber wheels immediately below the upper counter, and also because of the rather greater wire voltage required by the upper counter in order to counteract its larger cathode diameter. It is desirable that the gas multiplication in the three counters should be of the same order of magnitude, since this simplifies the choice of amplifier gain setting for a particular experiment. Ignoring the effect of gas pressure, which is the same for all the counters, the gas multiplication depends on wire voltage and cathode diameter according to the relation

$$M = M \left[\frac{V_0}{\log_{10}(b/a)} \right] \quad (1)$$

where M is the gas multiplication, V_0 the wire voltage, b the cathode diameter and a the wire diameter.⁽⁴⁴⁾

Hence if the middle counter has cathode diameter b_1 , and the upper counter b_2 , and both have a $1/10$ th mm. diameter wire, the ratio of the wire voltages must be given by

$$\frac{V_{01}}{V_{02}} = \frac{\log(10b_1)}{\log(10b_2)}$$

for the counters to have the same gas multiplication.

The dimensions chosen for the counter cathodes and guard-rings are of some importance, as may be seen by reference to Fig. 3, in which the counter geometry is reproduced approximately to scale. 1, 2 and 3 in Fig. 3 represent the counter cathodes, A is the polythene film, and B and C are the two guard-rings of importance in the consideration of the counter geometry. The two broken lines represent the paths of recoil protons originating in the extreme edge of the polythene film, A.

The guard-ring B is used as the defining 'stop' for the counter telescope system: it fixes the solid angle within which all recoil protons originating in the polythene film record a triple coincidence. As

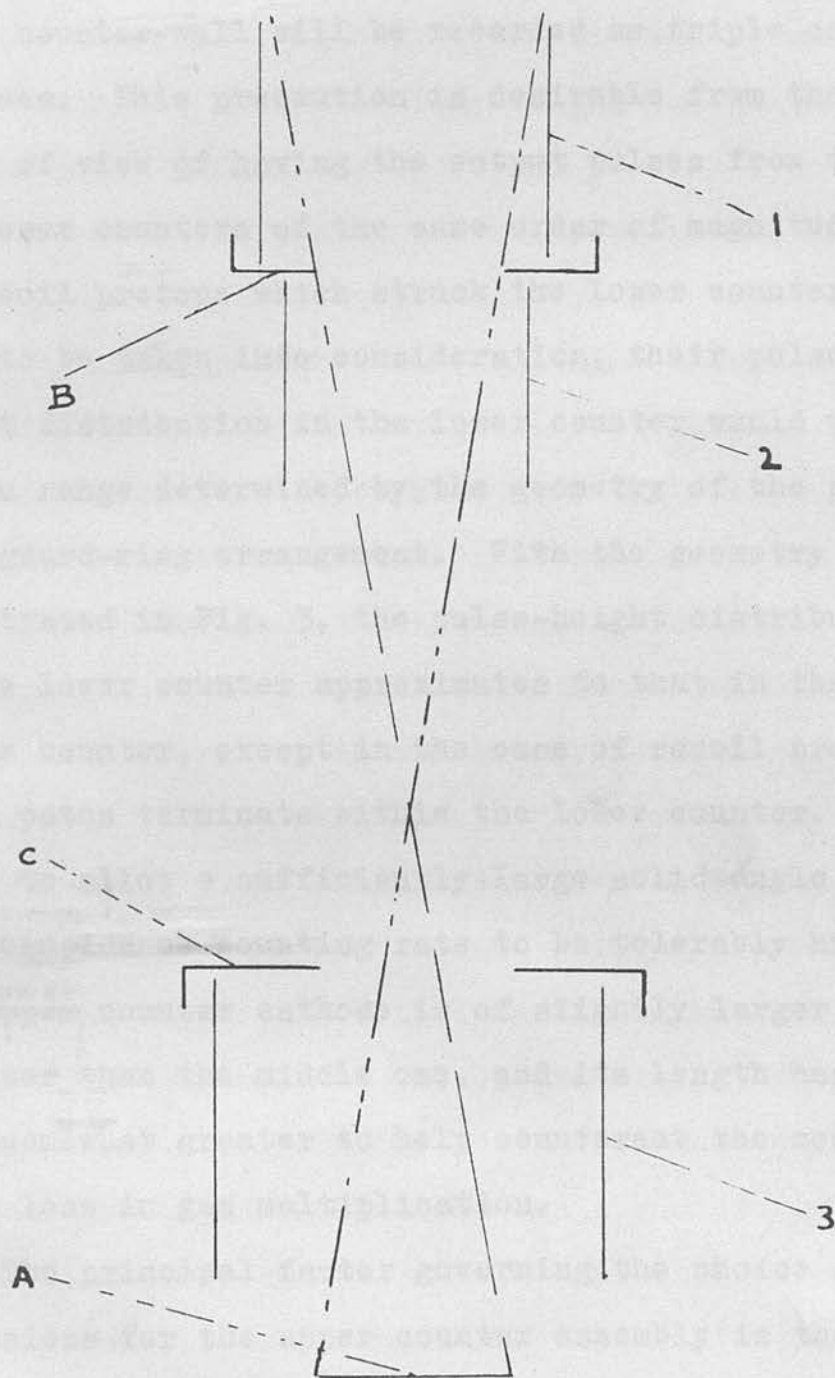


FIGURE 3. Proportional counter geometry.

can be seen from the diagram, its position has been fixed so that only those recoil protons which would traverse the counter telescope without striking the lower counter wall will be recorded as triple coincidences. This precaution is desirable from the point of view of having the output pulses from the two lower counters of the same order of magnitude. If recoil protons which struck the lower counter wall were to be taken into consideration, their pulse-height distribution in the lower counter would vary over a range determined by the geometry of the particular guard-ring arrangement. With the geometry illustrated in Fig. 3, the pulse-height distribution in the lower counter approximates to that in the middle counter, except in the case of recoil protons whose paths terminate within the lower counter. In order to allow a sufficiently large solid angle for the coincidence counting rate to be tolerably high, the ~~upper~~ ^{lower} counter cathode is of slightly larger diameter than the middle one, and its length has been made somewhat greater to help counteract the consequent loss in gas multiplication.

The principal factor governing the choice of dimensions for the upper counter assembly is the large number of recoil protons originating in the brass of the counter cathode, as has been mentioned

in the Introduction. These protons could constitute a serious drawback to the method if they were permitted to give rise to coincidences. This possibility has been eliminated by making the cathode of much larger diameter than the other two, as shown in Fig. 3. The guard-ring C then prevents recoils from cathode 3 from traversing the telescope. The larger cathode diameter is compensated for, as mentioned above, by using a higher wire voltage. There is a slight additional disadvantage in this method, however, in that the large cathode size provides a large solid angle for collection of recoil protons from the polythene. The resultant increased single counting rate increases the chance triple coincidence counting rate. This, however, is probably not of great significance, as will be seen later.

The other guard-rings, not shown in Fig. 3, have no geometrical significance, and merely serve as shields and supports for the counter cathodes.

The outer casing of the spectrometer, as can be seen from Fig. 1, is in two sections; the upper section, housing the radiators and absorbers as well as the first proportional counter, is a 10" diameter brass cylinder, sealed at either end by $\frac{1}{4}$ " thick brass plates, bolted on to the cylinder flanges, the

vacuum seal being made by conventional rubber ring gaskets, fitting into grooves in the surfaces of the plates. The lower section, containing the two lower counter systems, is a 6" diameter brass tube, similarly sealed on to the upper section. The pumping-out tube is at N.

The polythene radiators are mounted on a wheel of $3\frac{1}{2}$ " diameter, shown at O, which is free to rotate about the axis P. The radiators are situated in holes of diameter one inch, of which there are four, spaced symmetrically around the circumference of the wheel. The wheel is toothed, and is rotated by the smaller wheel Q, which is driven by a shaft passing out of the spectrometer through a Wilson-type rotating vacuum seal at the lower end. The wheel is located in position by a small spring-loaded ball-bearing contained in the screw, R. This ball-bearing locks into a punched hole near the circumference of the wheel when one of the radiator holes is centred on the counter telescope axis.

The aluminium absorbers are carried on two wheels situated in the upper section of the spectrometer immediately below the first counter. These wheels are of 5" diameter, and each contains eight one-inch diameter holes in which the absorbers are carried.

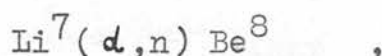
Hence there are available sixty-four different thicknesses of absorber, an ample number to cover the full range of neutron energies available for this work. The wheels are mounted centrally on driving shafts, similar to that used to rotate the radiator wheel, and both passing out of the spectrometer through Wilson seals in the end-plate. (In order to save confusion, these shafts and the corresponding Wilson seals have been omitted in Fig. 1; the absorber wheels are shown at S and S'). The wheels are located by screws containing spring-loaded ball-bearings, and the knobs which rotate the shafts are provided with pointers, indicating the thickness of the absorber in use.

Absorbers.

The absorbers used were of aluminium, a substance whose stopping-power for protons is fairly accurately known^{(45), (46)}. It was decided to place a series of comparatively thin absorbers in the upper of the two wheels, and a range of thicker ones in the lower wheel. The values of thickness chosen were dictated more by immediate availability than by choice, though as will be seen later, the range of values available was more than sufficient to cover all requirements.

The absorbers were cut in the form of discs of diameter $1\frac{1}{16}$ " from small pieces of sheet aluminium which were carefully cleaned, measured and weighed beforehand.

The most energetic neutrons available from bombardment of light elements by deuterons of up to 1 MeV energy are those resulting from the reaction



and have a maximum energy in the forward direction of about 15 MeV. Now the range in air at a pressure of 76 cms. of mercury and temperature 0°C ("standard air") of a proton of energy 15 MeV is 238.3 cms.

Hence, using the rough relation that 1 cm. of standard air is equivalent in stopping power to 1.52 mg/cm^2 of aluminium⁽⁴⁷⁾ the range in aluminium of a proton of 15 MeV energy is 362.2 mg/cm^2 . Hence this is the upper limit necessary for the absorber thickness.

After being carefully cleaned to remove all traces of grease, the pieces of sheet aluminium were cut into rectangles whose sides were measured to the nearest 0.1 mm. The weighing of the rectangles was carried out to 0.1 mg., and the absorber thickness expressed in mg/cm^2 . It will be seen that practically all the probable error in this thickness determination

arises in the measurement of area: the pieces available were mostly squares of approximately 5 cm. side, giving a probable error in area determination of the order of 0.3%, whereas the greatest probable error in mass determination is of the order of 0.05%.

The table below shows the constitution of the two absorber wheels.

TABLE I.

| <u>Position</u> | <u>Upper Wheel</u> (mg/cm ²). | <u>Lower Wheel</u> (mg/cm ²). |
|-----------------|--|--|
| 1 | 0 | 0 |
| 2 | 6.8 ± 0.02 | 63.2 ± 0.2 |
| 3 | 11.8 ± 0.04 | 81.7 ± 0.2 |
| 4 | 13.7 ± 0.04 | 122.5 ± 0.4 |
| 5 | 19.2 ± 0.06 | 160.3 ± 0.5 |
| 6 | 22.0 ± 0.06 | 194.5 ± 0.6 |
| 7 | 32.5 ± 0.10 | 256.9 ± 0.8 |
| 8 | 41.1 ± 0.1 | 344.3 ± 1.0 |

The absorber discs are mounted on small flanges around the circumference of the holes in the wheels, and are held in position by short lengths of steel wire pressing against the sides of the hole.

Radiators.

The recoil proton radiator used throughout the experimental work was a disc of polythene of thickness

1 mg/cm². This substance, a well-known commercial plastic, has the chemical formula (CH₂)_n, and was chosen for this work because of its large hydrogen content. A process for producing thin and reasonably uniform films of polythene has been devised, and will be described briefly here.

Polythene dissolves very easily in warm toluene (C₆H₅CH₃), and attempts were first made to produce films by pouring the solution on to a water surface, a method frequently used for thin film production. When the toluene evaporated, however, the polythene tended to coagulate, or at best to form a film with an irregular wavy surface, which was not very satisfactory. This difficulty was overcome by pouring the solution gently on to a horizontal glass surface, allowing the toluene to evaporate and then soaking the polythene film off in warm water. In a typical case, 30 mg. of polythene turnings were dissolved in 5 cc. of toluene by heating gently in a water-bath to about 80°C. The solution was then poured on a horizontal 3 inch square glass plate (a lantern slide cover glass), and left to settle and evaporate. When the toluene had gone, the plate was placed in nearly boiling water. The polythene quickly peeled off and rose to the surface, whence it was lifted on a wire

frame and allowed to dry. The quantities used produced a 3 inch square film of thickness 0.6 mg/cm^2 , uniform except at the edges.

The film is held in position in the radiator wheel by means of a thin brass ring fitting tightly into the hole. The untrimmed film is laid over the hole and the brass ring pushed into place. The edges of the film are then trimmed away. This arrangement keeps the film sufficiently taut to prevent any waviness appearing in it.

The major difficulty in the production of very thin films by this method appears to be in peeling them off the glass surface, but films of thickness greater than about 0.5 mg/cm^2 come off fairly easily. The thinnest film which has been produced by this method had a thickness of 0.2 mg/cm^2 . Films of this order of thickness, however, are extremely fragile, and from the point of view both of manipulation of the instrument and of obtaining an adequate coincidence counting rate, it was decided to use a film of thickness 1 mg/cm^2 . The following example will illustrate this latter point: the number of recoil protons projected into a small solid angle Ω in the forwards direction from a polythene film is given by

$$q_p = \frac{\nu}{r^2} N_p \sigma_p \frac{\Omega}{\pi} \quad (2)$$

where ν is the number of neutrons emitted from the source per unit solid angle per second, r is the distance of the polythene film from the neutron source, N_p is the number of effective hydrogen nuclei in the film (in the case of a thin film, the total number of hydrogen nuclei in the film) and σ_p is the neutron-proton scattering cross-section for the neutron energy under consideration. A 700 keV deuteron beam bombarding a target of heavy phosphoric acid produces nearly monoenergetic neutrons of energy 3.7 MeV at 0° to the beam; for these neutrons, the n-p scattering cross-section is about $2 \times 10^{-24} \text{ cm}^2$.⁽¹⁶⁾ According to the results of Kinsey, Cohen & Dainty⁽³⁾, this reaction produces a neutron flux of 5×10^5 neutrons/ μA /second/unit solid angle in the forwards direction. Thus with a resolved deuteron beam of $25 \mu\text{A}$, ν would be 12.5×10^6 .

A one-inch diameter disc of polythene of thickness 1 mg/cm^2 contains 4.2×10^{20} hydrogen nuclei, and in the geometrical conditions of the experiment, all of these are effective in producing recoils. Hence $N_p = 4.2 \times 10^{20} \cdot \Omega$, the solid angle for collection of recoil protons, is defined by the geometry as shown in Fig. 3, and is approximately 0.02 steradian. In a typical experiment, the distance of the

polythene film from the target, r , was about 5 cm.

These figures give as the coincidence counting rate $q_p = 2.8$ per second, or about 170 per minute, which is a convenient value.

Another factor which must be borne in mind is the presence of a recoil proton background from the brass end-plate immediately below the polythene film. The counting rate from this source was determined on several occasions by rotating the radiator wheel into one of its 'blank' positions, and was generally found to be of the order of 5% of the counting rate with the polythene film. Since the hydrogen producing these recoils is likely to be absorbed into the interior of the brass to a certain extent, and is not merely a surface film, the brass will act as a 'thick' hydrogen radiator, and the recoil protons will have a continuous energy distribution. If the polythene film gives few enough recoils for this effect to constitute a large percentage of the total counting rate, the resultant spectrum would be seriously affected.

Electronic Circuits.

The electronic apparatus associated with the spectrometer is outlined in Figure 4. The three

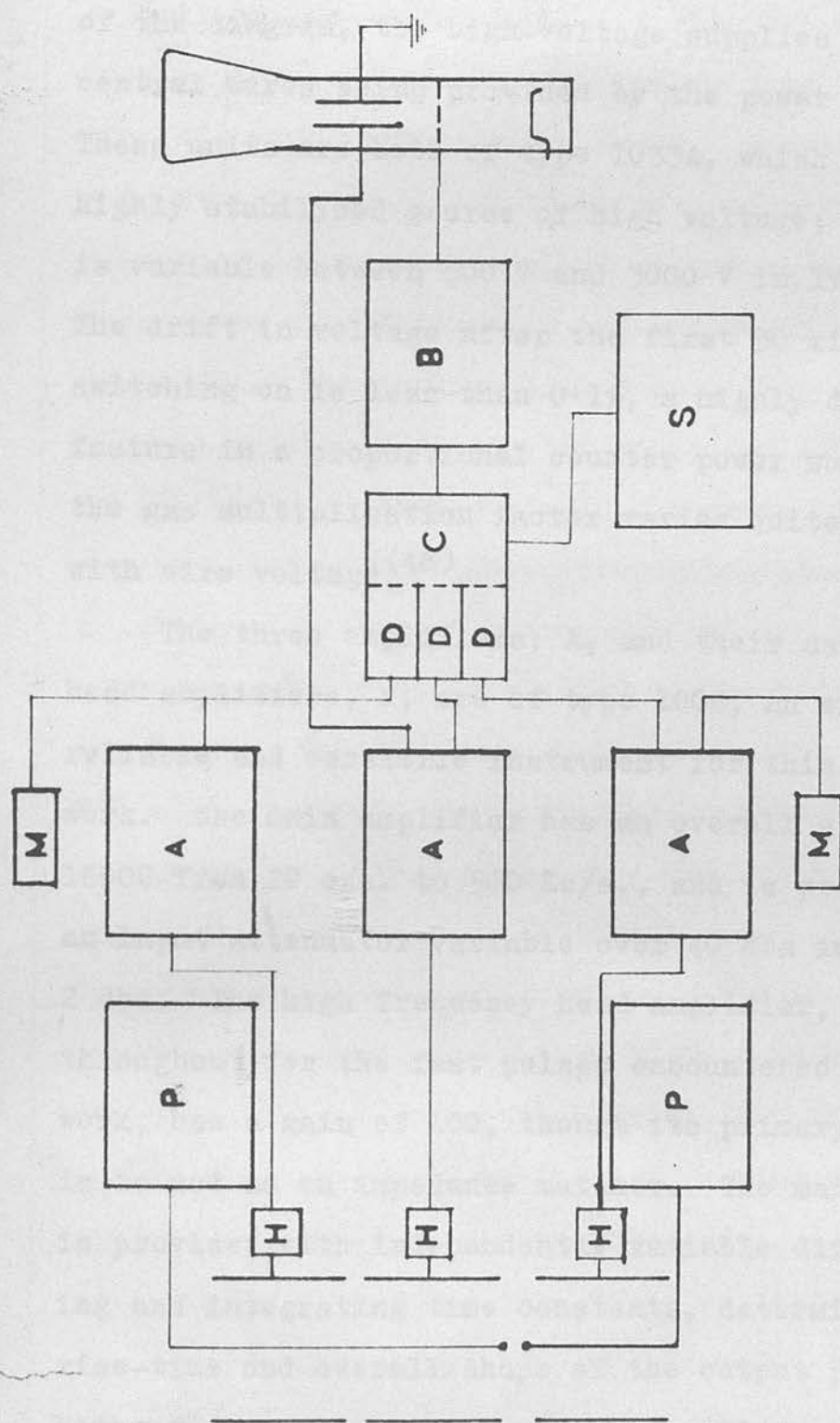


FIGURE 4. Block diagram of electronic circuits.

proportional counters are shown at the left-hand side of the diagram, the high-voltage supplies to the two central wires being provided by the power units, P. These units are both of type 1033A, which is a very highly stabilised source of high voltage; the output is variable between 500 V and 3000 V in IV steps. The drift in voltage after the first 30 minutes after switching on is less than 0.1%, a highly desirable feature in a proportional counter power supply, since the gas multiplication factor varies quite rapidly with wire voltage⁽⁴⁸⁾.

The three amplifiers, A, and their associated head amplifiers, H, are of type 1008, an extremely reliable and versatile instrument for this type of work. The main amplifier has an overall gain of 16000 from 20 c/s. to 500 Kc/s., and is provided with an input attenuator variable over 40 dbs in steps of 2 dbs. The high frequency head amplifier, used throughout for the fast pulses encountered in this work, has a gain of 100, though its primary purpose is to act as an impedance matcher. The main amplifier is provided with independently variable differentiating and integrating time constants, determining the rise-time and overall shape of the output pulses. Both of these time constants are continuously variable

between 1.5 milli-seconds and 0.2 microseconds, with a setting accuracy of $\pm 25\%$. A discussion of the problem of choosing the appropriate time constants for this work will be given later. For energy measurements, stability of gain is of paramount importance, and a great deal of attention has been devoted to this feature in the design of the amplifier. The makers claim a stability of 1% for a mains voltage variation of up to 10% and change in ambient temperature of 5°C . However, the resistors employed in the input attenuation circuit have a tolerance of 5%, so throughout the experimental work the gain of the amplifier on the middle counter was kept at the same value, except during some of the alpha-particle test experiments, where the large ionisation density necessitated the use of a lower gain. In addition there is provided an output plug

which The coincidence unit, C, used for most of the experimental work was of type 1036A, and contained three built-in discriminator units, D. The output pulses from the three amplifiers, having a rise-time of the order of 2.5 microseconds and amplitudes of up to 70 V, are fed into three separate channels for discrimination and shaping prior to reaching the coincidence unit proper. Each of these three

channels is provided with amplitude discrimination with a range from 2V to 50V for positive input pulses, variable paralysis time for the discriminator circuit from 5 to 500 microseconds, and a variable delay from 0 to 1 microsecond in steps of 0.05 microsecond. In the coincidence mixer, the outputs of the first two channels are put in coincidence with each other, with a resolving time which can be set to any of the approximate values 0.1, 0.2, 0.3, 0.4, 0.5, 1 or 2 microseconds. The resultant double coincidence pulses are then mixed with the pulses from the third channel, with a resolving time which can take any of the above values with the addition of a 4 microsecond position. The outputs of the three single channels, the double coincidence mixer and the triple coincidence mixer are all available at separate plugs, and in addition there is provided an output plug which can be switched to connect with any of these points. Also, by removing one input, it is possible to measure the counting rate of double coincidences between the first and third, and between the second and third channels respectively. The accuracy of the nominal resolving times is quoted as about $\pm 10\%$, and those times used in the experimental work have

been measured (see next section); their stability, however, is only $\pm 2\%$. The instrument produces a triple coincidence output pulse of about 16 volts amplitude and 15 microseconds width.

In the early stages of the work, before this coincidence unit became available, two experimental coincidence units were built and tested. In both cases, however, it was found to be difficult to obtain output pulses of the required amplitude and duration, together with a coincidence resolving time of the required length (at least 3 microseconds). The first unit tested was of the diode type⁽⁴⁹⁾. This was found to give pulses of the required type with a very short resolving time (less than 0.5 microsecond), and all attempts to lengthen the resolving time by comparatively simple methods seriously lengthened the pulse, as well as decreasing its amplitude.

The second coincidence unit built employed the well-known Rossi pentode circuit. This circuit was developed with a view to producing coincidence output pulses sufficiently large to produce the required degree of brightness modulation when applied to the oscilloscope grid. It consisted of three EF50 pentodes working as simple phase inverters, which

converted the positive input pulses supplied from external discriminator units to negative pulses of the same amplitude (about 12V). These pulses were fed into the control grids of three more EF50's arranged in a conventional Rossi circuit, and the coincidence output pulse brought out through an EF55 pentode acting as a cathode follower. This unit supplied output pulses of about 150V amplitude and a few microseconds long, but the resolving time of 0.6 microseconds was too short, and it was not found possible to lengthen it and still preserve the output pulse height. When the 1036A unit became available, this Rossi circuit was adapted to act as a brightness modulation unit, amplifying the coincidence pulses to the amplitude necessary for brightening the oscilloscope trace. The circuit as adapted is shown diagrammatically in Figure 5.

Output pulses from this unit are applied to the grid of the recording oscilloscope, whose D.C. voltage is just sufficient to produce a faint spot on the screen, to provide a base-line for the pulse-height analysis. The output from the amplifier connected to the middle counter is applied directly across the oscilloscope Y-plates, the normal Y-deflection amplifier being avoided, as its linearity and stability were suspect, and hence its use would nullify the

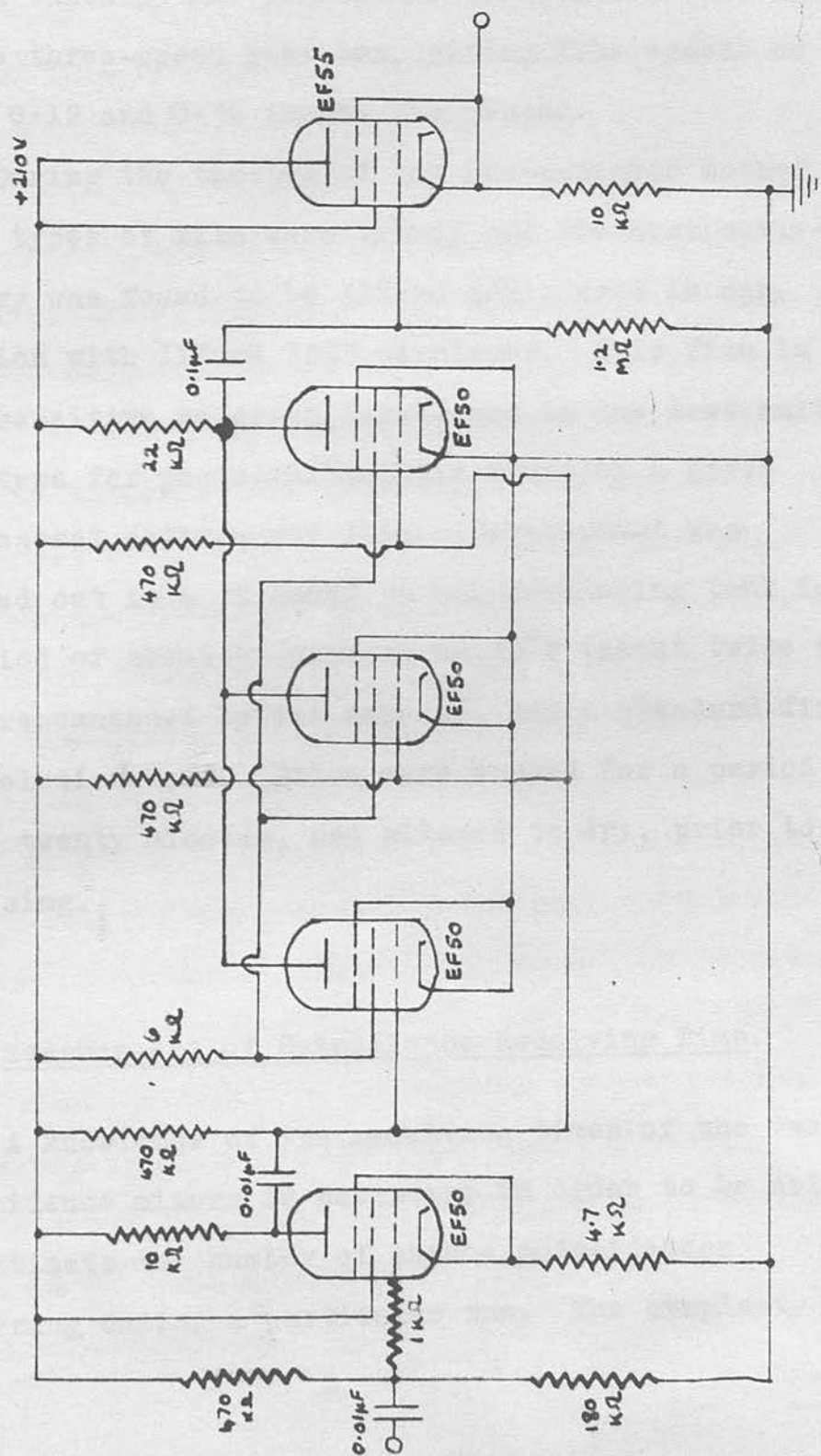


FIGURE 5. Circuit diagram of trace-brightening unit.

advantages of the 1008 amplifier. The oscilloscope used is the Cossor model 1035, in conjunction with the moving film recording camera type 1428. The camera takes 35 mm. perforated film, and is provided with a three-speed gear box, giving film speeds of 0.04, 0.12 and 0.36 inches per second.

During the testing of the photographic method, three types of film were tried, and the most satisfactory was found to be Ilford 5G91, used in conjunction with Ilford ID33 developer. This film is very sensitive to green light, and is the most suitable type for photographing the trace on a green fluorescent cathode-ray tube. Development was carried out in a standard 35 mm. developing tank for a period of about 10 minutes at 70°F (about twice the time recommended by the makers), and a standard fixing solution used. Films were washed for a period of about twenty minutes, and allowed to dry, prior to analysing.

Measurement of Coincidence Resolving Time.

A knowledge of the resolving times of the two coincidence mixers is necessary in order to be able to estimate the number of chance coincidences occurring during a particular run. The simplest

method of measuring this resolving time, τ , is to make use of the formulae for the chance coincidence rate, N_{12} , in terms of τ and the individual counting rates, N_1 , N_2 , For a double coincidence system, the formula is

$$N_{12} = 2N_1N_2\tau \quad (3)$$

Hence, by screening the two counters from each other and irradiating each one from a separate radio-active source, measurements of N_1 , N_2 and N_{12} can be made, giving a value for τ with an accuracy dependent on the statistics of the counting. This method is unsatisfactory in that for high accuracy long counting periods are necessary unless very strong sources are available, with their own obvious disadvantages. In this spectrometer, it is in any case necessary to place one of the sources inside the instrument itself in order to irradiate the upper counter, which might lead to radioactive contamination of the counter or the surroundings, and is in any case a laborious procedure.

Consequently, it was decided to examine the possibility of using the valve noise appearing at the outputs of two of the amplifiers as independent sources of random pulses for injection into the coincidence mixers. While the noise pulses are

probably somewhat different in shape from the pulses encountered in operation, the effect of the discriminators is to produce uniform pulses at the coincidence mixer input whatever the size or shape of the original pulses. The amplifiers are turned up to full gain (mean noise level about 7 to 8 volts) and the discriminator biases adjusted until suitable single counting rates are obtained. The optimum counting rate is determined by two factors: first, the desire to obtain reasonable accuracy in a short time, and secondly, the fact that at very high counting rates the simple formula above no longer holds and must be replaced by a much more complex relation. (50) In fact, in this work a high degree of accuracy in the values of the resolving times is not necessary, since only estimates of the chance coincidence rates are required. 2.70 ± 0.04 and 3.14 ± 0.03 microseconds.

both In general, this method has the great advantage over the radioactive method of permitting rapid tests of resolving time stability in fairly short times without the necessity for preparing and handling radioactive sources. It is, however, open to the objection that the two noise sources might not be completely independent. If, for example, there was present a certain amount of 50 c/s. hum at the

amplifier output, which is nearly always the case, the phase relationship between these would introduce some correlation between the two outputs which would invalidate the formula. The output hum levels of the amplifiers used for these measurements were checked, and found to be quite negligible even at full amplifier gain. The resolving time of the original Rossi coincidence unit was measured both by this method and by the radioactive source method, using two Thorium B sources, and the two values were found to agree within the statistical probable error.

As has been said above, the maximum resolving times of the two coincidence mixers in the 1036A unit were nominally 2 and 4 microseconds respectively. These values were checked from time to time by the noise method, and the mean values arrived at were respectively 2.70 ± 0.04 and 3.14 ± 0.03 microseconds, both of which differ considerably from the nominal values. A further check was provided under neutron bombardment by inserting an absorber thick enough to prevent any genuine recoil proton coincidences occurring, and measuring the counting rates in the upper and middle counters and their coincidence rate (here the pulses are provided by recoil protons from the counter cathodes). Values obtained in this way agree well

with those above.

The standard formula for the chance coincidence rate, N_{123} , in a triple coincidence system whose single counting rates are N_1 , N_2 , N_3 and resolving time τ is

$$N_{123} = 3N_1N_2N_3\tau^2 \quad (4)$$

but in the case of this instrument the conditions are such as to make the chance rate considerably greater than this. Since there are large numbers of protons recoiling from the counter walls, and since it is possible for these to produce genuine double coincidences with an adjacent counter, the chance coincidence rate is really determined by the double coincidence formula (3). Since a double coincidence between any pair of counters coinciding with a pulse in the third counter will produce a triple coincidence, the chance triple rate can be found by knowing any one of the double coincidence rates together with the single counting rate in the third counter. In the experimental work here, the double coincidence rate between the two lower counters and the single counting rate in the upper counter were measured, as this latter value provided a useful monitor of the neutron yield. In fact, the geometrical conditions make this latter case

the most likely chance coincidence source, since genuine double coincidences between the upper and middle counters must be rare, especially when an absorber is in use, and a genuine coincidence between the upper and lower counters necessarily implies a genuine triple coincidence.

The Neutron Source.

Fast neutrons are provided by bombardment of various target materials by deuterons accelerated by the 1.2 MeV Cockroft-Walton generator of the University of Edinburgh. The generator itself is of standard design, built and installed by Philips Ltd., and though the maximum voltage was nominally 1.2 MV, limitations of space made it difficult to go much beyond 800 kV. Most of the reactions investigated here were carried out with 750 keV deuterons, which gave quite satisfactory neutron yields with thick targets.

The ion source is of the Oliphant type, a simple discharge tube which has given a maximum total beam current when running on deuterium of about 150 μ A, and a maximum resolved deuteron beam of about 50 μ A. The beam of deuterons is accelerated vertically through a system of focussing electrodes into the

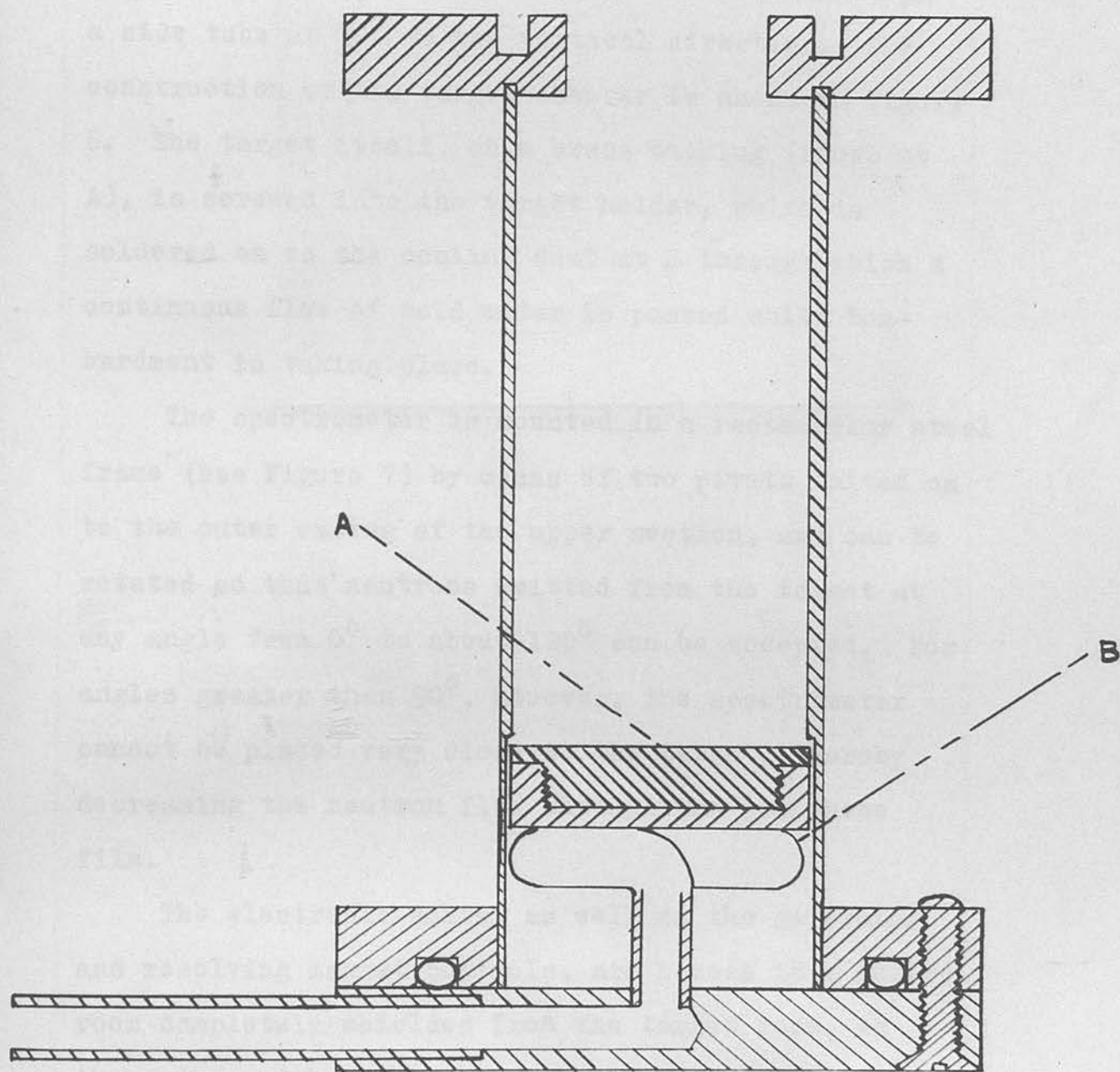


FIGURE 6. Target Construction.

target chamber, where it is analysed into its separate components by a large electromagnet, whose field strength is such as to pass the deuteron beam along a side tube at 30° to the vertical direction. The construction of the target chamber is shown in Figure 6. The target itself, on a brass backing (shown at A), is screwed into the target holder, which is soldered on to the cooling duct at B through which a continuous flow of cold water is passed while bombardment is taking place.

The spectrometer is mounted in a rectangular steel frame (see Figure 7) by means of two pivots bolted on to the outer casing of the upper section, and can be rotated so that neutrons emitted from the target at any angle from 0° to about 120° can be accepted. For angles greater than 90° , however, the spectrometer cannot be placed very close to the target, thereby decreasing the neutron flux through the polythene film.

The electronic units, as well as the generator and resolving magnet controls, are housed in a control room completely shielded from the target room, as there is a high flux of both neutrons and gamma-rays when the deuteron beam is running. The high-voltage supplies to the counters and the head amplifier power

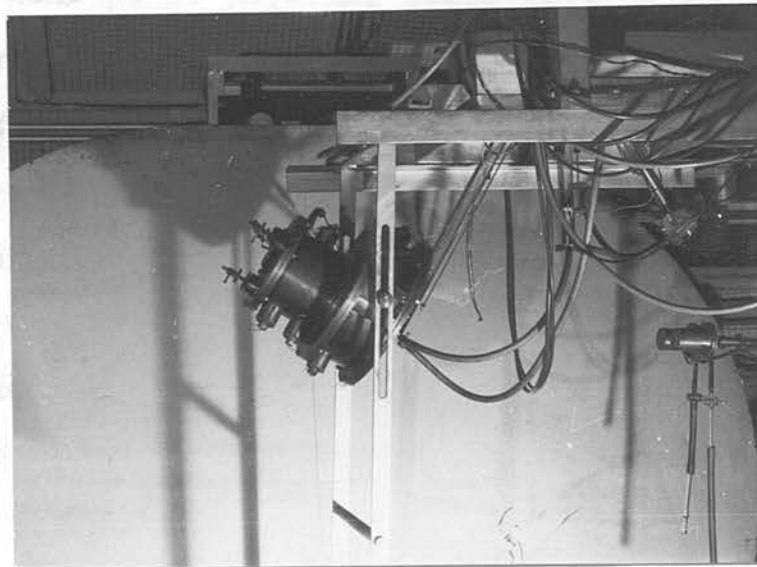


FIGURE 7. The Spectrometer mounting. The resolved deuteron beam passes down the long glass tube and strikes the target, which is partly hidden by the spectrometer. The resolving magnet is in the top right hand corner. The spectrometer is shown in the 90° position.

supplies and outputs are led into the target room by 30-foot lengths of shielded cable passing along a cable-way close to the ceiling. The head amplifiers are connected to the counter cathodes by very short lengths of coaxial cable, and are suspended from the spectrometer frame by lengths of string, a method of suspension which avoids any microphonic vibration, to which the head amplifiers are extremely sensitive. the proportionality of the three counters, and especially of the middle one, and the linearity of the amplifier response and of the deflection of the oscilloscope beam.

The Proportional Counters.

Three properties determine the proportionality or otherwise of a counter of a given design: the nature of the gas in the counter, the gas pressure, and the voltage between the central wire and the cathode. The choice of the gas to be used in the instrument described is partly determined by the fact that gas recoils resulting from neutron bombardment must not have a range long enough to register a triple coincidence. Since the maximum recoil energy imparted to a nucleus of mass M recoiling from a neutron of energy E_n is given by



CHAPTER IV.

TESTING OF THE INSTRUMENT.

During the course of the experimental work, routine tests of the performance of all the units were carried out from time to time, in order to prevent the occurrence of any systematic errors. The principal properties requiring frequent checking are the proportionality of the three counters, and especially of the middle one, and the linearity of the amplifier response and of the deflection of the oscilloscope beam.

The Proportional Counters.

Three properties determine the proportionality or otherwise of a counter of a given design: the nature of the gas in the counter, the gas pressure, and the voltage between the central wire and the cathode. The choice of the gas to be used in the instrument described is partly determined by the fact that gas nuclei recoiling from neutron bombardment must not have a range long enough to register a triple coincidence. Since the maximum recoil energy imparted to a nucleus of mass M recoiling from a neutron of energy E_n is given by

$$E_M = \frac{4M}{(M+1)^2} E_n, \quad (5)$$

this means that the gas must be fairly heavy, and rules out the use of hydrogen or helium or a compound containing hydrogen, such as methane. It was decided from the start to use argon as the principal gas, since its properties as a proportional counter gas are well-known, and it satisfies the above mass condition. As an example, a neutron of 4 MeV energy will produce argon recoils with a maximum energy of 400 keV, for which the range is about 1 mm. in standard air, or about 0.5 cm. in argon at a pressure of 15 cms. of mercury. Argon itself, however, is not very suitable as a proportional counter gas, since it has been found that at fairly low pressures the gas multiplication changes so rapidly with wire voltage that the counter is not very stable, and great care has to be taken in operation. The addition of a small amount of carbon dioxide, however, has been found to make the dependence of gas multiplication on voltage much less critical, and as the nuclei of both carbon and oxygen are sufficiently heavy to prevent long-range gas recoils occurring, this procedure was adopted here.

In order to test the counter properties, a small

hole was drilled in the end-plate of the spectrometer and covered with a mica window of thickness 1 mg/cm^2 , which allowed the passage of alpha-particles into the sensitive region. The alpha-particle source was in the form of a short length of brass screw with a flat and highly polished end. This screw was held in a short brass barrel with its polished end protruding, and the base of the barrel was attached to the inner surface of a shallow glass dish (in fact, the lower portion of a small beaker). The edge of the glass dish was provided with a brass flange, which rested on the base-plate of the spectrometer in such a way that the radioactive source was directed centrally down the hole in the plate. The sources were of thorium B, and were prepared by recoil collection of thorium A nuclei on the end of the small screw in a pot containing thoron gas. The thorium A decays by alpha-particle emission with a half-life of 0.14 secs. to thorium B, a beta-emitter, which yields thorium C with a half-life of 10.6 hours. Thorium C has two possible modes of decay, alpha-emission leading to Th C", or beta-emission giving Th C'. These two in turn decay by, respectively beta- and alpha-emission, leading to Th D, an isotope of lead. Hence the source, whose effective half-life is that of Th B, i.e. 10.6 hours, yields the alpha-particles of both

Th C and Th C', the respective energies and relative intensities of which are well-known. This type of source is ideal for testing counter proportionality.

The simplest method of testing a single counter is to pass the output of the amplifier through a pulse-height discriminator directly into a scaling unit, and to plot curves of counting rate against discriminator bias setting. These are known as 'bias curves'. During the period of testing, bias curves were plotted with many different gas mixtures and Wire voltages before the operating conditions were finally decided upon. The results of a typical series of such tests are shown in Figure 8; in fact, the conditions under which these curves were obtained were those under which most of the neutron work was later carried out. The gas used was a mixture of 90% cylinder argon and 10% carbon dioxide, with the common wire of the two smaller counters at 800V, and that of the larger counter at 900V. Cylinder argon was found to be sufficiently pure for this purpose not to require the use of dry ice or liquid air traps in the filling line.

As can be seen from the diagram, the bias curves consist of two well-marked plateaux, with reasonably sharp drops at the high-voltage ends; this is what

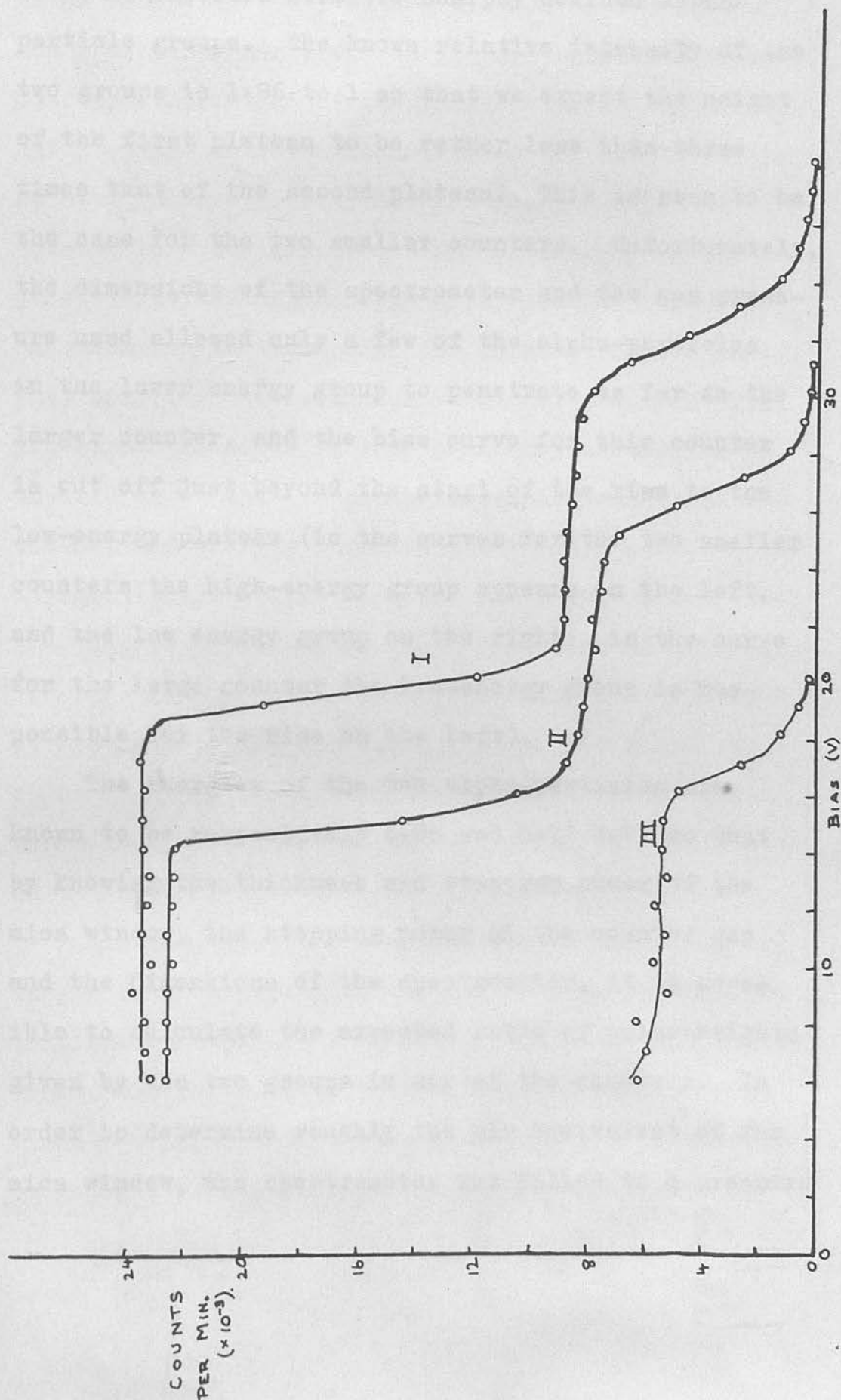


FIGURE 8. Bias curves of the ThC + C' alpha-particles from the three counters.

is to be expected from two sharply defined alpha-particle groups. The known relative intensity of the two groups is 1.86 to 1 so that we expect the height of the first plateau to be rather less than three times that of the second plateau. This is seen to be the case for the two smaller counters. Unfortunately, the dimensions of the spectrometer and the gas pressure used allowed only a few of the alpha-particles in the lower energy group to penetrate as far as the larger counter, and the bias curve for this counter is cut off just beyond the start of the rise to the low-energy plateau (in the curves for the two smaller counters the high-energy group appears on the left, and the low energy group on the right; in the curve for the large counter the low-energy group is responsible for the rise on the left).

The energies of the two alpha-particles are known to be respectively 6.08 and 8.78 MeV, so that by knowing the thickness and stopping power of the mica window, the stopping power of the counter gas and the dimensions of the spectrometer, it is possible to calculate the expected ratio of pulse-heights given by the two groups in any of the counters. In order to determine roughly the air equivalent of the mica window, the spectrometer was filled to a pressure

of 50 cms. of mercury with a mixture of 90% argon and 10% carbon dioxide, and irradiated with a Th B source. The output of the large counter (that farthest from the source) was amplified and displayed on an oscilloscope screen, and the gas pressure was reduced in intervals of 0.5 cm. of mercury until pulses from the high-energy group just appeared on the screen. At this point the alpha-particles are just entering the sensitive volume of the counter, and since the depth of this point beyond the window, the length of the air gap between the source and the window, and the gas stopping power are all known, the air equivalent of the mica can readily be calculated.

The required gas pressure was found to be approximately 34.5 cms. of mercury, yielding a rough value of 0.9 cms. as the air equivalent of the mica. This is in good agreement with the expected value of about 1 cm. from the nominal thickness of the mica of 1.5 mg/cm^2 .

Assuming that the stopping power of the mixture of gas used is approximately the same as that of the same pressure of air (a relation which is very nearly true), the expected pulse-height ratio of the two groups in the first counter traversed can be shown to be $7.5 : 4.5$, and that in the second counter to be

7.5 : 4. Both of these were found to be verified, within the limits of accuracy of the measurements.

A rather more accurate test of the proportionality of the counters is afforded by plotting a series of such curves for different wire voltages, the gas filling being kept constant. If the ratio of the pulse-heights remains the same, the counter may be assumed to be operating in the proportional region. This procedure was carried out in the case of the middle counter, and with a filling of 15 cms. of mercury pressure, the most reliable operating region was found to lie between 700V and 900V on the central wire. 800V was chosen as the operating potential for this counter. The bias curves for the other two counters shown in Figure 8 were then plotted in order to verify approximately their proportionality. The voltage on the large counter wire was set at 910V, approximately the value indicated by the relation on p. 28 to counteract the larger cathode diameter.

On development of the photographic method, it was decided to test the proportionality of the middle counter again, using triple coincidences to brighten the oscilloscope beam as described previously, and photographing the pulses appearing at the second amplifier output. Since only a few of the lower

energy group of alpha-particles penetrate to the third counter, however, the height of the high-energy peak in the pulse-height distribution was expected to be disproportionately high, but the relative position of the two peaks should agree with the calculated ratio of the energy losses of the two groups. The pulse-height distribution obtained is shown in histogram form in Figure 9. As can be seen, the height of the low-energy (high pulse-height) peak is very much less than the true value.

Testing of Amplifier and Deflection Linearity.

The linearity of the amplifier connected to the middle counter, and of the deflection of the spot on the recording oscilloscope can readily be checked using the photographic method. In order to do this, a standard pulse generator is used; this gives pulses of amplitude approximately 1 volt, with variable rise and decay times. These are fed at high recurrence frequency into a radio frequency attenuation network, whose output is passed into the head amplifier. The output of the main amplifier is connected to all three input terminals of the coincidence unit, so that each pulse produces a brightened trace on the oscilloscope screen. A time-base of

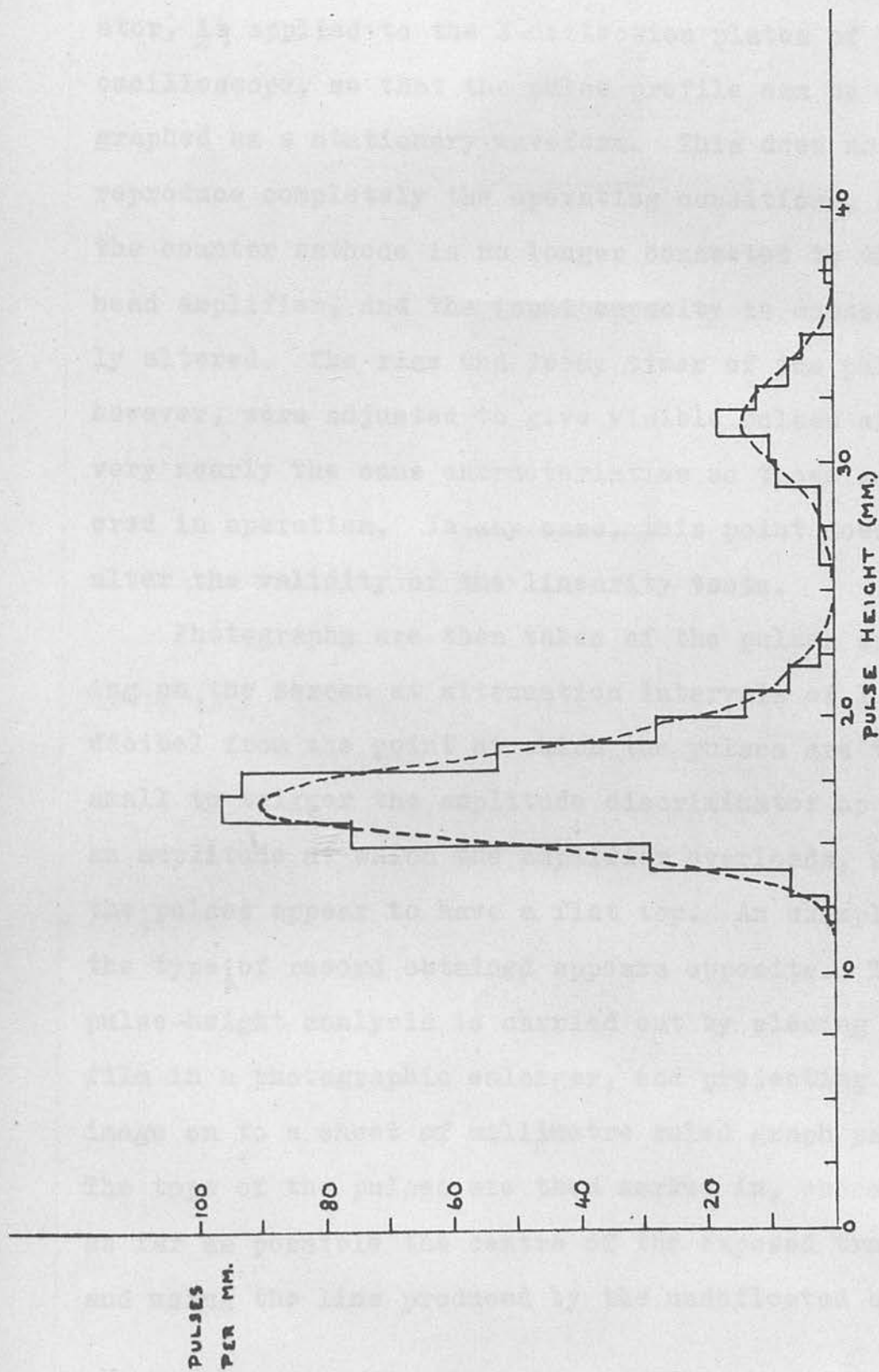


FIGURE 9. Pulse-height distribution of the ThC + C' alpha-particles.

50 microseconds sweep, triggered by the pulse generator, is applied to the X-deflection plates of the oscilloscope, so that the pulse profile can be photographed as a stationary waveform. This does not reproduce completely the operating conditions, since the counter cathode is no longer connected to the head amplifier, and the input capacity is consequently altered. The rise and decay times of the pulses, however, were adjusted to give visible pulses of very nearly the same characteristics as those encountered in operation. In any case, this point does not alter the validity of the linearity tests.

Photographs are then taken of the pulses appearing on the screen at attenuation intervals of 1 decibel from the point at which the pulses are too small to trigger the amplitude discriminator up to an amplitude at which the amplifier overloads, and the pulses appear to have a flat top. An example of the type of record obtained appears opposite. The pulse-height analysis is carried out by placing the film in a photographic enlarger, and projecting the image on to a sheet of millimetre ruled graph paper. The tops of the pulses are then marked in, choosing as far as possible the centre of the exposed trace, and using the line produced by the undeflected beam

as a base-line. The set of pulses has been used in the test to determine, using a constant reference voltage, the setting the flat-topped pulses at a fixed distance above the base-line; this is possible since the voltage for which the amplifier output is a constant property. The resultant pulses are of the height of the original pulses, and the obtained plotted log-log curves are shown in Figure 10. Such a curve is shown in Figure 10. It is noted that the linearity is not very good at low power.

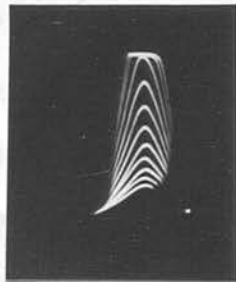
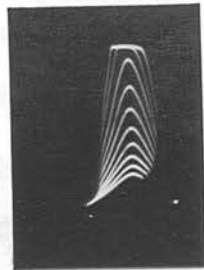


FIGURE 10. Typical test pulses. The upper set are at 2 db. intervals, and the lower set at intermediate 1 db. settings.

for low frequencies, the limit of pulses used is about 100 milliseconds. A particular example of the rise-time of 10 milliseconds, or 10 milliseconds, is shown in Figure 11.

as a base-line. This simple method of analysis has been used in all the neutron work to be described, using a constant enlarger magnification, obtained by setting the flat-topped overload pulses at a fixed distance above the base-line; this is justifiable, since the voltage for which the amplifier overloads is a constant property of the electronic circuit. The resultant pulse-heights are expressed as ratios of the height of the smallest pulse, and the values obtained plotted logarithmically against the corresponding attenuator settings. A typical example of such a curve is shown in Figure 11. It can be seen that the linearity is not very good at low pulse-height, but in any case this region was not used in any of the neutron work, since the energy resolution for low ionisation density is very poor. The lower limit of pulses used is shown by the arrow. In the particular example shown, the input pulses had a rise-time of 10 microseconds and decay-time of 1 millisecond, approximately.

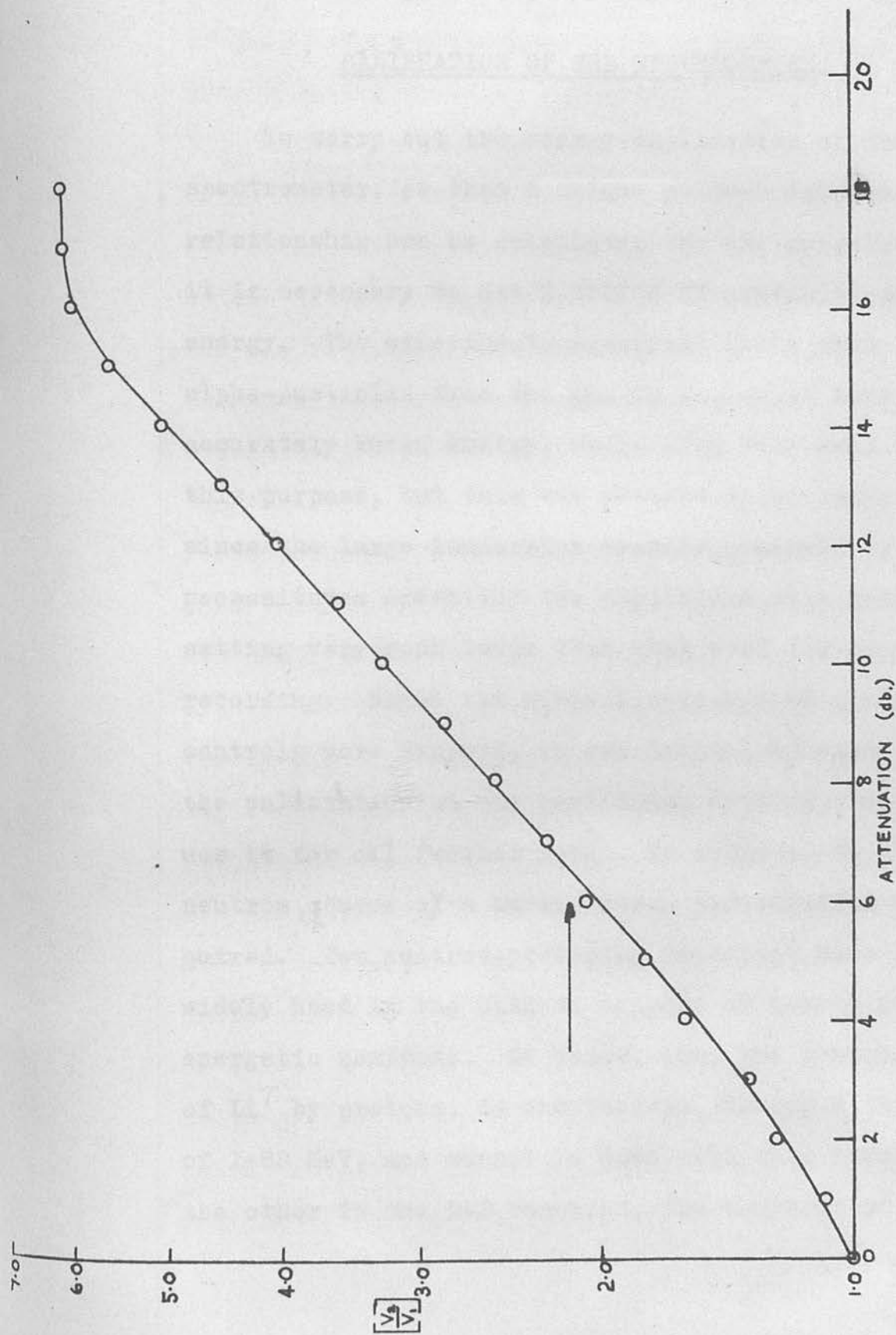


FIGURE 11. Amplifier and spot deflection linearity test.

CHAPTER V.

CALIBRATION OF THE SPECTROMETER.

To carry out the energy calibration of the spectrometer, so that a unique pulse-height-energy relationship can be calculated for any experiment, it is necessary to use a source of particles of known energy. The experiments described above with the alpha-particles from ThC and Th C', which have an accurately known energy, could have been used for this purpose, but this was thought to be undesirable, since the large ionisation density produced by them necessitates operating the amplifiers at a gain setting very much lower than that used for proton recording. Since the nominal settings of the gain controls were suspect, it was decided to carry out the calibration at one particular setting, and to use it for all further work. In order to do this, a neutron source of a known energy distribution is required. Two neutron-producing reactions have been widely used in the past as sources of nearly mono-energetic neutrons. Of these, one, the bombardment of Li^7 by protons, is endothermic, having a threshold of 1.88 MeV, and cannot be used with this apparatus; the other is the D-D reaction, the bombardment of

deuterium by deuterons, which has a positive Q-value of 3.25 MeV, and produces quite a high neutron yield even with low deuteron bombarding voltages.

Before presenting the results of the neutron work, some discussion of the operating conditions of the electronic apparatus would be desirable. The action of the proportional counter is such that almost all the ionisation responsible for the output pulse is formed within a very short distance of the positive central wire, since it is only in the neighbourhood of the wire that the field strength becomes great enough for secondary electrons to be produced. Hence, initially there will be a large positive space-charge around the wire, so that the pulse produced by the arrival of the electrons at the wire will be very small, and will occur within a very short time after the formation of the initial ionisation. By far the greater part of the pulse is produced by the motion of the positive ions towards the cathode, relatively a much slower effect, so that the total length of the pulse produced may be of the order of 100 microseconds or more. However, the initial rise of the pulse is quite rapid, so that the pulse reaches half its final height in a time of the order of 1% of the total pulse length. Differentiation of this portion of the pulse

by the input network of the amplifier can thus be made to provide short microsecond pulses, suitable for fast counting, although they are generated by positive ion movement. Very sharp differentiation by the amplifier is possible without affecting the proportionality, since the form of the pulse profile is the same wherever the initial ionisation is produced in the counter (if we neglect the effects of straggling).

The shape and height of the output pulse from the amplifier are also determined by the value of the integration time constant, which determines the high-frequency cut-off of the amplifier, and hence the rise-time of the output pulse for a unit step function input. It has been shown that for an optimum value of the signal/noise ratio, this time-constant should have the same value as the differentiation time-constant.

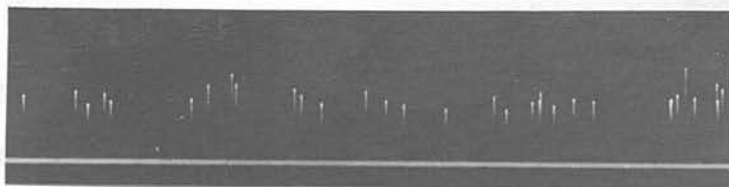
As regards the most suitable value of time-constant to use with this apparatus, two considerations must be borne in mind. Firstly, there is an inevitable delay of a few tenths of a microsecond between the appearance of a pulse at the output of the middle counter amplifier and the appearance of the trace brightening pulse (if a triple coincidence has occurred)

at the grid of the cathode ray tube. Thus if the pulse were very sharp (i.e. the differentiation time constant were very small), the brightening would not appear until the pulse was past its peak, and accurate pulse-height analysis would be impossible. Secondly, if the coincidence resolving time is less than the rise-time of the pulses, there is a possibility that one, or two, of the discriminators will not trigger in time to produce a coincidence, and genuine coincidences will be lost.

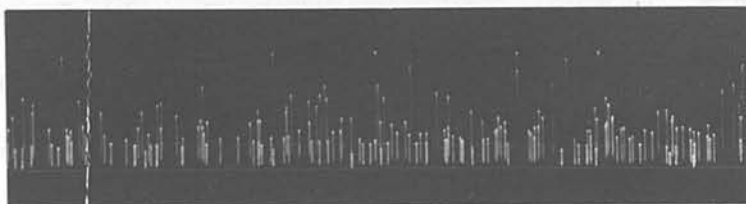
These conditions set the choice of time-constants within fairly narrow limits: the rise-time of the pulses must not be so short that the brightening pulse arrives too late, nor so long that a ridiculously high coincidence resolving time is necessary.

Some experiments were carried out to determine the optimum settings. It was found that with a nominal setting of 10 microseconds for both constants, the output pulses had broad tops, and the brightening appeared almost solely at the top, so that bright spots with very short tails were produced. This would be ideal from the point of view of pulse-height analysis, but measurement of the pulse rise-time on an oscilloscope with a calibrated time-base gave a value of approximately seven microseconds. As a

coincidence resolving time of this magnitude was not possible with the coincidence unit in use, and would in any case have given a very high chance coincidence rate, it was decided not to use this value. It was found that at a nominal setting of five microseconds for both constants, the output pulse rise-time was about 2.5 microseconds. Since the measured resolving times of the two coincidence mixers were 2.7 and 3.1 microseconds respectively (see Chapter III), this value satisfies the second of our conditions. Examination of the pulses under coincidence brightening showed that the top of the pulse was visible whatever its height, as well as the greater part of the down sweep (the test pulses shown in Figure 10 are of the same form as the pulses produced by recoil protons.) On films taken under operating conditions (see opposite), the pulses appear with long 'tails' but clearly defined tops, which make analysis relatively easy, although when the coincidence counting rate is high there is a tendency for two pulses of different heights to be superimposed, which might cause difficulty in determining the true height of the lower pulse. (This phenomenon is a superimposition merely of the images of the pulses on the film, not of the pulses at the amplifier output, an effect which occurs



(a) 10 microseconds time-constants.



(b) 5 microseconds time-constants.

FIGURE 12. Typical sections of films obtained under operating conditions.

appreciably only with very high counting rates).

The choice of amplifier gain is not very critical, provided that, as mentioned above, the gain is kept at the same value throughout the experimental work. Since the cathode ray tube screen, however, provides a limited range of deflection, it was thought desirable to confine the smaller pulses (i.e. those corresponding to low ionisation density, for which the energy resolution is inherently poor) to the region of spot deflection in which the linearity is least good, and to leave the linear deflection portion for those pulses corresponding to protons with residual ranges of 10 cms. of standard air or less. With the counter filling and wire voltage of the middle counter already decided upon (see Chapter IV), this condition was found to be realised approximately with a nominal input attenuation on the main amplifier of 16 dbs.

The optimum gain setting for the other amplifiers is decided by the desirability of obtaining output pulses from all three amplifiers of the same order of height, in order to trigger all the discriminators simultaneously. While this is obviously an impossible condition when a heteroenergetic group of recoil protons is present, it is possible to fulfil it in part by operating the large counter amplifier at a

slightly higher gain than the other two, since it records the least dense section of the proton track.

The operating conditions of the middle counter and its associated equipment may now be summarised as follows:

Counter filling : 90% argon, 10% carbon dioxide at a total pressure of 15 cms. mercury.

Wire voltage : 800 V.

Differentiation time constant : 5 microseconds.

Integration " " : 5 " of 110°.

Coincidence resolving time (1) : 2.7 "

" (2) : 3.1 "

The D-D Reaction

It was decided, then, to investigate the neutrons produced in the D-D reaction with a view to both energy calibration and the determination of the line-shape produced by the spectrometer for a monoenergetic neutron source. The reaction can be written as



and the known mass-values for H^2 , He^3 and the neutron give the formula (see appendix 1)

$$3.017Q = 4.026 E_n - 1.002 E_d - 2(2.033 E_d E_n)^{1/2} \cos \theta \quad (6)$$

for the energy of the emitted neutron, E_n , at angle θ to the deuteron beam of energy E_d . Q is the energy released in the reaction. The most reliable value for Q is probably that found by Livesey & Wilkinson,⁽²⁷⁾ using the photographic plate method, and quoted as 3.25 ± 0.02 MeV; this was the value adopted throughout this investigation. It can be shown ⁽⁵¹⁾ that at a particular value of θ , the dependence of E_n on the deuteron energy vanishes, so that a thick target can be used to produce a nearly monoenergetic neutron beam. This angle is in the neighbourhood of 110° , and this value was chosen for the calibration experiments. Unfortunately, the dimensions of the spectrometer and the geometry of the target chamber necessitated the polythene radiator being some distance away from the target, so that the recoil proton counting rate was rather low. Even so, quite good statistics were obtained in 15 minutes running time. The accelerating voltage used was 750 kV, and the resolved deuteron beam current about $25 \mu\text{A}$. The target was of heavy phosphoric acid, made by forming a thick paste of phosphorus pentoxide with a few drops of heavy water. This type of target is very easily prepared, and gives quite a high neutron yield, though the yield falls off quite rapidly with time, as the

heavy water evaporates under the intense heating of the deuteron beam.

Analysis of the pulse-height distribution was carried out as outlined previously, the magnification of the enlarger being set so that pulses which overloaded the amplifier, producing dense spots on the film, lay midway between 32 and 33 mm. above the baseline. This magnification was used throughout the remainder of the experimental work. The pulse-height distribution obtained in this way is shown in Figure 13, and can be seen to consist of one symmetrical group and a long tail of larger pulses, i.e. pulses corresponding to lower energy protons. The same effect appears in the results of Powell⁽²²⁾ on this reaction, and is almost certainly due to neutrons scattered from the material surrounding the target.

In order to calibrate the spectrometer from these results, it is necessary to calculate the energy spectrum of recoil protons to be expected under the conditions of the experiment, taking into account the geometry of the instrument, the thickness of the polythene film and the known features of the reaction. Firstly, it will be of interest to calculate the recoil proton spectrum produced by a truly monoenergetic neutron beam bombarding an infinitely thin polythene

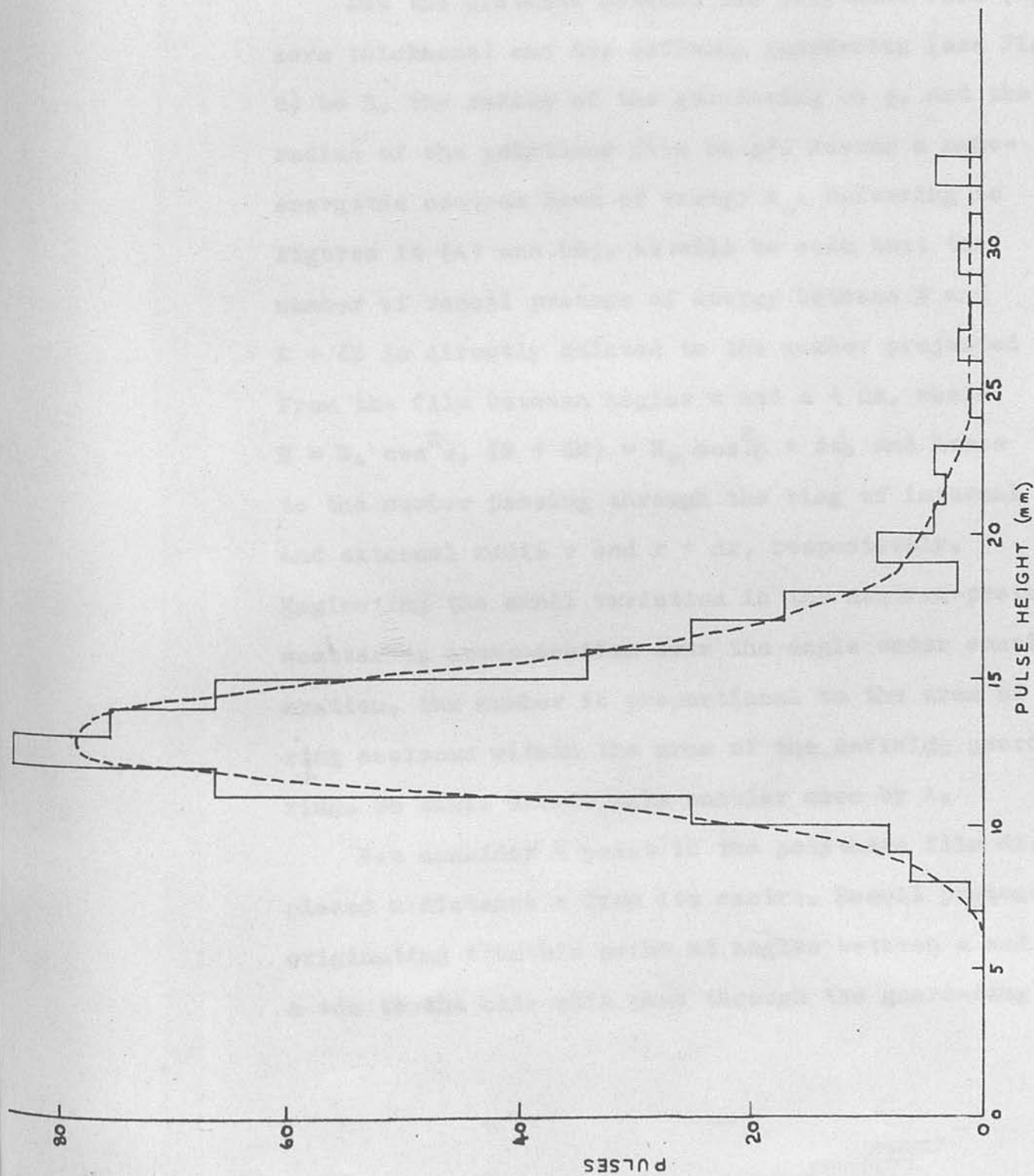


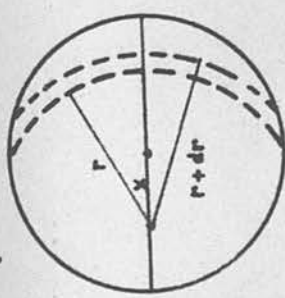
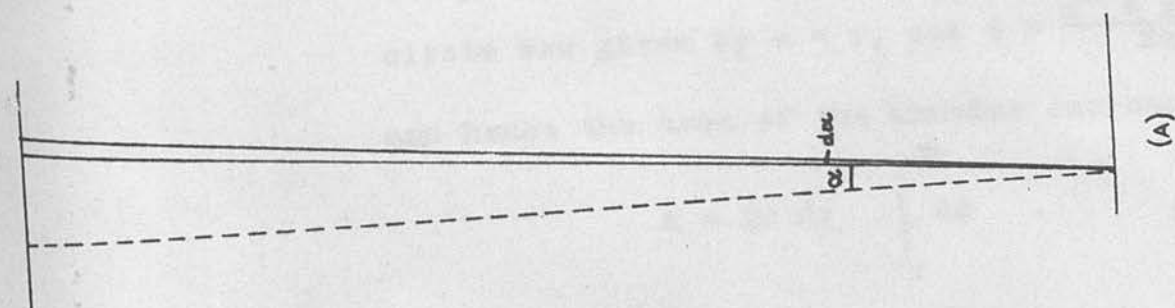
FIGURE 13. Pulse-height distribution from the D-D reaction at 1100 to the beam.

film, i.e. the effect of the geometrical conditions alone.

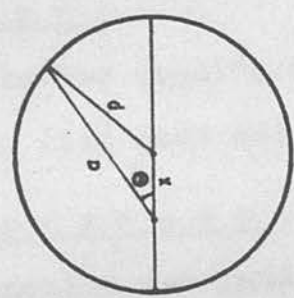
Recoil Spectrum from Monoenergetic Neutron Beam.

Let the distance between the polythene film (of zero thickness) and the defining guard-ring (see Fig. 3) be R , the radius of the guard-ring be p , and the radius of the polythene film be p' . Assume a monoenergetic neutron beam of energy E_0 . Referring to Figures I4 (A) and (B), it will be seen that the number of recoil protons of energy between E and $E + dE$ is directly related to the number projected from the film between angles α and $\alpha + d\alpha$, where $E = E_0 \cos^2 \alpha$, $(E + dE) = E_0 \cos^2(\alpha + d\alpha)$, and hence to the number passing through the ring of internal and external radii r and $r + dr$, respectively. Neglecting the small variation in the neutron-proton scattering cross-section over the angle under consideration, the number is proportional to the area of the ring enclosed within the area of the defining guard-ring. We shall denote this annular area by A .

Now consider a point in the polythene film displaced a distance x from its centre. Recoil protons originating from this point at angles between α and $\alpha + d\alpha$ to the axis will pass through the guard-ring



(B)



(C)

FIGURE 14.

plane at distances between r and $r + dr$ from the point vertically above the point of origin, where $r \approx aR$ (since a is small).

Now three cases must be considered:

(i) $x < p - r$:

All protons recoiling between a and $a + da$ are recorded, and hence A is the whole area of the annulus of radii r , $r + dr$, i.e.,

$$A = 4\pi r dr \quad . \quad . \quad . \quad (7)$$

(ii) $x > p + r$:

By similar considerations, $A = 0 \quad . \quad . \quad (8)$

(if $p' < p$, (ii) does not arise for any value of r).

(iii) $p - r < x < p + r$:

The annulus now intersects the guard-ring circle. Consider the point in the guard-ring plane vertically above the point of origin of the recoil protons. The equation of the guard-ring circle with respect to this point as origin is (see Fig. I4(C))

$$\cos \psi = \frac{x^2 + a^2 - p^2}{2ax} \quad . \quad . \quad (9)$$

The points where the circle of radius r meets this circle are given by $a = r$, $\cos \psi = \frac{x^2 + r^2 - p^2}{2rx}$,

and hence the area of the annulus enclosed is

$$A = 2r dr \int_0^{\psi_1} d\psi \quad . \quad . \quad (10)$$

where $\cos \psi_1 = \frac{x^2 + r^2 - p^2}{2rx}$, i.e.,

$$A = 2r \, dr \, \arccos \frac{x^2 + r^2 - p^2}{2rx} \quad . \quad . \quad . \quad (II)$$

If now there are emitted from the polythene film n protons per cm^2 per sec. per unit solid angle in direction around ψ to the axis ($\psi \ll 1$), then through area A at distance R from the film there pass $2\pi x \, dx \, n \frac{A}{4\pi R^2}$ protons per second which originate in an annulus of the film of area $2\pi x \, dx$.

From the values of A above, we can now calculate the rate of passage, Q , of protons of lateral spread between r and $r + dr$ through the guard-ring.

(i) if $r < p - p'$,

$$Q = \frac{n}{2R^2} \cdot 4\pi r \, dr \cdot \frac{p'^2}{2} = \pi p'^2 \frac{n}{R^2} r \, dr \quad (12)$$

protons per sec.

(ii) if $p - p' < r < p$,

$$Q = \pi(p - r)^2 \frac{n}{R^2} r \, dr + \frac{n}{R^2} r \, dr \int_{p-r}^{p'} x \arccos \frac{x^2 + r^2 - p^2}{2rx} dx \quad (13)$$

protons per sec.

(iii) if $p < r < p + p'$,

$$Q = \frac{n}{R^2} r \, dr \int_{r-p}^{p'} x \arccos \frac{x^2 + r^2 - p^2}{2rx} dx \quad (14)$$

protons per sec.

If this distribution is denoted by the function $N_1(r)$, the recoil proton energy spectrum $N_2(E)$ is given by

$$N_2(E) = N_1(r) \left| \frac{dr}{dE} \right| \quad . \quad . \quad . \quad (I5)$$

Since the acceptance angle is quite small, we can write $r = aR$, and hence

$$dr = R da \quad . \quad . \quad . \quad (I6)$$

Also, the dynamics of the neutron-proton collision lead to the relation

$$E = E_0 \cos^2 a,$$

and hence

$$\begin{aligned} dE &= 2E_0 \sin a \cos a da \\ &= 2E_0 a da, \end{aligned}$$

since $\sin a \approx a$ and $\cos a \approx 1$.

Hence

$$\left| \frac{dr}{dE} \right| = \frac{R}{E_0} \frac{1}{2a} \quad . \quad . \quad . \quad (I7)$$

and

$$\left| \frac{r dr}{dE} \right| = \frac{R^2}{2E_0} \quad . \quad . \quad . \quad (I8)$$

Substituting these relations in (I2), (I3) and (I4) above we have, apart from a numerical factor

(i) for $I > E/E_0 > \cos^2 \left(\frac{p - p'}{R} \right)$ (say $E_0 > E > E_1$)

$$N_2(E) = \frac{n}{2E_0} \pi p'^2 \quad (19)$$

(ii) for $\cos^2 \left(\frac{p - p'}{R} \right) > E/E_0 > \cos^2 \left(\frac{p}{R} \right)$ (say $E_1 > E > E_2$)

$$N_2(E) = \frac{n}{2E_0} \left[\pi (p - r)^2 + \int_{p-r}^{p'} x \arccos \frac{x^2 + r^2 - p^2}{2rx} dx \right] \quad (20)$$

(iii) for $\cos^2 \left(\frac{p}{R} \right) > E/E_0 > \cos^2 \left(\frac{p + p'}{R} \right)$ (say $E_2 > E > E_3$)

$$N_2(E) = \frac{n}{2E_0} \int_{r-p}^{p'} x \arccos \frac{x^2 + r^2 - p^2}{2rx} dx \quad (21)$$

The dimensions of p , p' , and R are respectively 1.5, 1.3 and 14.3 cms., and hence

$$E_1/E_0 = \cos^2 \left(\frac{p - p'}{R} \right) = 0.9998$$

$$E_2/E_0 = \cos^2 \left(\frac{p}{R} \right) = 0.9890$$

$$E_3/E_0 = \cos^2 \left(\frac{p + p'}{R} \right) = 0.9621.$$

The function $N_2(E)$ has been evaluated for values of E/E_0 between 1.00 and 0.962, at which point it vanishes. The integrals were determined numerically using the well-known Gregory formula. The results are tabulated on page 77, and the line-shape plotted against E/E_0 in Fig. 15.

The width of the peak in Fig. 15 at half-height, which can be taken as a measure of the resolution of an ideal instrument of this design using an infinitely thin radiator, is seen to be $E/E_0 = 0.004$, i.e. the energy spread is 0.4% of the incident neutron energy

TABLE II

| E/E_0 | r | Integration range | $\frac{\text{Integral}}{\pi(p-r)^2}$ | $\frac{\pi p^2 \text{ or } r^2}{\pi(p-r)^2}$ | $\frac{N_2(E)}{N_2(E_0)}$ |
|---------|------|----------------------|--------------------------------------|--|---------------------------|
| 1.000 | 0 | (i) | 0 | 5.31 | 5.31 |
| 0.999 | 0.44 | (ii) | 0.23 | 3.52 | 3.75 |
| 0.995 | 1.00 | (ii) | 0.91 | 0.78 | 1.69 |
| 0.990 | 1.43 | (ii) | 1.12 | 0.02 | 1.14 |
| 0.985 | 1.74 | (iii) | 0.80 | | 0.80 |
| 0.980 | 2.02 | (iii) | 0.53 | | 0.53 |
| 0.975 | 2.27 | (iii) | 0.30 | | 0.30 |
| 0.970 | 2.49 | (iii) | 0.13 | | 0.13 |
| 0.965 | 2.70 | (iii) | 0.02 | | 0.02 |
| 0.962 | 2.80 | (iii) | 0 | | 0 |

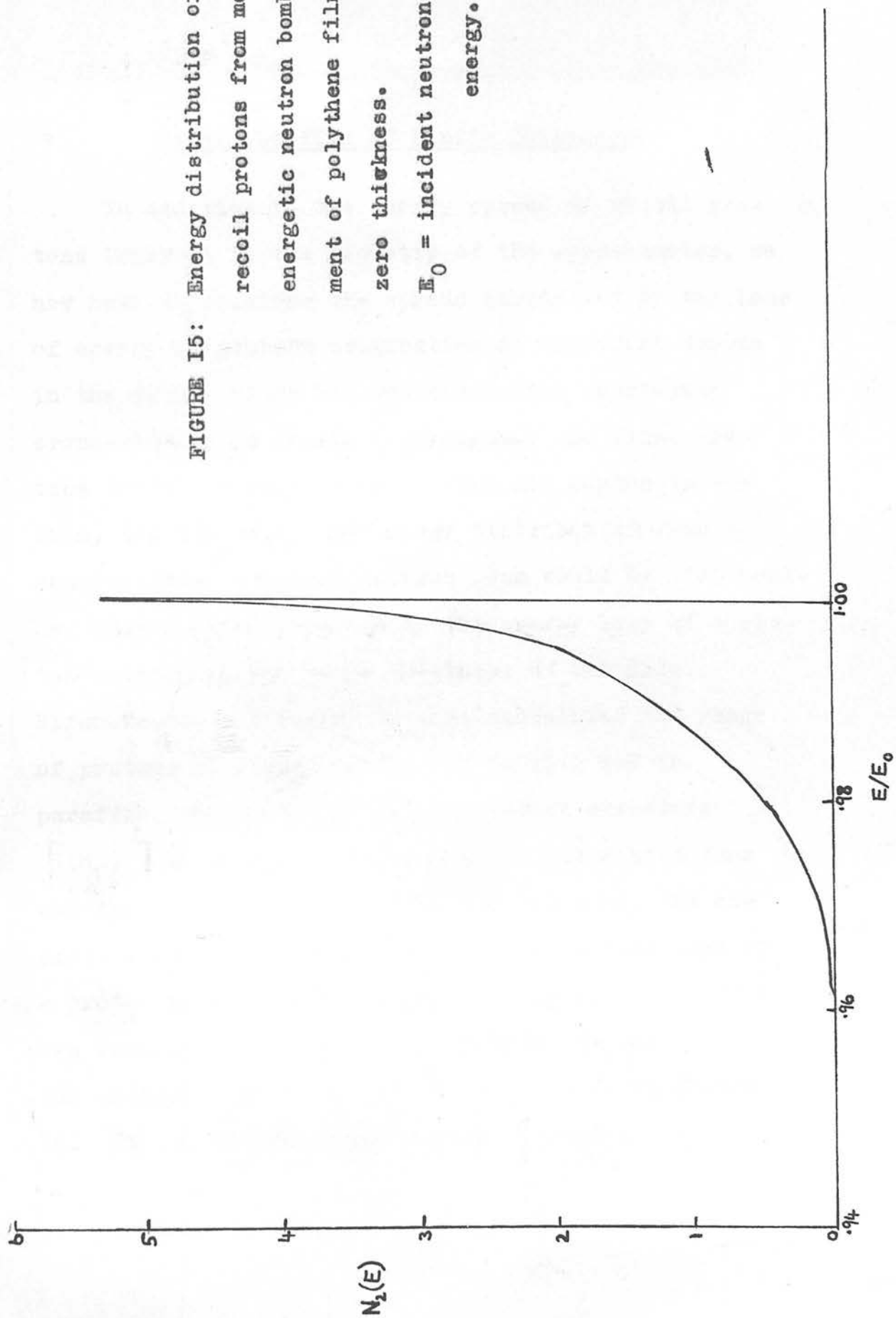


FIGURE I5: Energy distribution of
 recoil protons from mono-
 energetic neutron bombard-
 ment of polythene film of
 zero thickness.
 E_0 = incident neutron
 energy.

The maximum of the peak is seen to be displaced very little from $E/E_0 = 1$, the direct knock-on case.

Polythene Film of Finite Thickness.

In addition to the energy spread of recoil protons inherent in the geometry of the spectrometer, we now have to consider the spread introduced by the loss of energy of protons originating at different depths in the film. Since the neutron-proton scattering cross-section is constant throughout the film, protons recoil in equal numbers from all depths in the film, and the resultant energy distribution from a monoenergetic incident neutron beam would be rectangular, with a width governed by the energy loss of a proton traversing the whole thickness of the film. Hirschfelder and Magee⁽⁵²⁾ have calculated the range of protons of energy from 0.005 to 15.0 MeV in paraffin, which has the same molecular structure $[(CH_2)_n]$ as polythene. The ranges, calculated from the stopping powers of carbon and hydrogen, are expressed in $mg/cm.^2$, and from them the energy loss of a proton passing through a film of thickness $1\ mg/cm.^2$ can readily be computed as a function of initial proton energy. The resultant curve is shown in Figure 16. It can be seen that the energy loss at 2.3 MeV,

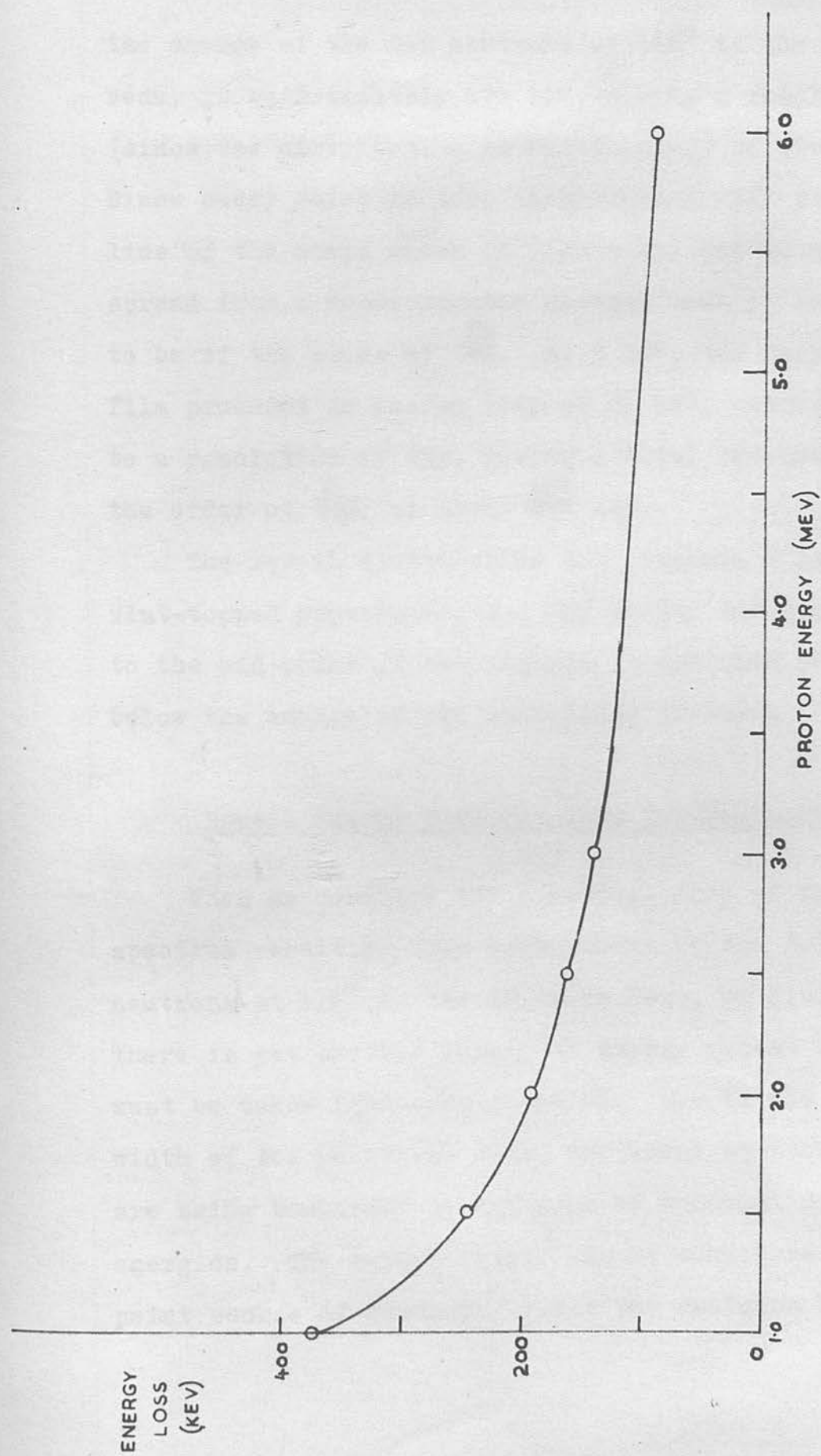


FIGURE 16. Energy lost by a proton in traversing 1 mg./cm.² of polythene.

the energy of the D-D neutrons at 110° to the deuteron beam, is approximately 170 keV, giving a resolution (since the distribution is rectangular) of about $7\frac{1}{2}\%$. Since every point in this distribution will produce a line of the shape shown in Figure 15, the total spread from a monoenergetic neutron beam is expected to be of the order of $\frac{7\frac{1}{2}}{3}\%$. At 6 MeV, the polythene film produces an energy loss of 85 keV, corresponding to a resolution of $1\frac{1}{2}\%$, giving a total resolution of the order of $\frac{2}{2\frac{1}{2}}\%$, or about $\frac{120}{150}$ keV.

The recoil distribution now presents a rather flat-topped appearance, and the energy corresponding to the mid-point of the maximum is now some 90 keV below the energy of the bombarding neutrons.

Recoil Energy Spectrum from D-D Neutrons.

When we consider the practical case of the recoil spectrum resulting from bombardment by the D-D neutrons at 110° to the deuteron beam, we find that there is yet another source of energy spread which must be taken into consideration. Due to the finite width of the polythene film, different sections of it are being bombarded by neutrons of somewhat different energies. The target itself can be considered as a point source of neutrons, since the deuteron beam is

is quite well focussed, so that, since there is no azimuthal variation in neutron energy, the polythene film can be divided into a series of strips, each of which is bombarded by neutrons whose energy depends on the angle between the beam and the line joining the mid-point of the strip to the target. The energy spectrum produced by this effect has been computed approximately by a graphical method (see appendix II), and found to be of the form shown in Figure 17. This is seen to rise to a maximum at 2.30 MeV, the energy of the neutrons bombarding the centre of the film, in the true 110° position, and to have a width at half-height of about 130 keV. The superimposition of the spectra due to the geometry of the instrument and the finite thickness of the polythene film should then produce a total spectrum of width of the order of 320 keV having a rather flat top whose centre point corresponds to a proton energy of 2.30 MeV minus half the energy lost in traversing the polythene film, i.e. an energy of 2.21 MeV.

Taking this value as the proton energy corresponding to the mid-point of the peak in the experimental spectrum shown in Figure 13, we are now in a position to calibrate the spectrometer for all energies. First, the energy lost in the middle counter by a proton

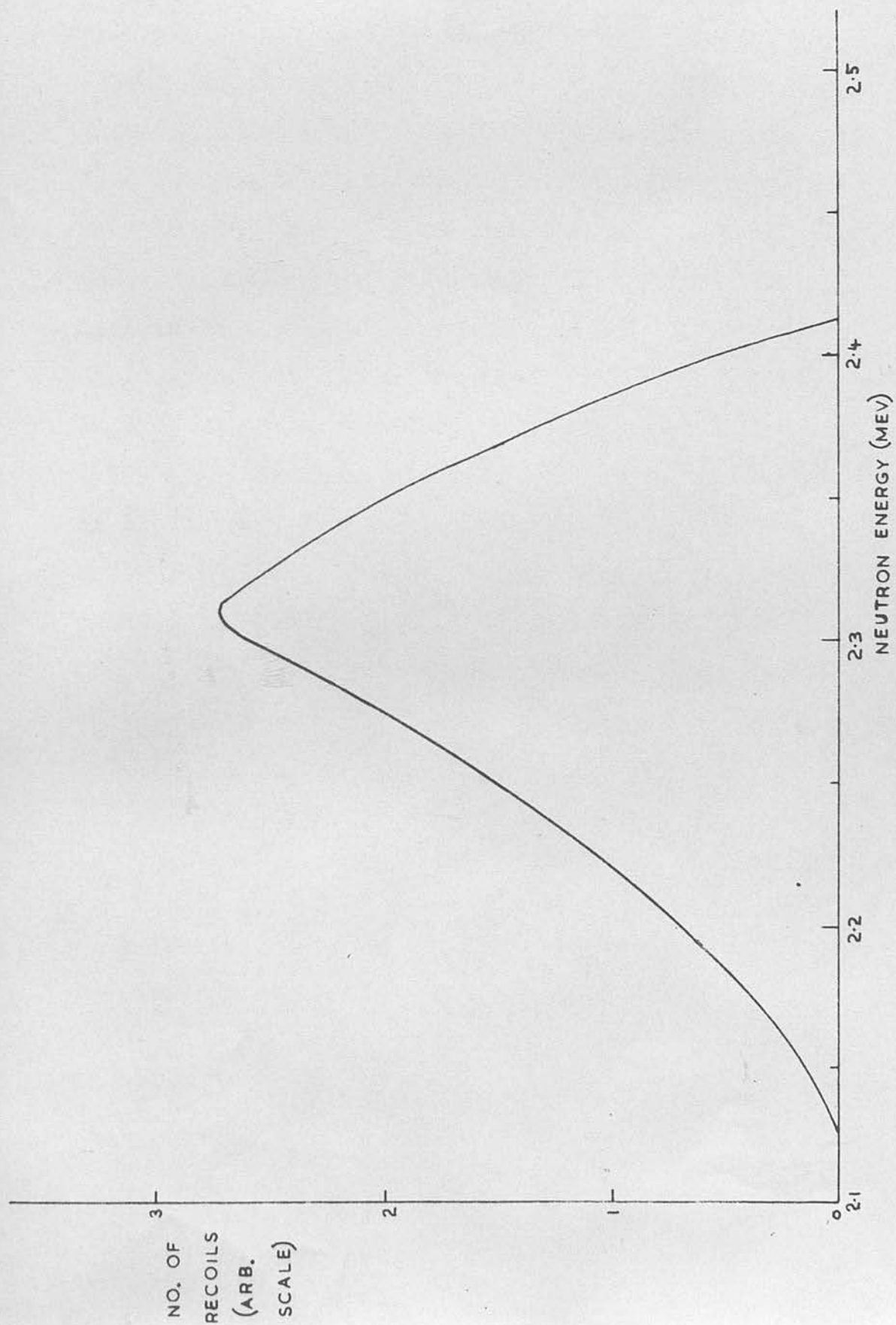


FIGURE 17. Theoretical recoil proton energy distribution from D-D neutrons at 110° .

leaving the radiator with initial energy 2.21 MeV must be calculated. To do this, it is necessary to determine the rate of energy loss by ionisation in the counter gas. The gas contains three components, argon, carbon and oxygen, whose effects can be computed separately and added. Hirschfelder and Magee⁽⁵²⁾ have tabulated values of $E \, dx/dE$ (E = proton energy, x = distance travelled) for protons in argon at atmospheric pressure, up to a proton energy of 3 MeV, and their values were used to find the rate of energy loss (dE/dx) in MeV/cm. Aron, Hoffman and Williams⁽⁵³⁾ have computed the rate of energy loss for protons in argon at 1 MeV intervals from 0 to 20 MeV, and at larger intervals up to 10,000 MeV. Their results, which are tabulated directly in MeV/cm., were used for higher energy protons.

Hirschfelder and Magee also list values for the 'stopping number', B , of oxygen and carbon, and show that this is related to dE/dx by the expression

$$\frac{dE}{dx} = 0.006094 \frac{B}{E} .$$

From these values, dE/dx for carbon and oxygen at atmospheric pressure was calculated.

The gas pressure used in the spectrometer, as mentioned previously, is 15 cms. of mercury, of which

90%, or 13.5 cms., is argon, and 10%, or 1.5 cms., carbon dioxide. Hence, to calculate the rate of energy loss in the gas, dE/dx for argon must be multiplied by 13.5/76, and dE/dx for carbon and oxygen by 1.5/76, and the values obtained added for each proton energy. The results are tabulated below:

TABLE III.

| E (MeV) | $(dE/dx)_A$ | $(dE/dx)_{O_2}$ | $(dE/dx)_C$ | Total (dE/dx) |
|---------|-------------|-----------------|-------------|----------------------|
| 0.2 | 0.1186 | 0.0122 | 0.0072 | 0.1380 |
| 0.4 | 0.0807 | 0.0094 | 0.0047 | 0.0948 |
| 0.6 | 0.0635 | 0.0075 | 0.0036 | 0.0746 |
| 0.8 | 0.0533 | 0.0064 | 0.0030 | 0.0627 |
| 1.0 | 0.0464 | 0.0055 | 0.0025 | 0.0544 |
| 1.5 | 0.0359 | 0.0043 | 0.0019 | 0.0421 |
| 2.0 | 0.0301 | 0.0035 | 0.0015 | 0.0351 |
| 2.5 | 0.0255 | 0.0030 | 0.0013 | 0.0298 |
| 3.0 | 0.0228 | 0.0028 | 0.0011 | 0.0267 |
| 4.0 | 0.0185 | 0.0022 | 0.0009 | 0.0216 |
| 5.0 | 0.0157 | 0.0019 | 0.0008 | 0.0184 |
| 6.0 | 0.0137 | 0.0016 | 0.0007 | 0.0160 |
| 7.0 | 0.0122 | 0.0014 | 0.0006 | 0.0142 |
| 10.0 | 0.0092 | 0.0011 | 0.0004 | 0.0107 |

These values are plotted against proton energy in Figure 18.

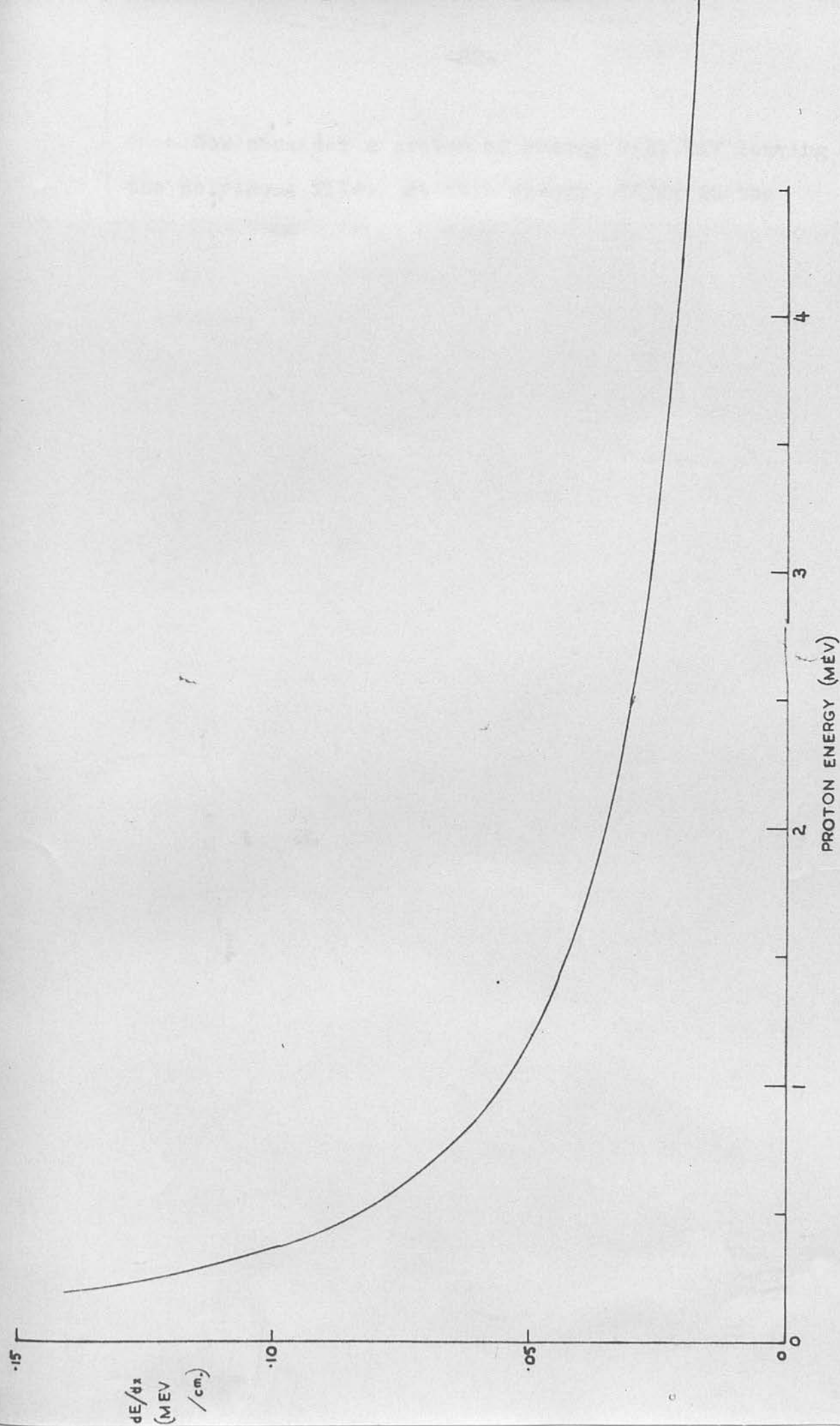


FIGURE 18. Rate of energy loss of protons in the counter gas.

Now consider a proton of energy 2.21 MeV leaving the polythene film. At this energy, dE/dx in the gas is 0.0325 MeV/cm. In order to reach the sensitive volume of the middle counter, the proton must traverse a distance of 11.9 cms. (The sensitive volume is taken as starting at the point where the counter wire enters the supporting solder). Hence, if the rate of energy loss remained constant over this distance, its energy on reaching the middle counter would be $2.21 - 11.9 \times 0.0325$ MeV, i.e. 1.82 MeV. But the rate of energy loss at this energy is now 0.0372 MeV/cm. A better approximation to the energy of the proton will be obtained by taking the true rate of energy loss over the distance traversed as the mean of the values for 2.21 and 1.82 MeV, i.e. 0.0348 MeV/cm. (This is roughly equivalent to considering the portion of Figure 18 between these energies as linear). Hence the corrected energy loss in reaching the middle counter is 0.41 MeV, and the energy of the proton is 1.80 MeV.

The energy loss in this counter can now be found by the same process. dE/dx at 1.80 MeV is 0.0373 MeV/cm., and since the length of the sensitive volume of the counter (taken as terminating at the guard-ring) is 2.5 cm., the approximate energy loss in the counter is 93 keV. This makes the energy on leaving

the counter 1.71 MeV, at which dE/dx has become 0.0383 MeV/cm. Taking the mean as the true value of dE/dx as before, we have $dE/dx = 0.0378$ MeV/cm., and the energy loss is 94.5 keV. 0.0145 6.85

Hence we can take the abscissa of the mid-point of the peak in Figure 13, i.e. 13 mm., as being the pulse-height corresponding to an energy loss in the middle counter of 94.5 keV. Since the pulse-height in a proportional counter is proportional to the energy dissipated in the counter, we can now construct a table of pulse-height against energy loss. From the energy loss can be calculated the mean rate of energy loss in MeV/cm., knowing the length of the counter. From this in turn, again assuming linearity of the curve in Figure 18 over the small range of energy of a proton in the counter, can be found the energy of the proton at the mid-point of the counter. These values are shown in Table IV, which follows. P represents the pulse-height in mm. (using the same magnification as was used in the D-D experiment), ΔE the energy loss in the middle counter, dE/dx and E_m the corresponding rate of energy loss and energy half-way through the counter, respectively.

TABLE IV.

| <u>P</u> | <u>ΔE</u> (keV) | <u>dE/dx</u> | <u>E_m</u> (MeV) |
|----------|------------------------------------|---------------------------|-------------------------------|
| 4 | 29.1 | 0.0116 | - |
| 5 | 36.4 | 0.0145 | 6.86 |
| 6 | 43.6 | 0.0175 | 5.36 |
| 7 | 50.9 | 0.0204 | 4.30 |
| 8 | 58.2 | 0.0233 | 3.61 |
| 9 | 65.4 | 0.0262 | 3.08 |
| 10 | 72.7 | 0.0291 | 2.65 |
| 11 | 80.0 | 0.0320 | 2.30 |
| 12 | 87.2 | 0.0349 | 2.01 |
| 13 | 94.5 | 0.0378 | 1.77 |
| 14 | 101.8 | 0.0407 | 1.58 |
| 15 | 109.1 | 0.0436 | 1.43 |
| 16 | 116.3 | 0.0465 | 1.31 |
| 17 | 123.6 | 0.0494 | 1.19 |
| 18 | 130.9 | 0.0523 | 1.08 |
| 19 | 138.1 | 0.0553 | 0.97 |
| 20 | 145.4 | 0.0582 | 0.89 |
| 22 | 160.0 | 0.0640 | 0.77 |
| 24 | 174.6 | 0.0699 | 0.67 |
| 26 | 189.2 | 0.0757 | 0.59 |

From the proton range-energy relations given by Livingston & Bethe⁽⁴⁵⁾, the ranges of the protons of energy E_m in standard air can now be found. By adding to these values the standard air equivalent

of the distance traversed by the proton in reaching the mid-point of the middle counter, the total range in standard air of a proton producing a pulse of any height can be found. When an absorber is inserted between the first two counters, its standard air equivalent must, of course, be added.

It has been seen in Chapter IV that the linearity of response of the amplifier and oscilloscope beam deflection is not very good below a pulse-height of 10 mm. From Table IX it can also be seen that the proton energy resolution is very poor in this region. Accordingly, it was decided to use only those pulses appearing above the 10 mm. line when the magnification is set as described above (i.e. 'overload' pulses at 32.5 mm.) In Table V below are listed the residual air ranges in cms. beyond the centre of the middle counter corresponding to pulse heights of 10 mm. and above.

TABLE V.

| <u>P (mm.)</u> | <u>R (cm.)</u> |
|----------------|----------------|
| 10 | 11.4 |
| 11 | 9.0 |
| 12 | 7.2 |
| 13 | 5.8 |
| 14 | 4.8 |
| 15 | 4.1 |
| 16 | 3.5 |
| 17 | 3.0 |
| 18 | 2.6 |
| 19 | 2.2 |
| 20 | 1.9 |
| 22 | 1.6 |
| 24 | 1.3 |
| 26 | 1.1 |

For pulse-heights greater than 26 mm., the linearity of response flattens out as the overload conditions are approached, but a rough estimate of the energy of a proton producing the maximum possible pulse height can be made by assuming that it just penetrates the sensitive volume of the last counter. This implies a residual range beyond the mid-point of the second counter of about 0.3 cms. of air, but cannot be considered as a reliable value, since the setting of the discriminator on the last counter determines how far the proton must penetrate to record a coincidence.

The calibration of the instrument is now complete, since the residual ranges given in Table V, together with a knowledge of the basic absorption in reaching the centre of the middle counter in any particular experiment, allow a pulse-height-energy relationship to be constructed from the known proton range-energy relations.

CHAPTER VI.

NEUTRONS FROM DEUTERON BOMBARDMENT OF BERYLLIUM.

The bombardment of beryllium by deuterons provides a large neutron yield even at quite low bombarding voltages, and this reaction has consequently been used widely as a convenient fast neutron source. As these neutrons were to be used in this laboratory for work on fast neutron dosimetry, it was decided to examine their spectrum at an angle of 0° to the deuteron beam. The deuteron bombarding voltage used throughout the experiments was 750 kV, and a thick beryllium target was used. Since none of the thick absorbers were necessary for these experiments (the upper limit of neutron energy at 0° is about 5 MeV), an absorber of thickness 3.3 mg/cm^2 was placed in the thick absorber wheel, so that a fine variation of absorption was possible by combining it with any of the thin absorbers listed in Table I (p. 34). In the 0° position, a series of films were taken at absorber thicknesses of 0, 3.3, 11.8, 16.8, 19.2, 32.5 and 41.1 mg/cm^2 , covering the complete neutron spectrum with good resolution.

Taking the run with no absorber as an example, details of the energy calibration and pulse-height

analysis will be given.

First, we must find the standard air equivalent of the distance traversed by a proton between the polythene film and the mid-point of the middle counter. This quantity will vary slightly with the energy of the proton, but may be taken as constant for all protons in the energy range under investigation with a particular absorber. In reaching this point, the proton has to traverse a distance of 7.6 cms. to reach the absorber, and 5.55 cms. after passing through the absorber. Hence, for the first 7.6 cms. of gas, we must use the value of stopping-power (relative to standard air) relevant to protons whose energy is that of the neutron energy range under investigation; for the absorber, we use the mean stopping power over the range from this energy down to about 2 MeV, and for the last 5.55 cms., the stopping power for protons of about 2 MeV energy. The small errors involved in this procedure are considered to be well within the geometrical and electronic resolution of the instrument.

At 2 MeV, dE/dx for the gas filling is (see Fig. 18) 0.035 MeV/cm., and the Livingston-Bethe range-energy curves⁽⁴⁵⁾ give a mean value for dE/dx at this energy of 0.169 MeV/cm. in standard air. Hence, 1 cm. of the gas filling is very nearly

equivalent to 0.2 cms. of standard air for 2 MeV protons. In the case where no absorber is in use, the total standard air length, r , traversed before reaching the mid-point of the middle counter is then given by $0.2 (7.6 + 5.55)$ cms., i.e. 2.7 cms.

We know from Table V the residual air range, r' , beyond the mid-point of the middle counter corresponding to any measured pulse-height, and so we can construct a table relating pulse-height to the total standard air range of the proton and hence to its initial energy.

TABLE VI.

Calibration for no Absorber.

| <u>P</u> (mm) | <u>r'</u> (cm) | <u>R = (r + r')</u> (cm). | <u>E</u> (MeV) |
|---------------|----------------|------------------------------|----------------|
| 10 | 11.4 | 14.1 | 3.00 |
| 11 | 9.0 | 11.7 | 2.69 |
| 12 | 7.2 | 9.9 | 2.43 |
| 13 | 5.8 | 8.5 | 2.23 |
| 14 | 4.8 | 7.5 | 2.07 |
| 15 | 4.1 | 6.8 | 1.95 |
| 16 | 3.5 | 6.2 | 1.84 |
| 17 | 3.0 | 5.7 | 1.75 |
| 18 | 2.6 | 5.3 | 1.68 |
| 19 | 2.2 | 4.9 | 1.60 |
| 20 | 1.9 | 4.6 | 1.54 |
| 22 | 1.6 | 4.3 | 1.48 |
| 24 | 1.3 | 4.0 | 1.42 |
| 26 | 1.1 | 3.8 | 1.37 |
| (33 | 0.3 | 3.0 | 1.19) |

The values in the last column are taken from the Livingston-Bethe range-energy curves.

It can be seen from this table that for low pulses the energy resolution is poor -- a change of 1 mm. in pulse-height gives an energy difference of over 300 keV -- while for large pulses a shift of 1 mm. gives considerably less than 100 keV energy shift.

Analysis of the pulse-height distribution is now carried out in 1 mm. intervals from 10 to 33 mm., and the pulses grouped in 100 keV intervals, as far as possible. The number of pulses in each group is then divided by the energy interval expressed in units of 100 keV, so that the resultant distribution gives the number of pulses per 100 keV interval at the mean energy of the interval.

The results of the run with no absorber are given in Table VII, which follows.

TABLE VII.

Recoil proton distribution - no absorber.

| <u>ΔP</u> | <u>Mean E (MeV)</u> | <u>D</u> | <u>P</u> | <u>P'</u> |
|------------------------------|---------------------|----------|--------------|--------------|
| 12-13 | 2.33 | 2.0 | 88 \pm 9 | 44 \pm 5 |
| 13-14 | 2.15 | 1.6 | 50 \pm 7 | 31 \pm 4 |
| 14-15 | 2.01 | 1.2 | 57 \pm 8 | 49 \pm 7 |
| 15-16 | 1.90 | 1.1 | 70 \pm 8 | 66 \pm 8 |
| 16-17 | 1.80 | 0.9 | 89 \pm 9 | 97 \pm 10 |
| 17-18 | 1.72 | 0.8 | 87 \pm 9 | 118 \pm 12 |
| 18-19 | 1.64 | 0.8 | 80 \pm 9 | 108 \pm 12 |
| 19-22 | 1.54 | 1.2 | 253 \pm 16 | 201 \pm 13 |
| 22-26 | 1.43 | 1.1 | 197 \pm 14 | 182 \pm 13 |
| 26-33 | 1.28 | 1.8 | 334 \pm 18 | 183 \pm 10 |

The third column gives the dividing factor, the fourth column the observed distribution of pulses, and the last column the number per 100 keV interval.

The second run was carried out with a 3.3 mg./cm² aluminium absorber. Here the standard air length of gas traversed can be taken as 2.7 cms. as above, but to this must be added the air equivalent of the aluminium. As mentioned previously, 1.52 mg./cm² of aluminium can be taken as roughly equivalent to 1 cm. of standard air; a small correction, given by Livingston and Bethe⁽⁴⁵⁾, must be added to this to arrive at the true air equivalent. For a thickness of 3.3 mg./cm² of aluminium, calculation gives the air equivalent as 2.1 cms.

Hence the total air length traversed by a proton in reaching the mid-point of the middle counter is $2.7 + 2.1$, or 4.8 cm. The total range, R , and thus the initial energy, E , of a proton causing a pulse of given height is thus shifted upwards. Analysis in this case is similar to that carried out in the last case, and gives the following results.

TABLE VIII.

Recoil proton distribution - 3.3 mg/cm.^2 absorber.

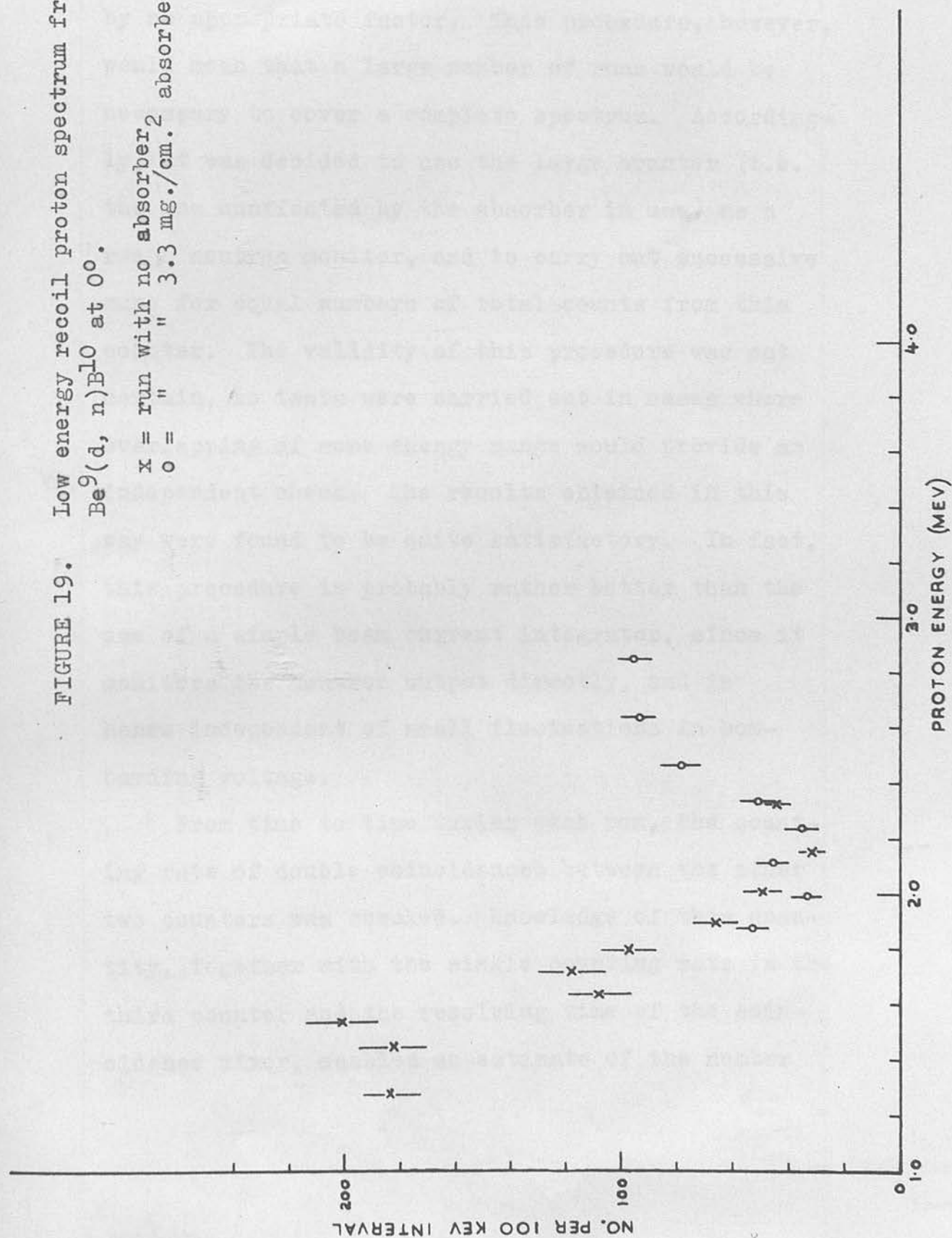
| <u>ΔP</u> | <u>Mean E (MeV)</u> | <u>D</u> | <u>P</u> | <u>P'</u> |
|------------------------------|---------------------|----------|--------------|------------|
| 11-12 | 2.85 | 2.3 | 220 ± 15 | 95 ± 6 |
| 12-13 | 2.64 | 1.9 | 176 ± 13 | 93 ± 7 |
| 13-14 | 2.47 | 1.5 | 117 ± 11 | 78 ± 7 |
| 14-15 | 2.34 | 1.0 | 50 ± 7 | 50 ± 7 |
| 15-16 | 2.24 | 1.0 | 35 ± 6 | 35 ± 6 |
| 16-18 | 2.12 | 1.4 | 63 ± 8 | 45 ± 6 |
| 18-20 | 1.99 | 1.2 | 40 ± 6 | 33 ± 5 |
| 20-24 | 1.88 | 1.1 | 57 ± 7 | 52 ± 6 |

By comparison with Table VII, it can be seen that at the overlapping points the numbers of pulses are nearly the same, so that these distributions can be joined directly. The spectrum is plotted in Fig. 19.

When runs with successive absorbers overlap in

FIGURE 19. Low energy recoil proton spectrum from $\text{Be}^9(d, n)\text{B}^{10}$ at 0° .

x = run with no absorber
o = " " 3.3 mg./cm.² absorber.



some energy range, it is comparatively simple to join the successive distributions by multiplying by an appropriate factor. This procedure, however, would mean that a large number of runs would be necessary to cover a complete spectrum. Accordingly, it was decided to use the large counter (i.e. the one unaffected by the absorber in use) as a rough neutron monitor, and to carry out successive runs for equal numbers of total counts from this counter. The validity of this procedure was not certain, so tests were carried out in cases where overlapping of some energy range would provide an independent check. The results obtained in this way were found to be quite satisfactory. In fact, this procedure is probably rather better than the use of a simple beam current integrator, since it monitors the neutron output directly, and is hence independent of small fluctuations in bombarding voltage.

From time to time during each run, the counting rate of double coincidences between the other two counters was checked. Knowledge of this quantity, together with the single counting rate in the third counter and the resolving time of the coincidence mixer, enabled an estimate of the number

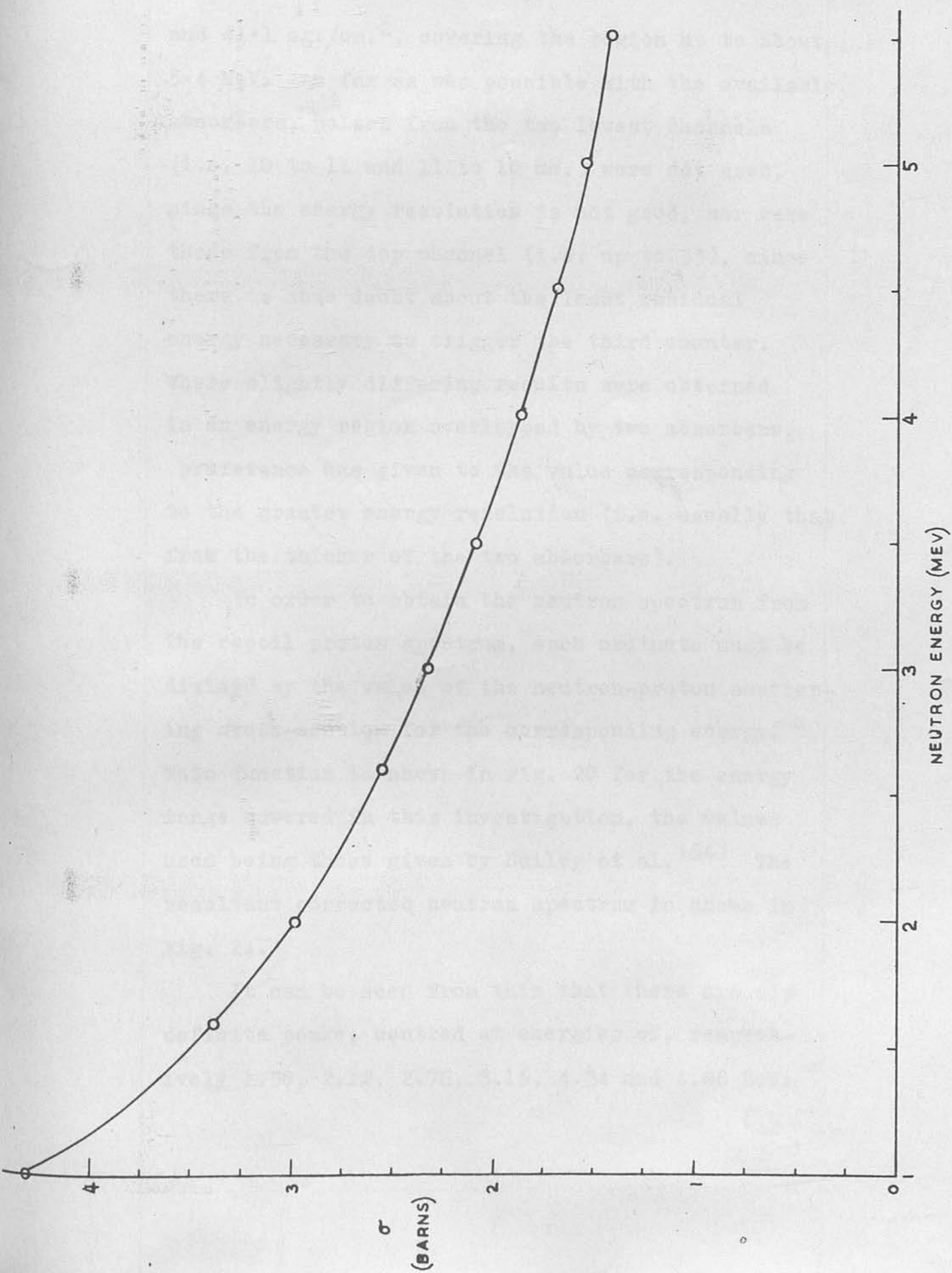


FIGURE 20. Neutron-proton scattering cross-section.

and 41.1 mg./cm.^2 , covering the region up to about 5.4 MeV. As far as was possible with the available absorbers, pulses from the two lowest channels (i.e. 10 to 11 and 11 to 12 mm.) were not used, since the energy resolution is not good, nor were those from the top channel (i.e. up to 33), since there is some doubt about the least residual energy necessary to trigger the third counter. Where slightly differing results were obtained in an energy region overlapped by two absorbers, preference was given to the value corresponding to the greater energy resolution (i.e. usually that from the thicker of the two absorbers).

In order to obtain the neutron spectrum from the recoil proton spectrum, each ordinate must be divided by the value of the neutron-proton scattering cross-section for the corresponding energy. This function is shown in Fig. 20 for the energy range covered in this investigation, the values used being those given by Bailey et al. (54) The resultant corrected neutron spectrum is shown in Fig. 21.

It can be seen from this that there are six definite peaks, centred at energies of, respectively 1.50, 2.12, 2.78, 3.16, 4.34 and 4.86 MeV.

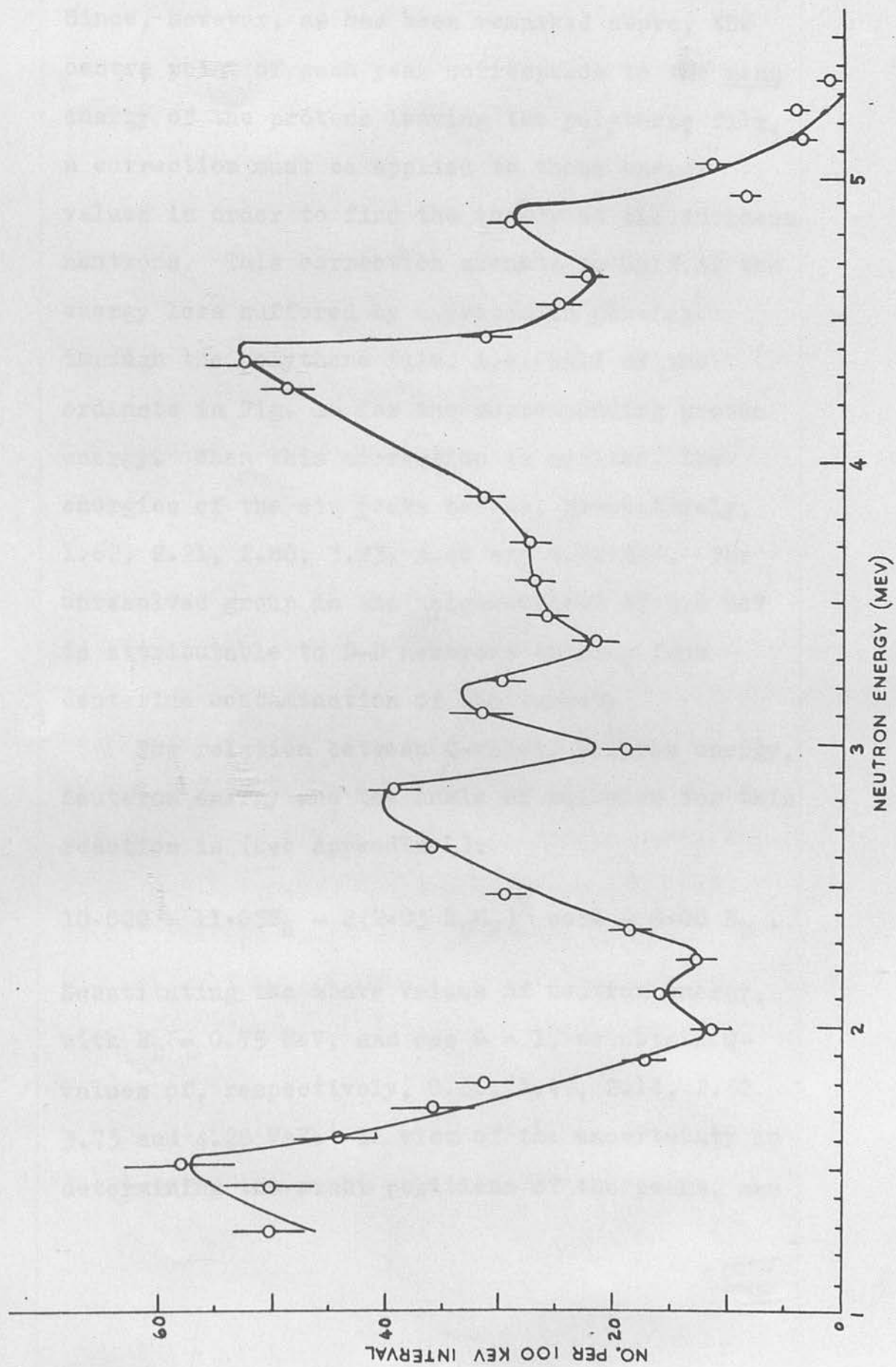


FIGURE 21. Neutron spectrum from $\text{Be}^9(\text{d},\text{n})\text{Be}^{10}$ at 0° to the deuteron beam.

Since, however, as has been remarked above, the centre point of each peak corresponds to the mean energy of the protons leaving the polythene film, a correction must be applied to these energy values in order to find the energy of the incident neutrons. This correction amounts to half of the energy loss suffered by a proton in passing through the polythene film, i.e. half of the ordinate in Fig. 16 for the corresponding proton energy. When this correction is applied, the energies of the six peaks become, respectively, 1.62, 2.21, 2.86, 3.23, 4.40 and 4.92 MeV. The unresolved group in the neighbourhood of 3.6 MeV is attributable to D-D neutrons arising from deuterium contamination of the target.

The relation between Q-value, neutron energy, deuteron energy and the angle of emission for this reaction is (see Appendix 1):

$$10.02Q = 11.03E_N - 2(2.03 E_D E_N)^{1/2} \cos\theta - 8.00 E_D .$$

Substituting the above values of neutron energy, with $E_D = 0.75$ MeV, and $\cos \theta = 1$, we obtain Q-values of, respectively, 0.86, 1.47, 2.14, 2.52, 3.73 and 4.28 MeV. In view of the uncertainty in determining the exact positions of the peaks, and

of the necessity for applying the polythene film correction, it is considered that the probable error in these values cannot be taken as less than ± 0.10 MeV in each case.

Early investigations of this spectrum, e.g. those by Staub and Stephens⁽⁵⁵⁾, and by Powell⁽²²⁾, were carried out at angles of about 100° , and showed the existence of four of the above groups. There is a slight indication in their results of the group with $Q = 1.47$ MeV, but no mention is made of it. Ajzenburg⁽⁵⁶⁾, using the photographic plate method, has recently carried out an extensive investigation of the neutron spectrum from this reaction at 0° using 3.41 MeV deuterons with a thin beryllium target. No neutrons from this group were reported, but neutrons corresponding to the group at 2.52 MeV were found. At the angles of emission investigated by the earlier workers this group would overlap the D-D neutrons, so that identification would be impossible.

Since this investigation was started, Dyer and Bird⁽⁵⁷⁾ have reported an investigation of the neutrons from this reaction with photographic plates at angles of 0° , 90° and 150° , using a thick target and 600 keV deuterons. In their

results for the 0° position, the peak corresponding to the 1.47 MeV group is clearly resolved, and the Q-value is quoted as 1.50 ± 0.03 MeV. There is a slight indication of the same group at 90° and 150° . By consideration of the relative energies of the group at the three angles, Dyer and Bird have shown that it results almost certainly from the reaction $\text{Be}^9 + \text{H}^2 \rightarrow \text{B}^{10} + \text{n}^1$, and corresponds to an excited level in B^{10} , the product nucleus. They also find a group corresponding to the 2.52 MeV group. In the table below are shown the Q-values found by Ajzenburg, by Dyer and Bird, and by the author.

TABLE IX.

| <u>Ajzenburg</u> | <u>Dyer & Bird</u> | <u>Author</u> |
|------------------|------------------------|-----------------|
| 0.83 ± 0.06 | 0.71 ± 0.02 | 0.86 ± 0.10 |
| - | 1.50 ± 0.03 | 1.47 ± 0.10 |
| 2.21 ± 0.06 | 2.15 ± 0.02 | 2.14 ± 0.10 |
| 2.61 ± 0.06 | 2.60 ± 0.02 | 2.52 ± 0.10 |
| 3.64 ± 0.06 | 3.62 ± 0.02 | 3.73 ± 0.10 |
| 4.35 ± 0.06 | 4.35 ± 0.02 | 4.28 ± 0.10 |

It is seen that the agreement is well within the quoted experimental errors in every case. Taking the Q-value for the ground-state transition as

4.35 MeV, the value deduced from the nuclear masses, the neutron group of Q-value 1.47 MeV corresponds to an excited level in B^{10} at 2.88 ± 0.10 MeV.

As a check on the existence of this group, it was decided to carry out an investigation of the low-energy neutron spectrum at 90° , again using 0.75 MeV deuterons. Two runs were carried out in this position, with no absorber and with the 6.8 mg./cm.² absorber. The resultant recoil proton spectrum is shown in Fig. 22, and it can be seen that there is some indication of the group, whose expected position is shown by the arrow. The peak at 2.37 MeV gives a Q-value of 2.09 MeV, in good agreement with the value obtained for the corresponding peak in the 0° position. The slope on the high energy side of this peak is attributable to both the D-D neutrons and the group of Q-value 2.52 MeV.

While it is not thought that the accuracy attainable by this method is as great as that of the photographic emulsion method, the above investigation demonstrates the usefulness of the instrument in allowing a rapid check to be made on the existence of a neutron group, whose energy can then be more accurately determined by the emulsion method.

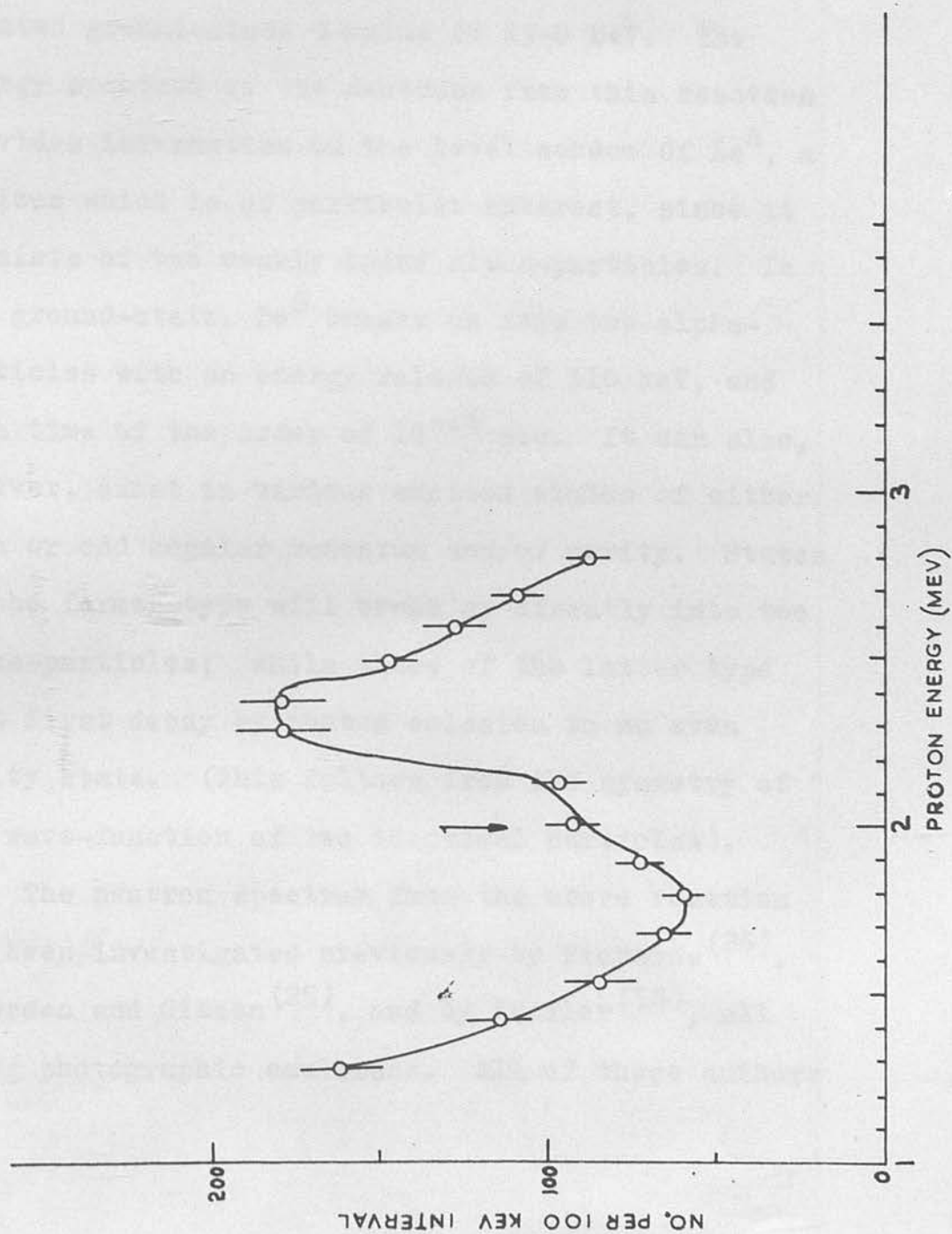


FIGURE 22. Low-energy neutron spectrum from $\text{Be}^9(\text{d},\text{n})\text{B}^{10}$ at 90° to the deuteron beam.

CHAPTER VII.

THE 4.9 MeV EXCITED STATE OF Be^8 .

The reaction $\text{Li}^7 (d, n) \text{Be}^8$ has long been known to provide a very large yield of both neutrons and gamma-rays, the former with a calculated ground-state Q-value of 15.0 MeV. The energy spectrum of the neutrons from this reaction provides information on the level scheme of Be^8 , a nucleus which is of particular interest, since it consists of two weakly bound alpha-particles. In its ground-state, Be^8 breaks up into two alpha-particles with an energy release of 110 keV, and in a time of the order of 10^{-16} sec. It can also, however, exist in various excited states of either even or odd angular momentum and/or parity. States of the former type will break up directly into two alpha-particles; while those of the latter type must first decay by photon emission to an even parity state. (This follows from the symmetry of the wave-function of two identical particles).

The neutron spectrum from the above reaction has been investigated previously by Richards⁽²⁶⁾, by Green and Gibson⁽²⁵⁾, and by Wäffler⁽⁵⁸⁾, all using photographic emulsions. All of these authors

found two strong high-energy neutron groups, corresponding to the formation of Be^8 in its ground-state and in a state of excitation about 3 MeV. From the apparent width of this latter group, Richards deduced the existence of another unresolved group, corresponding to an excitation of about 5 MeV, additional support for which was yielded by the subsequent discovery of a strong gamma-ray from the same reaction of about 4.9 MeV⁽⁵⁹⁾, implying the existence of a level of odd parity and/or angular momentum. Green and Gibson found some evidence for the existence of a neutron group at 4.9 MeV excitation, whereas Wäffler found none whatsoever.

Information about the low-lying even states of Be^8 can also be obtained from experiments on the scattering of alpha-particles by helium. A resonance has been observed by Devons⁽⁶⁰⁾ corresponding to a level in Be^8 at about 3 MeV, but any further observed resonances have been so broad as to be scarcely recognisable.

Recent work by the group at Canberra under Professor Titterton on the reactions $\text{B}^{11}(\gamma, t)\text{Be}^8$ and $\text{B}^{10}(\gamma, d)\text{Be}^8$ has yielded evidence for the existence of a broad level at about 5.3 MeV excitation, rather than at 4.9 MeV. This has been borne

out by the discovery⁽⁶¹⁾ of a gamma-ray of energy about 12.5 MeV from the reaction $\text{Li}^7 (p, \gamma) \text{Be}^8$, in addition to the already known gamma-rays of energy 17.6 and 14.8 MeV, corresponding to transitions to the ground-state and the 2.8 MeV level in Be^8 , respectively. The existence of this gamma-ray implies that the level at 5.3 MeV must be of even parity, since the highly excited state of Be^8 formed by proton bombardment of Li^7 decays to this level before breaking up into two alpha-particles.

Professor Titterton has suggested that the neutron spectrometer described here might be used in an attempt to detect neutron groups corresponding to the levels at 5.3 and/or 4.9 MeV, since its design allows a rapid survey of a particular range of neutron energy to be carried out.

A thick target of lithium metal was bombarded by 20 μA of 0.75 MeV deuterons, and the neutron spectrum at 0° examined using absorbers of total thickness 172.1, 155.0 and 141.7 mg./cm.², covering the energy range from 10.84 to 9.16 MeV with good resolution. The results are not very reliable, however, due to a peculiar difficulty associated with this reaction. The neutron spectrum extends from zero energy up to an energy of about 15 MeV, so that a very large number of neutrons is present;

the position is further complicated by the presence at low energies of neutrons from the reaction $\text{Li}^6(d, n) \text{Be}^7$ (Li^6 constitutes 7.5% of natural lithium), and of a continuum of neutrons arising from the three-body disintegration $\text{Li}^7(d, n) 2\text{He}^4$. Hence the single and double coincidence counting rates in the telescope system are very high, giving rise to a high chance triple coincidence rate; in fact, this chance rate was found to be of the same order of magnitude as the genuine coincidence rate. Since these chance coincidence pulses would in all probability mask the effect of any excited levels in Be^8 , it was decided to examine the possibility of eliminating their effect by some form of background subtraction. In order to do this, the operating conditions of the three counters must be preserved as nearly as possible, a condition which would not be realised merely by removing the polythene radiator. It is considered that by far the greater number of chance coincidences arise from single counts occurring in the counter nearest the target at the same time as a genuine double coincidence in the other two counters. The reasons for this are firstly, the greater distance between the first and second counters; secondly, the presence of the absorber, making it impossible for a proton of energy less

than about 10 MeV to cause a genuine double coincidence between the first two counters; and thirdly, the larger cathode diameter of the first counter, which prevents many double coincidences being caused by protons recoiling from the brass cathode. Accordingly, it was decided to insert an absorber thick enough to prevent any genuine recoils penetrating all three counters (i.e. having a thickness greater than the range of a 15 MeV proton), and to subtract the resultant pulse-height distribution from that obtained with the original absorber. Since the neutrons can penetrate the aluminium absorber without appreciable absorption or scattering, the number of recoils produced in the last two counters is nearly independent of the absorber in use, while the counting rate in the first counter is unaffected by the absorber. A rough check on the validity of the method is afforded by comparing the chance coincidence rates with the 'thin' and with the 'thick' absorbers inserted. These were found to be the same within the statistical probable error. Unfortunately, however, the subtraction process seriously affects the statistics of the resultant recoil proton spectrum, and large numbers of pulses have to be analysed to obtain a reliable spectrum.

It is thought that an improvement might be effected at the cost of resolution by using a thicker polythene radiator (say about 3 mg./cm.²), in order to increase the ratio of genuine recoils to recoils from the surrounding brass, though the gain would partly be offset by the resultant increase in the single counting rate in the first counter due to recoils from low energy neutrons. It is also thought that the use of a polythene film deposited on a thin aluminium backing would bring about an improvement by reducing the energy of the more energetic recoil protons in the first counter, and thereby enabling a lower amplifier gain to be used, so that the counting rate in the first counter is lowered. This would also tend to reduce the number of counts due to photo-electrons and Compton electrons resulting from the gamma-radiation, which may account for many of the smaller pulses.

The procedure used in carrying out the experiment and in the subsequent analysis was similar to that described in Chapter VI. The runs with the three absorbers and their respective background runs were all carried out for equal numbers of total counts from the first counter. This procedure was checked by comparing the pulse-height distributions from the background runs, which were found to be approximately the same. The pulses were analysed in intervals of approximately

100 keV, the number obtained being divided by the width of the interval.

The resultant recoil proton spectrum is shown in Fig. 23. Although the statistics are rather poor, there is definite evidence for the existence of a rather broad group centred at about 9.9 MeV. The relation connecting Q-value, neutron energy, deuteron energy and angle of emission for this reaction is

$$8.01 Q = 9.02 E_n - 6 E_d - 2(2.03 E_d E_n)^{1/2} \cos \theta ,$$

and substituting $E_n = 9.9$ MeV, $E_d = 0.75$ MeV, $\cos \theta = 1$, we obtain a value of 9.60 MeV for Q. The known mass-values give a calculated value of Q for the ground-state transition of 15.04 MeV. Subtraction gives the excitation of the corresponding level in Be^8 as 5.44 MeV. Again an accuracy of the order of ± 0.10 MeV is assumed. It can be seen that there is no evidence for a group in the neighbourhood of 4.9 MeV excitation, which would occur at about 10.5 MeV neutron energy.

While this cannot be regarded as decisive evidence for the existence of the new level, since no other groups are visible for comparison, it does afford at least an indication that the results of the Canberra group are correct, and that the supposed 4.9 MeV level does not exist.

The existence of the 4.9 MeV gamma-ray discovered

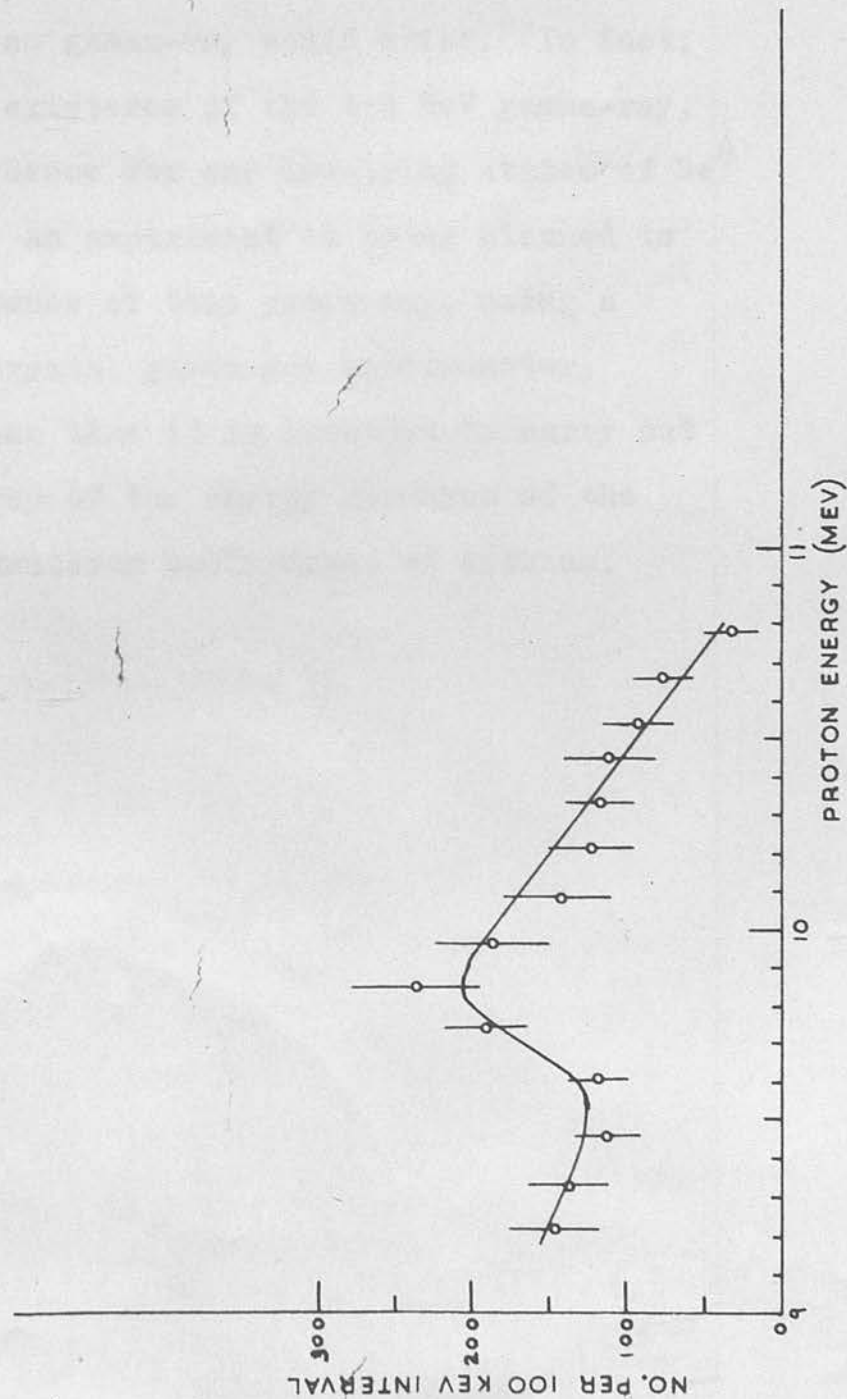


FIGURE 23. Section of recoil proton spectrum from $\text{Li}^7(d,n)\text{Be}^8$.

by Richards has not yet been explained. Titterton's discovery of the 12.5 MeV gamma-ray from $\text{Li}^7(p, \gamma) \text{Be}^8$ would imply that the 5.3 MeV state is of even parity, since the state formed by proton capture from Li^7 is of odd parity⁽⁶²⁾. Hence the 5.3 MeV level would break up directly into two alpha-particles, and no gamma-ray would arise. In fact, apart from the existence of the 4.9 MeV gamma-ray, there is no evidence for any low-lying states of Be^8 of odd parity. An experiment is being planned to check the existence of this gamma-ray, using a sodium iodide crystal gamma-ray spectrometer, while at the same time it is intended to carry out a complete survey of the energy spectrum of the neutrons from deuteron bombardment of lithium.

CHAPTER VIII.

SUMMARY

The design, construction and calibration of a recoil-coincidence-absorption fast neutron spectrometer has been described, and the theoretical resolving power of the instrument has been discussed, in so far as it is determined by the geometry of the proportional counter telescope and by the finite thickness of the polythene film radiator. The geometrical resolution has been seen to be of the order of 2% of the energy of the incident neutrons, so that the absolute resolution, expressed in units of energy, decreases with energy as the reciprocal of the neutron energy. At the same time, however, the energy spread introduced by the polythene film decreases as shown in Fig. 16. By combining the energy spreads from these two effects, we obtain a curve of the form shown in Fig. 24. Here the ordinate is the width at half-height of the line produced by monoenergetic neutrons whose energy is given by the abscissa. It can be seen that the theoretical resolution attains its best value (about 90 keV) in the neighbourhood of 3 MeV neutron energy, and is below 300 keV over the

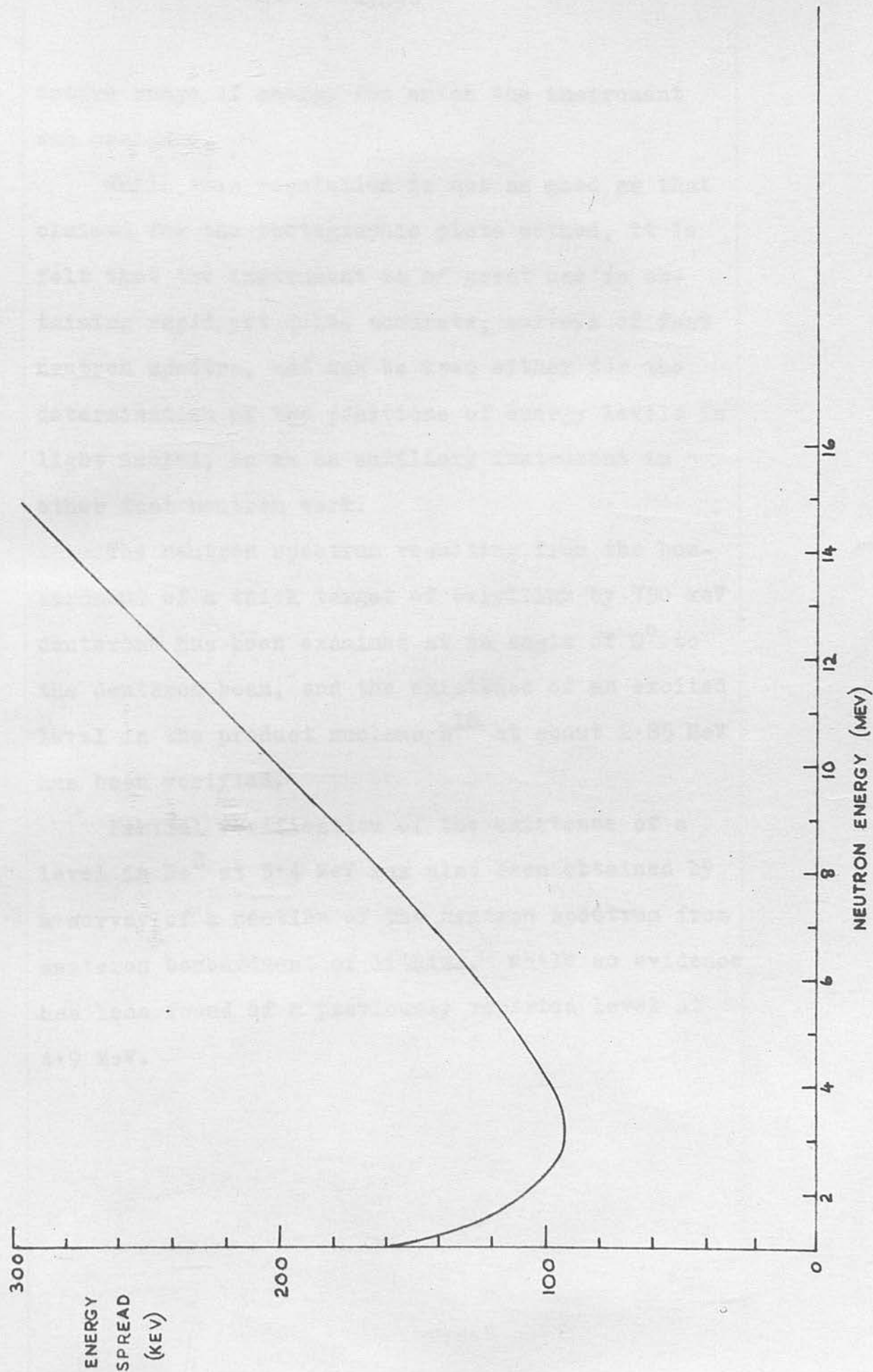


FIGURE 24. Theoretical spread of recoil proton energy due to counter geometry and polythene film thickness.

entire range of energy for which the instrument was designed.

While this resolution is not as good as that claimed for the photographic plate method, it is felt that the instrument is of great use in obtaining rapid, yet quite accurate, surveys of fast neutron spectra, and can be used either for the determination of the positions of energy levels in light nuclei, or as an auxiliary instrument in other fast neutron work.

The neutron spectrum resulting from the bombardment of a thick target of beryllium by 750 keV deuterons has been examined at an angle of 0° to the deuteron beam, and the existence of an excited level in the product nucleus B^{10} at about 2.85 MeV has been verified.

Partial verification of the existence of a level in Be^8 at 5.4 MeV has also been obtained by a survey of a section of the neutron spectrum from deuteron bombardment of lithium, while no evidence has been found of a previously reported level at 4.9 MeV.

APPENDIX I.

Derivation of the Reaction Formulae.

By consideration of the simple dynamics of a collision between a nucleus A and a deuteron D, giving rise to a product nucleus B and a neutron N, with an energy release Q, a simple relation can be derived expressing the Q-value in terms of the individual particle masses, the neutron energy and the angle of emission of the neutron in laboratory space.

Let the masses of the reacting particles be respectively m_A , m_D , m_B , m_N , and their energies E_A , E_D , E_B , E_N . Since the nucleus A is at rest in laboratory space, $E_A = 0$.

Let the angle between the direction of emission of the neutron and the initial direction of the deuteron be Θ , and that between the direction of recoil of the nucleus B and the initial deuteron direction be ϕ .

Applying the laws of conservation of energy and momentum, we have

$$E_B + E_N = E_D + Q \quad (1)$$

$$(m_B E_B)^{1/2} \cos \phi + (m_N E_N)^{1/2} \cos \Theta = (m_D E_D)^{1/2} \quad (2)$$

$$(m_B E_B)^{1/2} \sin \phi = (m_N E_N)^{1/2} \sin \Theta \quad (3)$$

From equation (3),

$$\cos \phi = \left[1 - \frac{m_N E_N}{m_B E_B} \sin^2 \theta \right]^{\frac{1}{2}}$$

and substituting this in equation (2) leads to

$$m_B E_B = m_D E_D + m_N E_N - 2(m_D m_N E_D E_N)^{\frac{1}{2}} \cos \theta \quad (4)$$

Hence, from the energy relation (1), we obtain the general reaction formula

$$\begin{aligned} m_B Q &= (m_B + m_N) E_N - (m_B - m_D) E_D \\ &\quad - 2(m_D m_N E_D E_N)^{\frac{1}{2}} \cos \theta \end{aligned} \quad (5)$$

By substitution of the known mass-values, it is now possible to obtain relations for each of the reactions investigated:

(1) $H^2(d,n)He^3$; $E_D = 0.75 \text{ MeV}$, $\theta = 110^\circ$.

$$m_D = 2.01471 \text{ a.m.u.}$$

$$m_N = 1.00893 \quad " \quad \cos \theta = -0.342$$

$$m_B = 3.01700$$

Hence,

$$3.017Q = 4.026E_N + 0.684(1.525E_N)^{\frac{1}{2}} - 0.752 \quad (6)$$

(2) $Be^9(d,n)B^{10}$; $E_D = 0.75 \text{ MeV}$, (a) $\theta = 0^\circ$
(b) $\theta = 90^\circ$

$$m_D = 2.01471 \text{ a.m.u.}$$

$$m_N = 1.00893 \quad " \quad (a) \cos \theta = 1$$

$$m_B = 10.01618 \quad " \quad (b) \cos \theta = 0$$

Hence,

$$(a) \quad 10.016Q = 11.025E_N - 2(1.525E_N)^{1/2} - 6.001 \quad (7)$$

and

$$(b) \quad 10.016Q = 11.025E_N - 6.001 \quad (8)$$

$$(3) \quad \text{Li}^7(d,n) \text{Be}^8; \quad E_D = 0.75 \text{ MeV}, \quad \theta = 0^\circ.$$

$$m_D = 2.01471 \text{ a.m.u.}$$

$$m_N = 1.00893 \quad " \quad \cos \theta = 1.$$

$$m_B = 8.00785 \quad "$$

Hence

$$8.008Q = 9.017E_N - 2(1.525E_N)^{1/2} - 4.495 \quad (9)$$

TABLE X.

| Strip No. | Energy |
|-----------|--------|
| 1. | 3.190 |
| 2. | 3.213 |
| 3. | 3.232 |
| 4. | 3.249 |
| 5. | 3.267 |
| 6. | 3.283 |
| 7. | 3.298 |
| 8. | 3.317 |
| 9. | 3.334 |
| 10. | 3.352 |
| 11. | 3.368 |
| 12. | 3.386 |
| 13. | 3.400 |

APPENDIX II.

Computation of Energy Spread of Recoils from D-D Neutrons at 110° .

As explained in Chapter V, the polythene film is divided into strips, thirteen in number, and the angles between the beam and the line joining the centre of each strip to the target are calculated, taking the distance of the polythene film from the target as 10 cm., and assuming that the centre strip corresponds to an angle of 110° . The corresponding energy of the neutrons bombarding each strip is then found from formula (5) in Appendix I. The values for each strip (each of which is of width 0.2 cm.) are tabulated below.

TABLE X.

| <u>Strip No.</u> | <u>Energy</u> |
|------------------|---------------|
| 1. | 2.198 |
| 2. | 2.215 |
| 3. | 2.232 |
| 4. | 2.249 |
| 5. | 2.266 |
| 6. | 2.283 |
| 7. | 2.300 |
| 8. | 2.317 |
| 9. | 2.334 |
| 10. | 2.351 |
| 11. | 2.368 |
| 12. | 2.385 |
| 13. | 2.402 |

The resultant recoil proton energy spectrum is found graphically, using the diagram shown in Fig. 25. Here the inner circle, divided into thirteen strips horizontally, represents the polythene film, or its projection on the plane of the defining guard-ring, and the outer circle the circumference of the guard-ring. Each strip is divided into squares by a series of vertical lines, shown dotted.

Now, taking the uppermost strip as an example, a series of values of r is chosen. (The parameter r , defined in Chapter V, is simply related to the ratio of recoil energy to incident neutron energy). Since the polythene film diameter is 2.8 cms., and the guard-ring diameter is 3.0 cms., the maximum possible value of r is 2.8 cms. This corresponds to the case of a proton recoiling from the edge of the film and travelling in such a direction that it just grazes the opposite edge of the guard-ring. The values of r chosen for the computation were 0, 0.5, 1.0, 1.4, 1.8, 2.2, 2.6, and 2.8 cms.

The numerical values of the quantities listed in Table II were then determined graphically by drawing circles of radii r with centres at the centres of the successive small squares. The angles between the points

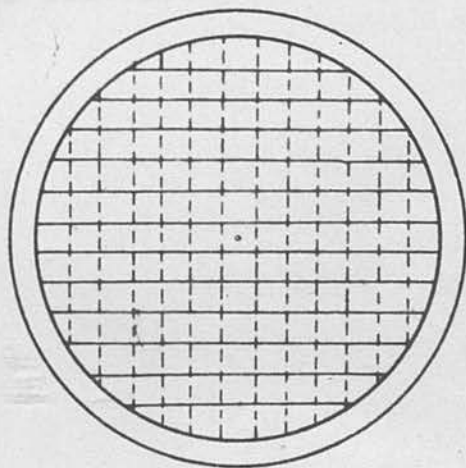


FIGURE 25.

at which these circles intersect the guard-ring circle give the values of the integrals in Table II. Where the square under consideration intersects the edge of the polythene film (e.g. the left-hand square of the first strip), the value obtained must be multiplied by the ratio of the area of the section of the square inside the film to the area of the whole square.

In this way the recoil proton energy spectra from all the strips in turn were calculated and plotted. By adding the successive ordinates the final distribution shown in Fig. 17 was obtained.

APPENDIX III.

The Level Scheme of B^{10} .

Taking the Q-value for the ground-state transition in the reaction $Be^9(d,n)B^{10}$ as 4.35 MeV, the value obtained from the individual masses, the neutron groups found in this reaction correspond to levels in B^{10} at 0.62, 1.83, 2.21, 2.88 and 3.49 MeV, all with probable errors of about ± 0.10 MeV. Rasmussen, Hornyak and Lauritsen⁽⁶³⁾ have found gamma rays from this reaction of energies 412, 713, 1016, 1424, 2138, 2853 and 3580 keV respectively. Ajzenburg⁽⁵⁶⁾ and Dyer and Bird⁽⁵⁷⁾ have proposed decay schemes which account for all of these on the basis of the levels given above.

The 412 keV gamma-ray could correspond to a transition from the 2.21 MeV to the 1.83 MeV level, though the possibility of an unresolved neutron group corresponding to 400 keV excitation above the ground-state cannot be ruled out. The 2.21 MeV level could also give rise to the 1424 keV gamma-ray by decaying to the level at about 0.7 MeV, and to the 2138 keV gamma-ray by direct decay to the ground-state, although it is difficult to see how these three gamma-rays can compete successfully. The 2138 keV gamma-ray can also arise from

a transition between the 2.88 MeV and 0.7 MeV levels. The 1016 keV gamma-ray is explained as a transition from the 1.8 MeV level to the 0.7 MeV level, and a transition to this same level from the level at 3.5 MeV could give rise to the 2853 keV gamma-ray. On the other hand, the 2853 keV gamma-ray could also arise from a direct ground-state transition from the 2.88 MeV level. The 3580 keV gamma-ray is probably due to a ground-state transition from the 3.5 MeV level.

It can be seen that no unique decay scheme can be proposed until more is known about the spins and parities of the various states, so that selection rules can be applied. It is, however, worth noting that the spin of the ground-state of B^{10} is known to be $3^{(64)}$, a rather high value, which might point to transitions to the 0.7 MeV level being preferred to direct ground-state transitions. If this were the case, the 713 keV gamma-ray would be expected to be relatively very intense, since it represents the decay of the 0.7 MeV level to ground. This has been verified experimentally⁽⁶⁵⁾.

The level scheme, together with all possible transitions giving rise to the observed gamma-rays, is shown in Fig. 26. The levels on the right are

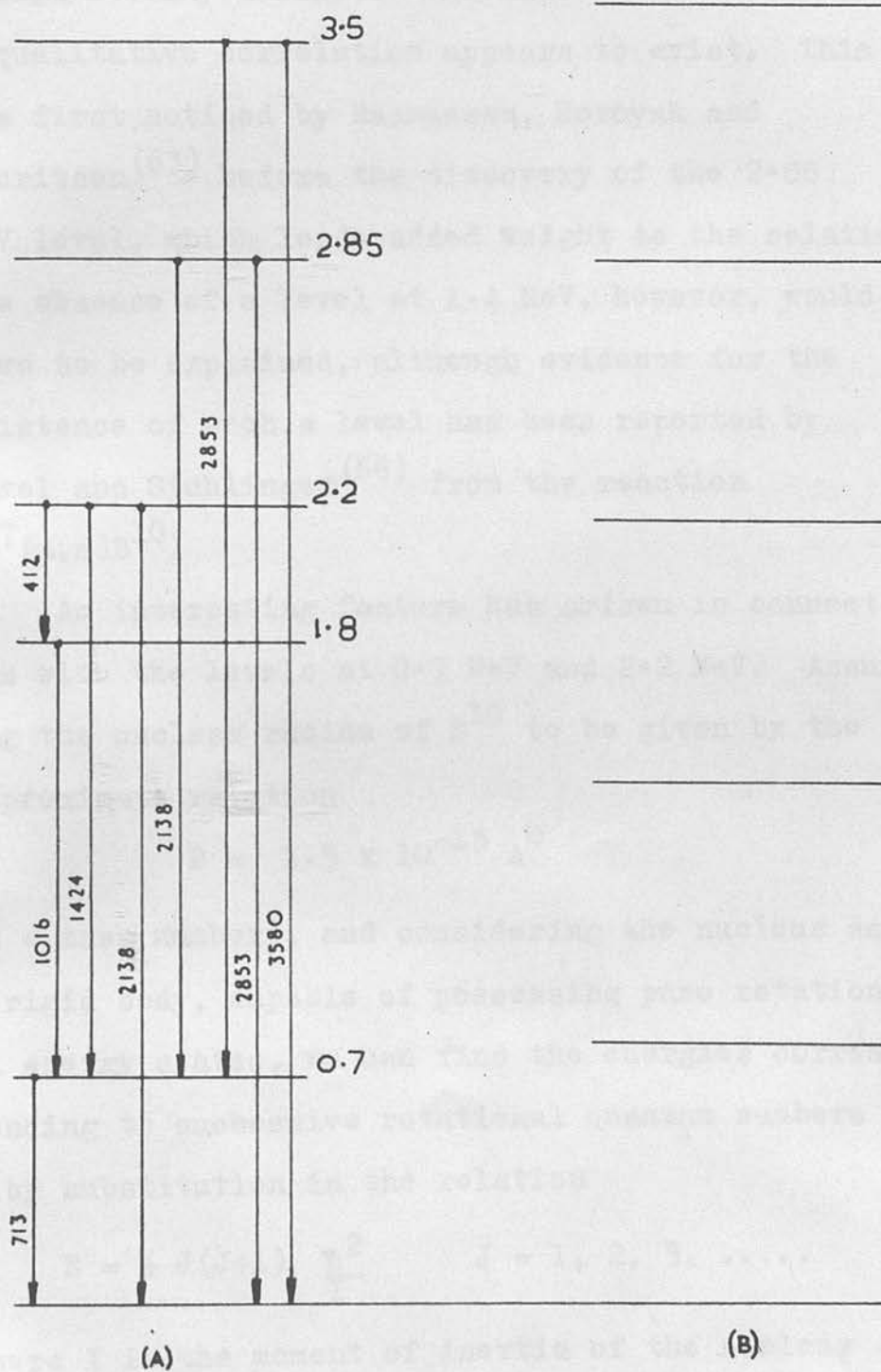


FIGURE 26. Energy Levels of B^{10} .

those obtained by assuming an equal spacing of 0.72 MeV. While the positions of the experimentally determined levels are not known accurately enough for any definite conclusions to be drawn, a qualitative correlation appears to exist. This was first noticed by Rasmussen, Hornyak and Lauritsen⁽⁶³⁾ before the discovery of the 2.88 MeV level, which lends added weight to the relation. The absence of a level at 1.4 MeV, however, would have to be explained, although evidence for the existence of such a level has been reported by Haxel and Stuhlinger⁽⁶⁶⁾ from the reaction $\text{Li}^7(\alpha, n)\text{B}^{10}$.

An interesting feature has arisen in connection with the levels at 0.7 MeV and 2.2 MeV. Assuming the nuclear radius of B^{10} to be given by the approximate relation

$$R = 1.5 \times 10^{-13} A^{1/3}$$

(A = mass number), and considering the nucleus as a rigid body, capable of possessing pure rotational energy states, we can find the energies corresponding to successive rotational quantum numbers J by substitution in the relation

$$E = \frac{1}{2} J(J+1) \frac{\hbar^2}{I} \quad J = 1, 2, 3, \dots$$

where I is the moment of inertia of the nucleus

(regarded as a sphere) about its diameter.

Taking E as 0.72 MeV and \hbar as 1.054×10^{-27} erg.-secs., the corresponding quantum number J is slightly less than 1. If the nuclear radius be taken as 3.81×10^{-13} cm., a value which is somewhat larger than that given by the relation above, the quantum number becomes exactly 1.

Substitution of $J = 2$ leads to a level at 2.16 MeV, which is close to the energy of the well-known level at about 2.2 MeV. $J = 3$ would give a level at about 4.32 MeV, corresponding to no known level.

While it is realised that this relationship is probably coincidental, it is perhaps worth noting that recent work has indicated that the nuclei Be^9 and B^{10} do in fact possess anomalously large radii (67).

Department, and in particular to Mr. A. Headridge, for many invaluable suggestions.

Finally, the author wishes to express his thanks to the Department of Scientific and Industrial Research for the award of a Maintenance Grant which enabled him to devote his time to this work.

ACKNOWLEDGMENTS.

In conclusion, the author wishes to express his thanks to all who have assisted in the work described, and in particular to Professor N. Feather and Mr. J. Dainty for general facilities, advice and encouragement, and to Messrs. R.M. Sillitto and M.D. Carter, of the University of Edinburgh High Voltage Laboratory, without whose assistance in the operation and maintenance of the Cockroft-Walton generator the work could not have been carried out. The author is also indebted to Messrs. Sillitto and Carter for much helpful discussion and advice, and to the technical staff of the University of Edinburgh Natural Philosophy Department, and in particular to Mr. A. Headridge, for many invaluable suggestions.

Finally, the author wishes to express his thanks to the Department of Scientific and Industrial Research for the award of a Maintenance Grant which enabled the work to be carried out.

REFERENCES

- (1) Wilkinson: Ionisation Chambers and Counters (Cambridge Monographs), p. 169.
- (2) Amaldi, Bocciarelli, Ferretti & Trabacchi: Ric. Sci., 13, 502 (1942).
- (3) Kinsey, Cohen & Dainty: Proc. Camb. Phil. Soc., 44, 96 (1948).
- (4) Feld, Scalettar & Szilard: Phys. Rev., 71, 464 (1947).
- (5) Bretscher & Wilkinson: Proc. Camb. Phil. Soc., 45, 141 (1949).
- (6) Klema & Hanson: Phys. Rev., 73, 106, (1948).
- (7) Report of Fast Neutron Data Project: AEC Unclassified Report.
- (8) Taylor: Proc. Phys. Soc. Lond., A, 47, 873 (1935).
- (9) Lattes & Occhialini: Nature, 159, 331 (1947).
- (10) Keepin & Roberts: Phys. Rev., 76, 154 (1949).
- (11) Keepin & Roberts: Rev. Sci. Inst., 21, 163 (1950).
- (12) Goldsmith, Ibser & Feld: Rev. Mod. Phys., 19, 259 (1947).
- (13) Roberts, Nakaji & Solano: Phys. Rev., 81, 327 (1951).
- (14) Keepin: Phys. Rev., 80, 768 (1950).
- (15) Feld: Phys. Rev., 70, 429 (1946).
- (16) Adair: Rev. Mod. Phys., 22, 249 (1950).
- (17) Curie & Joliot: Comptes Rendus, 194, 1229 (1932).
- (18) Whaling & Butler: Phys. Rev., 78, 72 (1950).
- (19) Dee: Nature, 133, 564 (1934).

REFERENCES (Contd).

- (20) Blau & Wambacher: S.B. Akad. Wiss. Wien,
141, 617 (1932).
- (21) Taylor: Proc. Roy. Soc. A, 150, 382 (1935).
- (22) Powell: Proc. Roy. Soc. A, 181, 344 (1943).
- (23) Peck: Phys. Rev., 73, 947 (1948).
- (24) Nereson & Reines: Rev. Sci. Inst., 21, 534,
(1950).
- (25) Green & Gibson: Proc. Phys. Soc. A, 62, 407,
(1949).
- (26) Richards: Phys. Rev., 59, 796 (1941).
- (27) Livesey & Wilkinson: Proc. Roy. Soc. A, 195,
123 (1948).
- (28) Baldinger, Huber & Staub: Helv. Phys. Acta,
11, 245 (1938).
- (29) Barschall & Bethe: Rev. Sci. Inst., 18, 147,
(1947).
- (30) Coon & Nobles: Rev. Sci. Inst., 18, 44 (1947).
- (31) Willard & Preston: Phys. Rev., 81, 480 (1951).
- (32) Hanson & McKibben: Phys. Rev., 72, 673 (1947).
- (33) Bonner & Butler: Phys. Rev., 83, 1091 (1951).
- (34) Worth: Phys. Rev., 78, 378 (1950).
- (35) Baldwin: Phys. Rev., 83, 495 (1951).
- (36) Falk: Phys. Rev., 83, 499 (1951).
- (37) Cohen & Falk: Phys. Rev., 84, 173 (1951).
- (38) Poole: Proc. Phys. Soc. Lond., A, 65, 453,
(1952).
- (39) Allen, Beghian & Calvert: Proc. Phys. Soc.
Lond. A, 65, 295 (1952).
- (40) Beghian, Allen, Calvert & Halban: Phys. Rev.,
86, 1044 (1952) .

REFERENCES (Contd).

- (41) Owen, Neiler & Wheatley: Pittsburgh Radiation Laboratory Report N7 onr - 32505.
- (42) James & Treacy: Proc. Phys. Soc. Lond. A, 64, 847 (1951).
- (43) Giles & Silverleaf: Private Communication.
- (44) Rossi & Staub: Ionisation Chambers and Counters.
- (45) Livingston & Bethe: Rev. Mod. Phys., 9, 245, (1937).
- (46) Smith: Phys. Rev., 71, 32 (1947).
- (47) Rosenblum: Ann. d. Physik, 10, 408 (1928).
- (48) Korff: Electron and Nuclear Counters.
- (49) Howland, Schroeder & Shipman: Rev. Sci. Inst., 18, 551 (1947).
- (50) Pfozter: Zeits. f. Phys., 102, 23 (1936).
- (51) Bretscher & Martin: Helv. Phys. Acta 23, 15 (1950).
- (52) Hirschfelder & Magee: Phys. Rev., 73, 207 (1948).
- (53) Aron, Hoffman & Williams: Range-Energy Curves (UCRL - 121).
- (54) Bailey et al.: Phys. Rev., 70, 583 (1946).
- (55) Staub & Stephens: Phys. Rev., 55, 131 (1939).
- (56) Ajzenburg: Phys. Rev., 82, 43 (1951).
- (57) Dyer & Bird: Aust. J. Phys., 6, 45 (1953).
- (58) Wäffler: Helv. Phys. Acta, 23, 239 (1950).
- (59) Bennett, Bonner, Richards & Watt: Phys. Rev., 59, 904 (1941).
- (60) Devons: Proc. Roy. Soc. A, 172, 559 (1939).
- (61) Titterton: Report of the Birmingham Conference on Nuclear Physics (1953), p. 11.

REFERENCES (Contd).

- (62) Fermi: Nuclear Physics (Revised Edition) p. 150.
- (63) Rasmussen, Hornyak & Lauritsen: Phys. Rev.,
76, 581 (1949).
- (64) Gordy, Ring & Burg: Phys. Rev., 74, 1191 (1948).
- (65) Hornyak, Lauritsen, Morrison & Fowler: Rev.
Mod. Phys., 22, 291 (1950).
- (66) Haxel & Stuhlinger: Zeits. f. Physik, 114,
178 (1939).
- (67) Bonner: Report of the Birmingham Conference
on Nuclear Physics (1953), p. 11.